The Role of Endoglin in the Immunomodulatory Capacities of Mesenchymal Stem Cells and the Relationship to Hyperbaric Oxygen Therapy

By

Amy Rose Cantilena

Submitted to the graduate degree program in Molecular and Integrative Physiology and the Graduate Faculty of the University of Kansas in partial fulfillment of the requirements for the degree of Doctor of Philosophy

_____

Chairperson: Dr. Buddhadeb Dawn, MD, FACC, FAHA, FACP

_____

Dr. Brenda J. Rongish, PhD

_____

Dr. Timothy A. Fields, MD/PhD

_____

Dr. John G. Wood, PhD

_____

Dr. Patrick E. Fields, PhD

_____

Dr. Rajasingh Johnson, M.Phil, PhD, HCLD

Date Defended: May 8, 2017

The Dissertation Committee for Amy Rose Cantilena

certifies that this is the approved version of the following dissertation:

The Role of Endoglin in the Immunomodulatory Capacities of Mesenchymal Stem Cells and the Relationship to Hyperbaric Oxygen Therapy

_____

Chairperson: Dr. Buddhadeb Dawn, MD, FACC, FAHA, FACP

Date approved: May 8, 2017

Abstract

Mesenchymal stem cells (MSCs), a type of "adult" stem cell found in most organs, represent an emerging tool in the field of regenerative medicine. In the setting of myocardial injury, for example, MSCs have been shown to promote repair and recovery. Studies have been hampered, however, by variation in MSC phenotypes, as defined by cell surface marker expression, and the absence of a clear consensus of what MSC phenotypes are best able to support regeneration. Providing insight into the regenerative capabilities of varying MSCs phenotypes is crucial to their continued success in therapies.

One cell surface marker that has been shown to have functional relevance to regenerative medicine is endoglin (CD105). Endoglin is a type I transmembrane protein that functions as an auxiliary receptor for the TGFβ receptor complex. The absence of endoglin on MSCs reportedly defines a population with a greater propensity for cardiovascular differentiation and greater capacity to support myocardial repair. However, despite their ability to improve post-infarct cardiac function and reduce the size of resultant scars, the retention of these cells in myocardial tissue varies from only 3%-6%. Thus, transdifferentiation seems an unlikely explanation for the regenerative effects. In addition to their capacity for multipotential differentiation, MSCs also have a reported ability to suppress various immune responses, including suppression of stimulated T-cell proliferation. I hypothesized that the absence of CD105 may identify a population of MSCs with an altered capacity to modulate the immunologic milieu at the time of myocardial injury, and this difference in immunomodulatory function accounts for the improved outcomes.

To investigate this idea, MSCs that either express endoglin ($CD105^+$) or not ($CD105^-$) were co-cultured with T-cells and effects on stimulated T-cell proliferation examined. Surprisingly, neither $CD105^+$ nor $CD105^-$ MSCs were able to suppress proliferation of either $CD4^+$ or $CD8^+$ T-cells. In light of this observation, effects of MSCs on T-cell differentiation were assessed. Notably, co-culture of both

$CD105^+$ and $CD105^-$ MSCs with $CD4^+$ T-cells showed a striking effect on T-cell differentiation. Syngeneic MSCs induced Th2 skewing, with increased expression of IL-4 and IL-10 and a marked decrease in IL-17 expression. The presence of CD105 in the MSCs influenced this outcome, with a more pronounced decrease in IL-17 expression and increased IL-4 secretion.

Effects of allogeneic MSCs on T-cell differentiation were also examined. Due to the reported "immune privilege" of MSCs, it has been proposed that allogeneic MSCs may be utilized to expand the pool of MSCs available for clinical use. In an allogeneic co-culture system, both $CD105^+$ and $CD105^-$ MSCs significantly affected T-cell differentiation. Compared to syngeneic MSCs, allogeneic MSCs stimulated higher expression of IL-4, IL-5, and IL-10, as well as increased secretion of IL-4 and IL-10. There were fewer differences between $CD105^+$ and $CD105^-$ MSCs. However, $CD105^-$ MSCs induced much less IL-2 and IFNγ compared to $CD105^+$ MSCs. These results indicate that MSCs influence T-cell differentiation, resulting in a Th2 skewing with increased production of the immunosuppressive cytokine IL-10 and, in the case of syngeneic cells, diminished Th17 differentiation. This effect could be essential for the previously described MSC-induced cardiac functional preservation, and could explain differences between $CD105^+$ and $CD105^-$ phenotypes.

In addition to these mechanistic studies, I also examined potential clinical relevance of CD105 expression in MSCs in umbilical cord blood transplantation. This question arose from a clinical study was underway at the University of Kansas Cancer Center that focused on using hyperbaric oxygen (HBO) for improving clinical outcomes post umbilical cord blood (UCB) transplant. In the observation of post-transplant transfusion requirements, HBO-treated patients required less supportive blood products than historic UCB-recipients. Furthermore, they experienced decreased time to transfusion independence. However, upon examining the correlation between levels of erythropoietin in these HBO-patients to their transfusion requirements, the data did not match with animal studies, which showed a reduction in erythropoietin was the causative method by which HBO improved engraftment.

Therefore, we examined the supportive role of MSCs in response to HBO in the hematopoietic niche. This included observing changes in CD105 on MSCs after exposure to HBO, as endoglin is a known hypoxia response gene. While the observation of immunomodulatory factors produced by MSCs as a result of HBO is still underway, a downregulation of CD105 12 hours after exposure to HBO was observed. This correlates to the homing window of hematopoietic stem cells in the context of transplant and may be indicative of changes in MSCs providing a more supportive bone marrow microenvironment after exposure to HBO-therapy.

Dedication

I dedicate this work to my parents, Drs. Louis and Cathy Cantilena. You have dedicated your lives to the happiness of your children, and taught us everything we know.

Acknowledgements

I would first like to thank my mentor, Dr. Buddhadeb Dawn for the opportunity to conduct research under his guidance for the last five years. Despite the fact that I chose an ambitious project that was only tangentially related to his other studies, he was always consistently supportive of my work. I will always appreciate your encouragement and allowing me an unprecedented degree of investigative freedom in my project.

I would also like to acknowledge the contributions of the other members of the Dawn laboratory, who often provided their services and knowledge when I needed it most. They kindly tolerated my late-night phone calls, and calmly provided instruction to remedy my (clearly urgent) needs on more than one occasion.

Dr. Omar Aljitawi , who has since continued his accomplished career at the University of Rochester, took a chance on this MD/PhD student by allowing me to navigate my first independent clinical research project. Under his pilot study for using hyperbaric oxygen in his transplant patients, Dr. Aljitawi guided me through my first IRB submissions and other administrative hurdles. The results of his support and expertise created my first, primary-authored abstract as a scientist. For this, I cannot begin to express my gratitude.

The University of Kansas Medical Center has created a wonderful, cohesive academic environment in which to perform my dissertation work. Without brilliant, approachable faculty members and knowledgeable core facility personnel, my research would not have been possible.

I am particularly indebted to Dr. Thomas Yankee, Dr. Patrick Fields, and the members of their respective laboratories for their very patient assistance with my projects. They were able to provide everything: from help with data analysis to lending reagents/mice – often at the last minute – to save my experiments. I probably still owe you a few ELISA plates.

I am incredibly grateful to Dr. Brenda Rongish, Dr. Timothy Fields, and Janice Fletcher for their magnificent work in the coordination of the MD/PhD Program. They work tirelessly to ensure all my fellow students can navigate the administrative quagmire of a dual-degree program. They are also our strongest advocates and our biggest cheerleaders. I know I speak for all the students in the program when I say that we are truly appreciative of your efforts. The members of my dissertation advisory committee have most likely learned to dread the moments when I pop my head inside their offices and ask them if they have a minute – but it would never show. Each one of my committee members has taken the time out of their extremely busy schedules to help me with scientific guidance. Whether it was to help troubleshoot a freshly failed experiment, or to suggest a future direction for a project, their guidance has been invaluable. I would simply be lost without them.

I experienced some challenges in my personal life during the course of my doctoral studies – I wouldn't have made it through them without my friends. Some of whom flew from the coasts of our country when I needed them most. I know I am the luckiest person in the world to have you in my life.

Most importantly, there are not words to express how grateful I am for my family. For my parents, who have worked tirelessly their entire lives to ensure their children would have every opportunity. I could give you my organs, and it could not begin to repay the lifetime of love and dedication that you have given me. To my brother Tim, who has called me every single day during my studies – your inquiries and updates are one of the favorite parts of my day. My sister Anna, who has taken it as her personal duty to make me laugh, I would have less happiness in my life without you. And finally, I am perennially indebted to my sister Carly. I would not have been able to complete my research if you hadn't been a wonderful "aunt," taking care of my incorrigible mutts when I spent late nights in lab. We both know that you're holding me together. Thank you.

Table of Contents

List of Figures

List of Tables

Chapter 1: Introduction

Endoglin (CD105) is an elusive, multifaceted protein that plays a critical role in the development and functionality of many mesoderm derived tissues. Initially discovered 30 years ago, the protein has gained prominence as a marker of mesenchymal stem cells (MSCs) in the last 15 years. However, there is still debate about CD105-expression on MSCs, and its causative role for observed variation in MSC-performance. In 2007, *Kolf et al* published a review discussing the inconsistencies of MSC markers and lack of a cohesive surface protein profile, evidenced by a survey of 91 original papers investigating MSC properties. Of these, 8 listed CD105 as a "marker," thereby stating its necessity for the identity of a MSC in both human and murine lines.[1] In recent years, there has been debate as to the presence or absence of endoglin distinguishing a unique population of MSCs. Some groups have successfully proven that CD105 is a useful marker for differentiation and preservation of cardiac function. [2] Others have determined that the lack of endoglin is necessary for achieving optimal immunologic modulation. [3] There has not been consensus, therefore, about the function of endoglin and how it serves MSCs. The purpose of this introduction is to examine the function of endoglin as it has been explored in a variety of tissues, determine the consistency of its signaling pathway in those tissues, and extrapolate the function of its signaling and the consequences it has in a population of MSCs.

Protein Structure and Function

Structure and Variants

The protein of endoglin has been identified to subsist in several forms. The predominant variant, the long form (L-endoglin), is a 180 kDa homodimeric membrane bound glycoprotein. [4] Unless otherwise specified, this review will discuss endoglin as it relates to the L-endoglin form. Its identity as the

dominant form is derived from its constitutive presence on endothelial cells.[5] The two other forms discovered, and less frequently explored are the short, membrane bound form described as having a role in tumor development.[6 7 8] S-endoglin and L-endoglin vary only by their cytoplasmic tails. The short form has seven unique intracytoplasmic residues which alter its function. [9]The long form containing 47 intracytoplasmic residues has been well characterized in its function in several tissues, to be discussed in a separate portion of this review. Additionally there exists a soluble form of endoglin, known as S-endoglin. The structural form of soluble endoglin is considerably smaller than its cytoplasmic bound counterparts, at only 65 kDa. Mass spectrometry data has revealed that this variant corresponds with the N-terminus of L-endoglin structurally. S-endoglin has been demonstrated to play a role in preeclampsia, as a disruptor of vascular modulation in response to TGFβ during pregnancy.[10] While an interesting mechanism of action was demonstrated in *Venkatesha et al's* paper for this clinical phenomenon, there has not been any documentation of S-endoglin associated with *in vitro* MSC observations.

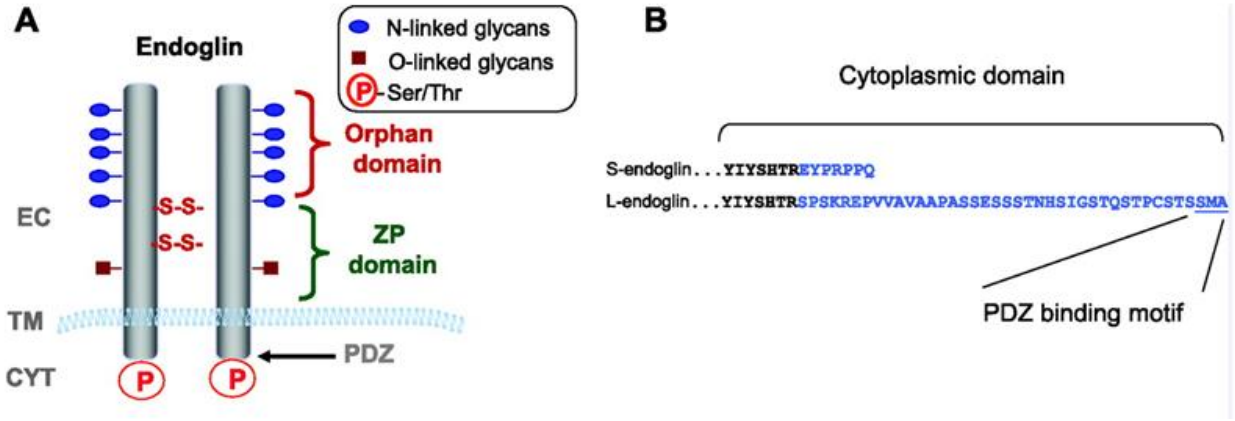

Figure 1.1: Structural configurations of L- and S-endoglin.
(A) Surface expression of Endoglin containing an N-terminal orphan domain and a zona pellucida (ZP) domain immediately juxtaposed to the membrane surface. A postsynaptic density 95/Drosophila disk large/zonula occludens-1 (PDZ)-binding motif is found to be intracytoplasmic at the C-terminus. **(B)** Differences in amino acid sequences for S-and L-endoglin for the cytoplasmic domain. Figure adapted from *Lopez-Novoa et al* and the *American Journal of Physiology*;[11] reproduction did not require permission.

Signaling and TGFβ Associations

The structural components of L-endoglin, which correspond to their signaling functionality in the TGFβ family, have been well characterized. *Koleva et al* in their 2006 paper characterize the phosphorylation sites of endoglin as a TGFβ type III receptor and the physiologic consequences of the intracytoplasmic serine and threonine phosphorylation, accomplished by TBRII and the TGFβ type I receptor family. [12] This family includes activin-like kinase 1 (ALK1) and TBRI (sometimes known as ALK5). Previous literature has demonstrated that TGFβ ligand binding on the TGFβRII receptor permits the interaction between the TGFβ type 1 receptor family and TBRII. The latter activates the kinase activities of ALK1 and ALK5. These kinases have been characterized to propagate Smad signaling for the effects of TGFβ. This work is based on documented evidence which highlights that endoglin is also a substrate for ALK5 and TBRII, and that phosphorylated endoglin is the result of this interaction.[13] Notably *Koleva et al's* studies made use of constitutively active forms of ALK1 (caALK1) and ALK5 (caALK5) in order to study their phosphorylation function on their substrate, endoglin. Using primarily mass spectroscopy data for their analysis, this group proved that caALK1 is the direct kinase substrate which phosphorylated endoglin on its intracytoplasmic threonine residues. They also provide evidence that the carboxyl terminal PDZ-liganding motif regulates this phosphorylation. This kinase action on the threonine residues of endoglin allows this group to conclude that the association of endoglin with TBRII is necessary prior to its phosphorylation via caALK1. The group discusses their results with an inclination stating that the association of the TGFβ type I and TBRII receptors with endoglin is a way in which TGFβ modulates the cell in a Smad-independent function. These findings correspond with the hypotheses tested by other groups, which state that endoglin alone cannot bind TGFβ1 and TGFβ3 without TBRII.[14] This group also finds that endoglin can bind to and associate with the kinase complexes signaled by activin-a, BMP2 and BMP 7 – but can only bind these ligands in the presence of their corresponding receptors. It has been demonstrated by *Barbara et al* that endoglin interacts with activin-a and BMP7 via

activin type II receptors (ActRII and ActRIIB), and that BMP2 associates with endoglin in the presence of ALK3 and ALK6. These functions, as they have been described in several papers, are necessary for migration, cell structural integrity and cell to cell adhesion. [15-17]

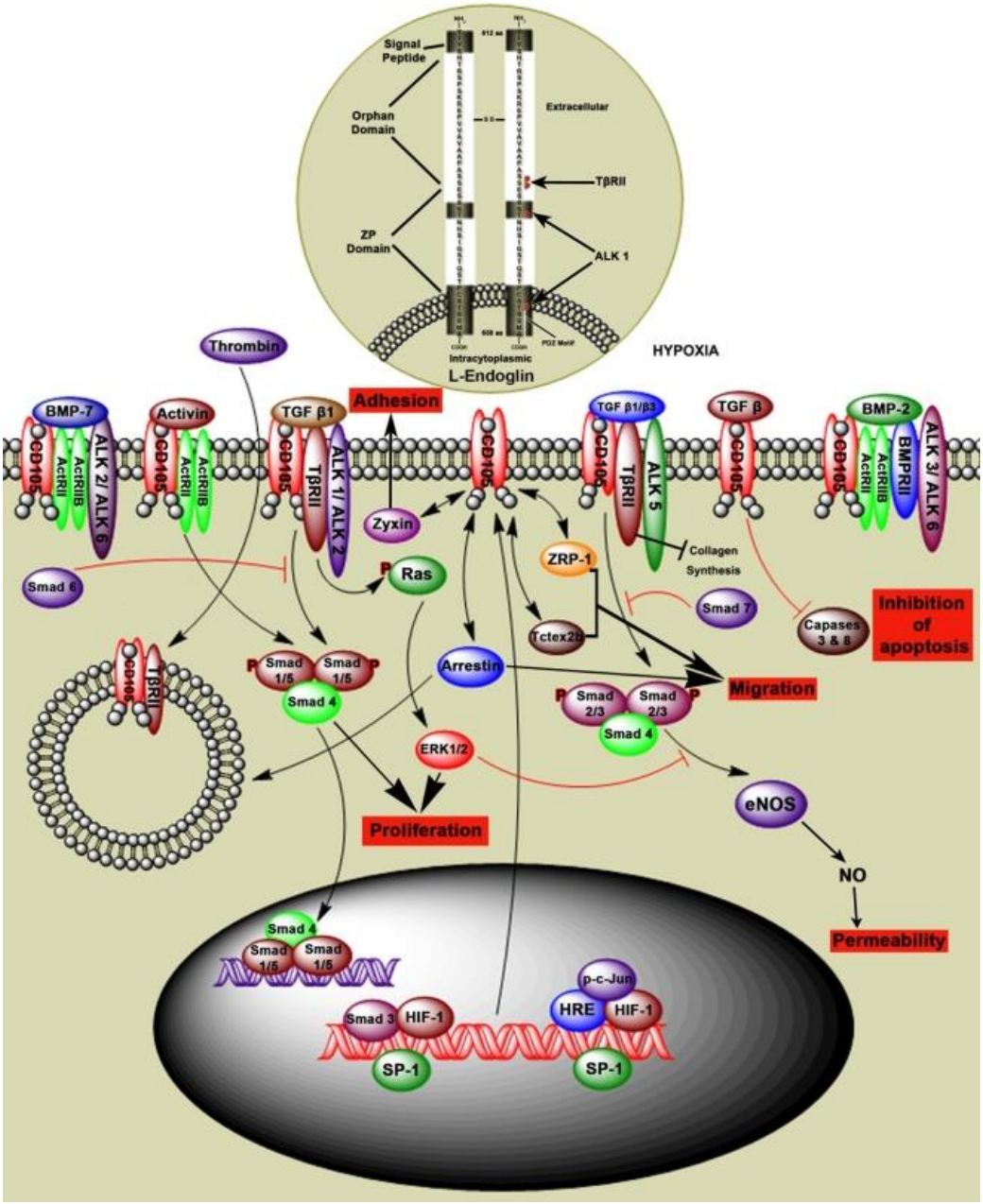

Figure 1.2: Hypothetical model of endoglin functionality
L-Endoglin binds to TGF-β1, TGF-β2, activin, BMP-2, and BMP-7 via its association with TGF-β type II receptors (ActRII, ActRIIB, ALK1, ALK2, ALK3, ALK5, ALK6, BMPRII, and TβRII). Sp1 modulates Endoglin transcription through other factors in a hypoxic environment. TGF-β1 and β3 propagate intracellular Smads 1/5, 2/3, and 4 by way of the TGF-β receptor complex. Smad6 and 7

block the effects of Smad 1/5 and Smad 2/3, respectively. TGF-β signaling through Endoglin inhibits apoptosis by prohibiting the function of caspases 3 and 8. Interaction between Zyxin, ZRP-1, Tctex2b, and endoglin alters migration and cell adhesion. CD105/TGFbRII complexes are internalized by endocytosis in the presence of thrombin. This figure was adapted from the work of *Valluru et al*[18] from their publication in *Frontiers in Physiology* and did not require permission as it is derived from an open-access article distributed under the Creative Commons Attribution Non Commercial License.

Cytoskeletal Modifications

The cytoplasmic domain of endoglin, serving as a substrate as described above, has been shown to interact with one protein highly associated with actin assembly, zyxin-related protein I (ZRP-1). This protein has been found at focal adhesion sites.[19] *Sanz-Rodriguez* et al determined via proteinalysis that the LIM domain of the ZRP-1 protein interacted with the cytoplasmic domain of endoglin, which they confirmed using transgenic myoblasts in vivo. In cells that did not express endoglin, ZRP-1 maintained its position at focal adhesion points on the cytoskeleton. However, upon the induction of the expression of endoglin, ZRP1 moved to associate throughout the cells along fibrillar structures, reminiscent of stress fibers. They also conducted a comparative study to determine the role of endoglin's presence in actin organization. Those cells made to express endoglin had parallel actin fibers constructing a concentric array which left the center of the cell free of fibers – reminiscent of the actin structure of endothelial cells. The cells which did not contain endoglin had F-actin localized in peripheral bands and dense bundles at cell-substrate contacts. One of the most important assays from this paper demonstrated that when endoglin is engaged (via monoclonal anti-endoglin antibodies); it appears in aggregates at the cell surface, bringing the actin skeleton along with it. While this shows interactions anchoring endoglin in the cytoskeleton, it also demonstrated the importance of endoglin as a molecule dictating a cell's structural integrity.

Embryogenesis and Developmental Significance

Early Angiogenesis

It therefore comes as no surprise that endoglin is a necessary component for development. In models of Hereditary Hemorrhagic Telangiectasia type I, the knocking out of endoglin results in embryonic lethality.[20] *Jonker et al* describe the course of endoglin during embryogenesis as it relates to murine development.[21] This paper provides exquisite detail of the global expression of endoglin during development. Making gratuitous use of a LacZ controlled β-galactosidase from a reporter cassette downstream of endoglin, this team observed crucial findings for where endoglin is first seen. Endoglin makes its debut at post-coital day (PCD) 6.5 in mice, in the amniotic fold and developing allantois. In mice, these tissues rapidly develop and by PCD 7 endoglin can be seen in the amnion. Not 12 hours later, endoglin is found prominently in the cardiogenic plate. As early organogenesis ensues, endoglin can be found in areas where vascular development is crucial. Most notably, this group found that endoglin was most prominent in the developing endocardium as opposed to the myocardium. They offered no evidence or speculation as to the functionality of its presence. With the entirety of the circulatory system involving and depending upon the functionality of endoglin, it is no surprise that it is crucial for proper vascular development.

Neural Crest Associations

The presence of endoglin has been noticed in the importance of neural crest cell differentiation. As endoglin had been observed in the cells surrounding the neural tube, its expression has been co-localized with neural crest markers HNK-1 and SOX-10.[22] However, not all identified neural crest cells expressed endoglin, thereby indicating a subpopulation of neural crest cells that were endoglin positive. As the embryo is examined in a rostrocaudal manner, it was determined that the neural crest cells expressing endoglin correlated with the cells that gave rise to vascular smooth muscle cells (SMC). The overexpression of endoglin in neural crest tissues leads to aberrant SMC development, however, it was determined that this was not due to defects in cell migration, but rather defects in the organization of

the vascular smooth muscle. These actions were also determined to be independent of TGFβ or BMP signaling, as there was no noticeable change in phosphorylation of pSmad 1/5/8 (BMP signaling) or pSmad2/3 (TGFβ signaling).

Cardiogenesis

The above findings have been confirmed in human embryo studies, and endoglin has been demonstrated to play a later role in cardiac development. This was initially investigated because of previous studies demonstrating the presence of TGFβ during cardiac development,[23] and the receptor profile for these factors had yet to be explored. *Qu et al* studied developing human embryos aged 4-8 weeks for their expression of endoglin, and made the noteworthy observation that the expression of endoglin corresponded with TGFβ type I and type II receptors, along with betaglycan.[24] These studies looked at the presence of endoglin in later organogenesis, and found its expression to correlate with the developing vasculature of kidney, lung, liver, neural tissues, and stomach. They further focused their studies on the developing human heart. Using qualitative antibody staining, it was found that endoglin was highly expressed on the primitive heart tube at 4 weeks development, and that endoglin co-stained with PECAM-1 on these tissues. Both endoglin and PECAM-1 were absent from myocardium. As the endocardial cushions make their first appearance from mesenchymal tissues at 5 weeks, a low-to-medium amount of endoglin was detected. However upon the pronounced development of endocardial cushion tissues of the AV outflow tract, the mesenchymal cells produced a strong signal corresponding to a high expression of endoglin. The endoglin-expressing endocardium was also found to line the spongy myocardium at this 5 week mark. During the crucial 6-7 week period of development, endoglin again was found to be highly expressed in the mesenchymal cushions as they gave rise to the atrioventricular and semilunar valves. Endoglin was also found during this period to continue to be co-expressed on the expanding endocardium with PECAM-1. High levels of endoglin were also found

during the fusion of endocardial cushions to form the intermediate septum. At 9 weeks, when the septation between the ascending aorta and pulmonary trunk has occurred and the semilunar valves are formed, endoglin expression finally decreased. By 12 weeks, a low, constant level of endoglin is found to be expressed on the residual mesenchymal cells on the semilunar and AV valves, and the intermediate aorticopulmonary septum.

Table 1.1 CD105, associated molecules, in embryo/organogenesis

Location	Developmental Age (Human)	Expression Level	Colocalized Proteins
Amniotic Fold[21]	Week 1	Moderate	
Amnion[21]	Week 2	High	
Cardiogenic Plate[21]	Week 3	High	
Neural Crest Cells[22]	Week 3	Moderate	HNK-1, SOX10
Primitive Heart Tube[24]	Week 4	Low/Moderate	PECAM-1
Endocardial Cushions[24]	Early Week 5	Low/Moderate	
Endocardial Lining[24]	Week 5	Low/Moderate	PECAM-1
AV Outflow Tract[24]	Late Week 5	High	
Mesenchymal Cushions[24]	Week 6-7	High	
Expanding Endocardium[24]	Week 6-7	Moderate	PECAM-1
Atrioventricular and Semilunar Valve Formation[24]	Week 6-7	High	
All Cardiac Locations[24]	Week 9	Low	

Endoglin in Adult Tissues

Endothelium and eNOS-signaling

The presence of CD105 has been found on numerous normal cell types in adult tissues, and its presence has been noteworthy in the development of several pathological states. As previously stated, endoglin is constitutively expressed in the adult endothelium. The role of endoglin for normal endothelial function has been well characterized.[25] *Toporsian et al* show that endoglin is central to the

NOS-dependent dilation of arteries. Using vessels from haploinsufficient *Eng*$^{+/-}$ mice, HUVEC cells from patients with endoglin mutations, and proteinalysis, this group was able to determine that endoglin increases the stability of eNOS four-fold and that Ca^{2+} activation of eNOS is dependent on endoglin. It was also determined via immunoprecipitation assays that the endoglin-deficient HUVEC cells possessed Ca^{2+}-activated eNOS with impaired interaction with HSP90. The interactions of these two proteins are necessary for maintaining NO levels.[26] Because of this impaired interaction, cells deficient in endoglin had increased NOS-dependent O_2^- production, suggesting that the role of endoglin is important for eNOS coupling. These findings correspond with their larger-scale findings of impaired myogenic responses in endoglin insufficient mice. They postulate that this crucial role of endoglin in regulating vascular tone is responsible for the venular dilation and capillary loss observed as early events in HHT1.

Vascular Injury

As endoglin is involved in the development of vasculature and its normal regulation, several groups have investigated its presence and role during vascular injury. [27, 28] A definitive study published by *Ma et al* involved the observation of endoglin expression in porcine coronary arteries following balloon injury. In their work they document the expression of endoglin on endothelium, adventitial fibroblasts, and some medial smooth muscle cells prior to injury. In each of these cell types they determined a marked overexpression of endoglin that was sustained for two weeks after balloon injury to the arteries. Twenty-eight days following injury, the levels of endoglin were found to be low or nearly absent. Also, by staining human arterial sections removed from coronaries with complex plaques, they found there was an abundance of endoglin compared to a normal artery of the same subject. The interesting portion of their studies related to endoglin as a modulator of the effects of TGFβ1 on smooth muscle cells. In previous studies, smooth muscle cells (SMCs) were modulated and increased their migration potential when stimulated with Platelet Derived Growth Factor (PDGF), and this increased

migration was mitigated by the addition of TGFβ1 to cultures.[29] *Ma et al* demonstrates here that decreasing endoglin lead to a decrease in TGFβ1's ability to slow a PDGF-induced SMC migration.

Among other types of vascular injury, there has been much study and conjecture regarding endoglin's presence in diseased arteriovenous malformations (AVMs). HHT1 patients suffer from AVMs globally,[30] and therefore it is a point of interest to study the relation of endoglin to AVMs in patients who are not afflicted by phenotypic deficiencies in endoglin. *Matusurba et al* used samples from AVMs and normal cerebral vasculature in their 2000 study, localizing endoglin to several areas within the pathologic and normal cerebral vasculature.[31] Namely, they found an expected expression of endoglin on the endothelium consistent with vasculature in other tissues, but also found endoglin in the adventitial layer in the leptomeningeal arteries, associating with the outer fibroblastic layer of the vessel wall. Surprisingly, it has been noted that endoglin positive adventitial cells were increased in cerebral AVMs, possibly as a result of shear stress on the vessels. The presence of endoglin in areas of shear stress on vasculature has also been studied. In fact, in contrast to ALK1, endoglin mRNA is upregulated in *in vitro* conditions mimicking shear stress.[32] These studies were performed in the context of examining endoglin insufficient ($Eng^{+/-}$) mice after induction of limb ischemia.

Ischemia

From all these data, it is clear that CD105 plays a role not only in maintaining normal vascular tone in the adult, but is also important for embryonic vascular development. However, angiogenesis in the adult – particularly with regard to reperfusion to ischemic areas, is where endoglin is most crucial. Hypoxia has been shown to be a potent signal for the expression of endoglin. *Sanchez-Elsner et al* describe the expression of endoglin regulated by hypoxia on a transcriptional level, as their studies conclusively show an increase in surface protein, transcript, and promoter activity of the endoglin gene.[33] They also determined that a hypoxic response element exists downstream of the main

transcriptional start site of endoglin. HIF-1 modulates a suite of hypoxia response elements, including VEGF, erythropoietin, and iNOS.[34-37] This group found that by binding a functional consensus HRE in the endoglin promoter, endoglin is also activated by HIF-1. They determined that when exposed to TGFβ, Smad3 works with Sp1 and HIF1 to cooperatively increase the expression of endoglin. *Li et al* have shown that the expression of CD105, however, blocks the ability of TGFβ to promote endothelial migration in HUVEC cells. This blockade contributes to angiogenesis.[38] These two studies together would perhaps propose that endoglin expression as modulated by TGFβ is a form of negative feedback on the affected cell types.

Hyperoxia

With hypoxia being an important mediator for the expression and function of endoglin, as described above, it is surprising that there have been very few studies related to the presence of CD105 induced by converse, hyperoxic environments. Documentation of changes in eNOS in hyperoxia have been reported in the context of vascular formation for preterm-infants.[39] Disruptions caused by the sudden increased oxygen tension in the underdeveloped infant tissues create problems in the eNOS and VEGF-related vascular development. eNOS and CD105 have also shown linked functionality through TGFβ-dependent Smad2 signaling.[40] However, there have not been direct, correlative links between hyperoxia and the expression of CD105. The only documentation of changes in CD105 as a result of increased oxygen tension have been in the clinical contexts of neonatal bronchopulmonary dysplasia, where there was an upregulation in the expression of CD105 in pulmonary vasculature.[41] This could be a direct, unanticipated result of the increased oxygen exposure in these tissues, or the by-product of fully differentiated (if aberrant) vascular tissue development, mediated by other oxygen-tension response elements.

Angiogenic Properties and Oncology Therapies

The propensity of endoglin expression to yield neovascularization has been of great interest to the field of oncology. CD105 as a target to halt angiogenesis in solid tumors is an attractive candidate for anticancer therapy. As CD105 is upregulated on activated endothelial cells, targeting CD105 during solid tumor development has been shown to thwart the necessary angiogenesis that would supply said tumor, limiting its growth.[42] *Burrows et al*, having created a murine IgM monoclonal antibody that specifically binds to endoglin, claim that it binds exclusively to activated, developing tumor vasculature. They did not speculate as to the safety of using this in human therapy. However, more recently, anti-CD105 antibodies bearing antitumor therapy have been demonstrated to home to and increase the permeability and retention of novel treatments.[43]

CD105 and Adult Stem Cell Populations

Hematopoietic Progenitors

Despite claims from groups which state that their anti-endoglin therapies target tumors specifically;[44, 45] endoglin has shown to be a marker of cell types other than the vasculature. In fact, a long-term, repopulating hematopoietic stem cell population has been defined by the presence of endoglin.[46]. *Chen et al* isolated a side population of hematopoietic stem cells (HSC) marked by expression of SCL, which is needed for definitive hematopoiesis in the mouse,[47] and characterized their marker profiles. The most notable finding was their confirmation that the endoglin-expressing early HSCs were more adept at producing long term repopulation of bone marrow cells in irradiated mice. Additionally, studies have been performed using embryonic stem (ES) cells to study endoglin's role in the hemangioblast.[48]. *Perlingeiro et al* made use of $Eng^{-/-}$, $Eng^{+/-}$, and control ES cells and differentiated them toward the hemangioblast phenotype, and found that the presence of endoglin was necessary in CFC assays for the formation of blasts. Using flow, they determined that colocalization of endoglin and FLK-1 marked a very active hemangioblast population during differentiation.

In addition to these important HSC and early hemangioblast lineages, endoglin is a marker for early erythroid progenitor cells. Several studies have demonstrated that endoglin increases concomitantly with CD235a in early erythrogenesis delineating from myeloid commitment, as CD45 expression decreases. [49, 50] This is intuitive, as the previously discussed role for endoglin in hypoxia is well documented, and TGFβ signaling plays a role in erythropoietin synthesis. [51] *Machherndl-Spandl et al* characterize the immunophenotype of early erythroid progenitors from the mononuclear fraction of whole, uncultured bone marrow. Flow analyses provide distinct phenotypes of stages of early erythroid development, with the signal for CD105 being faint in stage A, but then becoming strongly pronounced in stages B and C. They note that as erythrogenesis progresses toward its terminal differentiation, CD105 is lost.[52]

Cardiospheres

Another regenerative cell population has very recently been found to have endoglin as an important mediator for function. Heart-derived cardiosphere cells have been documented to show regenerative function in injured myocardial models, both by direct regenerative and paracrine effects.[53] *Tseliou et al*, of the same group, has recently elucidated a mechanism by which endoglin acts as a mediator for the TGFβ suppressing effects of cardiosphere cells in a chronic-ischemic model in rats. With the end goal to reduce fibrosis, they studied the paracrine effects of cardiospheres and found that soluble endoglin was present in the cardiosphere-conditioned media. They attributed the presence of endoglin in this soluble form to the presence of Metalloproteinase MMP14 on cardiospheres. Their findings are interesting as they demonstrate that soluble endoglin inhibits pSmad2/3 phosphorylation in a dose-dependent manner, and that the effects can be neutralized using an antibody directed against the extracellular domain of endoglin (which structurally corresponds to soluble endoglin). They also

demonstrate that the neutralization of soluble endoglin correlates to a decrease in collagen production by the dermal fibroblasts they utilized as target cells.[54]

Mesenchymal Stem Cells

MSC Identification

The MSC is an interesting population in which to finally examine the role of endoglin. As previously stated, there are inconsistencies in the marker profile as to whether or not CD105 should be considered as a marker for the MSC, as there exists a lack of consensus regarding MSC cell surface antigens. MSCs have been shown to differentiate *in vitro* into cardiac tissue, vascular tissue, adipose tissue, chondrocytes, and osteocytes. [55-59] They also exhibit the capacity for self-renewal and inherent mechanisms for immunomodulation. [60 61]. Established methods of MSC isolation require a plastic selection phase of mononuclear cells, the source of which varies. Bone marrow, umbilical cord blood, Wharton's jelly cells, and even adipose tissue manipulations have yielded cell populations which have been accepted as MSCs.[58, 62-64]

MSC, Endoglin, and TGFβ Signaling

With such heterogeneity in the field, it is difficult to come to conclusions about the role of endoglin in the MSC, as the interaction between CD105 and other MSC "markers" (which may or may not be present) has not been identified. However, previous studies have been undertaken to investigate the role of TGFβ in this diverse population of cells. TGFβ1 signaling in bone resorption, as linked to osteoarthritis, caused migration and aggregation of MSCs, [65] and the inhibition of TBRI decreases this migration. *Zhen et al* observed the effects of TGFβ1 on Smad signaling in MSCs that were documented as only being positive for nestin. Their model was for the study of osteoarthritis, induced by a method of ischemic bone injury. The group did not investigate whether the hypoxia response elements were upregulated in this disease model of MSCs, as it would be anticipated that the $CD105^{+}$ population of

cells increased in response to hypoxia. However, in their examination of Smad phosphorylation, this group determined that treatment with TGFβ1 of these isolated MSC groups resulted in a consistent dose-dependent increase in phosphorylation of Smad1/5/8. Interestingly, a marked contrast was evident in the MSCs from their ischemic model, with an increase in pSmad2/3 positive cells. They did not investigate whether this was facilitated by hypoxia response elements on the MSC, such as endoglin, but did note that it was mitigated by TBRI-inhibitors. [66]

ERK-MAPK and PDGF Signaling

Other signaling pathways, as we have previously described, are modulated by endoglin. While not specifically studying the role of endoglin, there has been a massive transcriptome study of the differentiation capacity of MSCs into different lineages and the molecular signaling involved in each. *Ng et al* differentiated mixed-sample MSCs (Lonza) into chondrogenic, osteogenic, and adipogenic lineages, and observed the whole-transcriptome changes in mRNA during each stage of differentiation. This group determined that ERK-MAPK signaling is globally important in the process of commitment and growth for all these lineages. PDGF signaling in these differentiated, mixed MSCs was associated strongly with the chondrogenic and adipogenic differentiation, and TGFβ signaling pathways were important in chondrogenesis specifically. They tested the importance of these two signaling pathways by blocking PDGF in addition to ALK5 of the TGFβ pathway. Their results were as predicted from their transcriptome studies. They also found that these two pathways are important for MSC growth, as their populations did not expand as easily as their uninhibited controls. [67] Other groups, however, have shown TBRII inhibition via microRNA-21 at the transcriptional and protein level to be important for adipogenesis.[68] However, as neither group characterized the expression of endoglin in these cells, the effect of CD105 on the signaling pathways of differentiation can only be extrapolated.

MSC Origin and Endoglin Expression

The heterogeneity in both source and marker profile has not gone unnoticed by all groups, however. Several papers have sought to characterize MSCs based on their source of origin and surface antigens. *Gaafar et al* undertook a large scale characterization of MSCs from endometrium and bone marrow to characterize their cytokine profile and expression levels of genes associated with multipotency and regeneration potential. In both populations, they detected a high concentration of CD105, but reported endometrial-derived cells had mildly greater (1.31-fold) expression of endoglin by mRNA analysis. While they did not speculate on the role of endoglin in the determination of the cytokine profile of each type, they did note that there was a greater propensity for these cells to express markers commonly associated with angiogenesis such as G-CSF, GM-CSF, KDR, WVF, WNTa and – to a lesser extent - GDF15,7, IL1b, ICAM1, ITGA6, NTE5, and BMP2 genes.[69]

CD105 in MSCs for Regeneration

The source of origin of MSCs and the heterogeneity of marker profiles have also been explored in a functional capacity. *Gaebel et al* observed differences in CD105 expression in MSCs as it relates to healing performance capacity for cardiac regeneration, and used MSCs from different human sources. The primary analysis of this paper revealed that bone-marrow derived MSCs (BMMSC) and adipose-tissue derived MSCs (ATMSCs) had a significantly higher proportion of cells which expressed CD105 as compared to cells derived from umbilical cord blood (CBMSCs). They also noticed that when taking a CD105-enriched population of CBMSCs for *in vitro* expansion, the amount of cells expressing CD105 decreased. They did not determine if this resulted from down-regulation of endoglin expression within the MSCs, or if the $CD105^{+}$ cells failed to expand as proficiently as their $CD105^{-}$ counterparts. The group further investigates the role of CD105 for preservation of cardiac function after ischemic injury. Using *SCID* mice, they examined the CD105-enriched CBMSCs and found their capacity for improving ejection

fraction was greater than their unaltered CBMSC correlates after LAD ligation. This improved function correlated well to the BMMSCs and ATMSC. They also demonstrated similar capacities of BMMSCs and their CD105-enriched CBMSCs to limit infarction size 6 weeks post-MI. Their subsequent analyses examine capillary density, fibrosis data, engraftment, apoptosis, and *in vitro* metabolic assays of the MSCs themselves. All of which were found to correlate the CD105-enriched CBMSCs with BMMSCs. They also performed an assay which observed capillary tube formation of only BMMSCs, one with endogenous expression of CD105, and the other which knocked out CD105 function using antisense phosphothiate-ODN. The untreated BMMSC group showed more favorable tube formation, indicating a predilection for neovascular formation. To date, this publication has been the most comprehensive in its characterization of $CD105^+$ vs. $CD105^-$ MSCs. [2]

The differentiation capacity of MSCs with respect to other lineages, however, has found that the lack of endoglin is a pro-osteogenic marker. *Chung et al* focused their studies on CD90 expression in the MSC, but nonetheless found that a low level of CD105 in the MSC population corresponded to an increased expression of osteoponin and osteocalcin at both 7 and 14 days into osteogenic differentiation.[70] These data, along with studies that document greater propensities for $CD105^-$ MSC to expand in culture,[71] may indicate that the lack of CD105 on MSCs identifies a more primitive population for self-renewal.

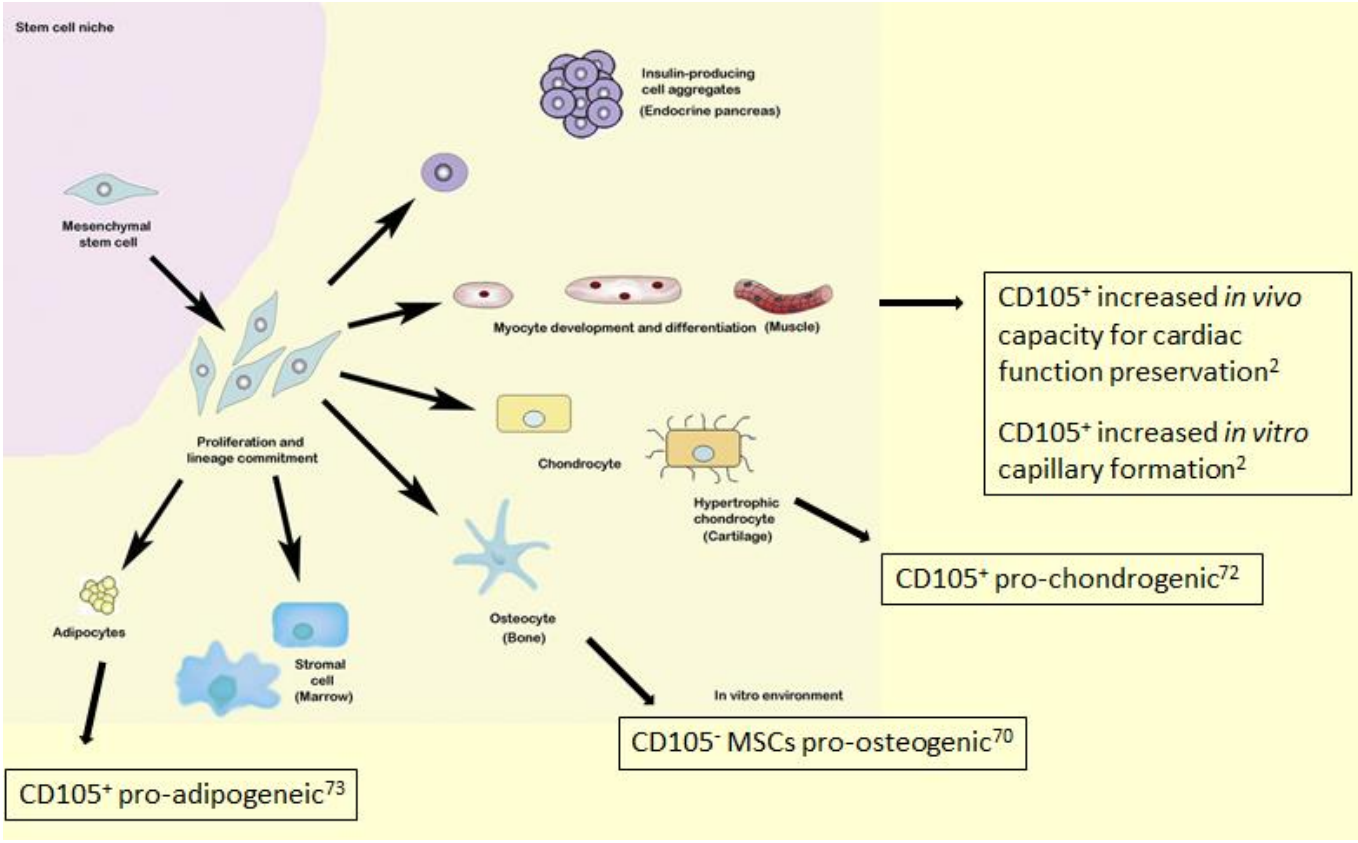

Figure 1.3: Differentiation potential of MSC
An illustration of the differentiation and expansion capacity of MSCs *in vitro* from various sources into several lineages, following exposure to specific growth/differentiation factors. The propensity for differentiation into several of these lineages has been studied with respect to CD105 expression. [2, 70, 72, 73] This figure was adapted and modified with permission from the work of *Kode et al* found in *Cytotherapy* 2009; Volume 11, Issue 4, Pages 377-391, under license agreement number 4074420424818 from Elsevier and the Copyright Clearance Center.

Role of Endoglin in MSC Immunomodulatory Capacity

However, in the immunomodulatory capacity of MSCs, the expression of endoglin has found to be limiting in capacity. In a paper which initially seeks to characterize MSCs derived from adipose tissue with respect to CD105 expression, there were some novel findings in both the expression on CD105 and characterization of some interesting multipotency markers. *Anderson et al* determined that $CD105^{+/-}$ ATMSCs had similar marker profiles with regard to CD29, CD44, CD49f, sca-1 and MHC class I positivity, and CD45 negativity. It was also noteworthy that they gathered data seeking to prove that $CD105^{-}$ cells were not of a more-differentiated phenotype. This was achieved by comparative studies where they

found no difference in cell size, proliferative CFU-F capacity, or expression of the following lineage markers: nanog (multipotency), PPAR-γ and LPL (adipogenesis), ALP and osteocalcin (osteogenesis) or Sox-9 (chondrogenesis). There was an additional attempt to stimulate expression of CD105 with TGFβ1, but this did not yield an increased CD105 positivity. One interesting data point was that at confluency, their ATMSC's surface expression of endoglin was decreased, but CD105 mRNA levels increased, however they failed to demonstrate that this was the action of MMP14 cleavage activity at the cell surface. However, subsequent analyses showed other important markers of the TGFβ signaling family to be equivalent in both populations. This group showed that betaglycan, ALK1, ALK5, and TBRII were expressed at equivocal levels between $CD105^{+/-}$ ATMSCs by mRNA analysis.

The most novel portion of this paper, however, was the documentation of the differential capacity of CD105 on MSCs to modulate immune cells. Initially, there was a non-statistically significant increase in the production of TGFβ1 by $CD105^{-}$ cells. Subsequently, TNFα and INFγ were used as proinflammatory cytokines on the $CD105^{+/-}$ cells. Stimulation with these compounds increased iNOS and IL-6 mRNA expression to a much greater extent in the $CD105^{-}$ group. Because both iNOS and IL-6 are important for T-cell expansion, an assay was devised using mitomycin-C treated MSCs of both groups with CFSE-labeled splenocytes. In a dose-dependent fashion of MSCs, $CD105^{-}$ cells proved more adept at suppressing $CD4^{+}$ T-cell expansion *in vitro.* Because of this previously undescribed effect of a $CD105^{-}$ population as a more potent immunosuppressant, the group also sought to see if $CD105^{-}$ cells generated a propensity for activated macrophages to mature to a regulatory phenotype by the secretion of IL-10 and IL-12. There were no differences seen between the $CD105^{+/-}$ groups in that final assay.[3]

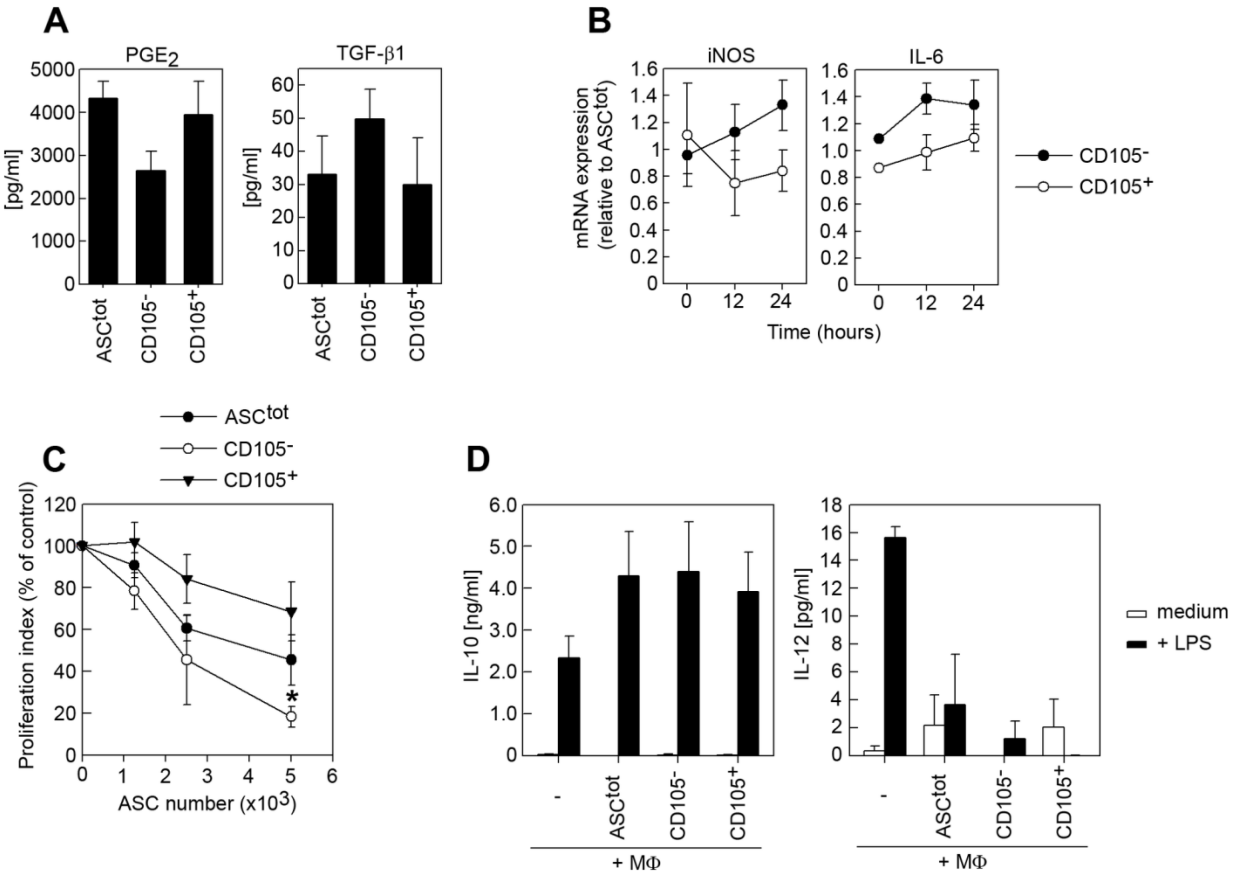

Figure 1.4: CD105 signaling for immunomodulation of specific immune-cell lineages
Definitions: ASC^{tot} – total adipose derived MSCs, LPS – lipopolysaccharide, PGE_2 – prostaglandin E2, MΦ – macrophage. **(A)** The levels of PGE_2 and TGF-β1 concentration from supernatants by ELISA, measuring relative concentrations for CD105+/- ASCs compared to the total fraction (B) ASC^{tot}, $CD105^-$ and $CD105^+$ mASCs were stimulated with TNF-α (10 ng/ml) and IFN-γ (10 ng/ml) for 12 and 24 hours, and the expression of iNOS and IL-6 was analyzed using qPCR. (C) Dose-response of mitomycin C-treated ASC^{tot}, $CD105^-$ and $CD105^+$ ASCs were cultured with splenocytes (200,000 cells/well) and stimulated with anti-CD3 (1 μg/ml) for 72 hours, and proliferation of $CD4^+$ splenocytes was quantified. (D) BM-MΦs cultured in presence or absence of ASC for 48 hours followed by restimulation with LPS (1 μg/ml) for 24 hours. Concentration of IL-10 and IL-12 from the co-culture supernatants were measured using ELISAs. Data are shown as mean (SEM). This figure was adapted from the work of *Anderson et al* from their publication in *PLoS One*,[3] and did not require permission as it is derived from an open-access article (PLoS One, 2013; Volume 8, Issue 10, Pages e76979) distributed under the Creative Commons Attribution Non Commercial License.

Summary

There are several pieces of evidence that have yet to be determined which will complete the picture of CD105 in the MSC. The first is a consensus marker profile by which to define the mesenchymal stem cell. As previously stated, there are contradictory reports regarding the use of CD105 as a marker for a sub-set of MSCs with distinct capabilities, because there is such heterogeneity in the population. The second is that the mechanism by which endoglin functions to provide these differing MSC

capacities, which has been demonstrated of endoglin in other cell types. As the field stands, the characterization of $CD105^+$ versus $CD105^-$ cells is primarily characteristic instead of mechanistic. Discussed here were several papers commenting on differentiation and functional capacities of these two different cell types, but there was very little decisive, conclusive evidence of how endoglin plays a role in its capacities. Additionally, there has been work on cytoskeletal organization of the MSC,[74-76] none of which even consider the differential expression of endoglin as a target for investigation, as it was in endothelial cells. A greater understanding of endoglin's role in TGFβ, BMP signaling, and TGFβ independent mediated effects should be undertaken in order to explain the variety of phenotypic differences in these two distinct MSC populations.

Chapter 2: Exploration of the Immunomodulatory Capacity of Mesenchymal Stem Cells on $CD4^+$ and $CD8^+$ T-cells with respect to Endoglin Expression in both Syngeneic and Allogeneic Systems

ABSTRACT

The immunomodulatory capacities of MSCs and their suppressive mechanisms have been extensively explored. However, a lack of consensus in the definitive, identifying marker profile for MSCs may have consequences in terms of a given MSC-population's immunomodulatory efficacy. Endoglin (CD105) expression is one such debated marker, and its presence indicates a cell type with a modified functional capacity compared with the $CD105^-$ counterparts. Additionally, MSCs are presently used in trials for cell-therapy, some in allogeneic settings. This study seeks to replicate immunosuppressive syngeneic *in vitro* effects of MSCs on $CD4^+$ and $CD8^+$ T-cells, and apply the created methods in an allogeneic context. It also explores the differentiation of $CD4^+$ T-cells in co-culture with $CD105^{+/-}$ MSC populations in the syngeneic and allogeneic settings.

Bone marrow MSCs were harvested from C57BL/6J mice, and sorted for a $CD45^-$/c-kit^- /$CD90^+$/Sca-1^+ expression profile. This population was sorted for CD105 for the establishment of experimental groups. Splenocyte and experimental $CD4^+$ and $CD8^+$ subgroup proliferation was tracked using CFSE. CFSE-signal tracking was employed in titrating doses of stimulation antibodies for proliferation cultures, and determining effective methods for MSC-splenocyte co-culture. From the results of these experiments, a ratio of 1 MSC for every 5 splenocytes was employed in a transwell culture system. Experimental splenocyte populations were stimulated with a combination of plate-bound anti-CD3 and anti-CD28. The $CD105^{+/-}$ MSCs were subsequently irradiated and placed in a transwell co-culture system with stimulated $CD4^+$ or $CD8^+$ splenocytes in syngeneic and allogeneic co-culture systems, respectively. In the differentiation culture, the $CD4^+$ cells and supernatants were harvested after differentiation and restimulation. mRNA levels of Th1/Th2/Th17/Treg-associated factors were assessed from the differentiated $CD4^+$ populations. Th1/Th2-cytokine production was quantified in

these supernatants to determine functional differences between differentiation in the experimental groups.

Previously documented proliferation analyses that employed antibody-only stimulation used the anti-CD3 concentration of 10μg anti-CD3/mL (plate bound) and 5μg/mL of anti-CD28 in the soluble phase. This method consistently produced no stimulatory effect for all splenocyte populations. Titration and manipulation of the antibody method led to the necessary combination of 10μg anti-CD3/mL and 5μg/mL of anti-CD28 being plate bound. Comparison of direct co-culture and transwell co-culture methods produced an MSC-washout artifact in the direct co-culture group. This necessitated that all MSC/splenocyte co-cultures be performed in a transwell system. This system was further optimized by examining the necessary doses of MSCs to induce suppression, and the appropriate timeframe in which to examine the results. It was found that a ratio of 1 MSC for every 5 splenocytes was optimal at producing expression without exhausting the cultures, and the most consistent suppression was seen at 48 hours after induction of co-culture.

Using these optimized co-culture conditions, the effect of CD105 expression on MSCs for the suppression of $CD4^+$ and $CD8^+$ syngeneic and allogeneic co-cultures was examined. Though no results reached significance, $CD105^-$ MSCs produced the highest degree of suppression compared to their $CD105^+$ counterparts in both syngeneic and allogeneic $CD4^+$ co-cultures. However, while the trend was maintained for $CD8^+$ syngeneic cultures, there was a slight stimulatory effect produced in the $CD8^+$ allogeneic model.

For the $CD4^+$ differentiation assays, changes in transcription favoring a Th2-phenotype were most pronounced in the allogeneic contexts. In the case of IL-10, IL-4, and GATA3, CD105- allogeneic co-culture groups also demonstrated increased expression compared to the $CD105^+$ allogeneic populations. Th1/Th17 associated transcription factors were largely downregulated in all allogeneic experimental

populations. The syngeneic groups, showed consistent downregulation corresponding with the lack of CD105 expression. Confirmation of these phenotypes by quantification of Th1/Th2-secreted factors revealed consistent patterns with IL-4 and IL-10 production and their corresponding expression data. The Th1-associated cytokines, IL-2 and IFNγ, did not follow the pattern associated with expression. IFNγ production was markedly increased compared to controls in the $CD105^+$ and $CD105^-$ experimental populations, though the $CD105^-$ group produced less IFNγ than the CD105 in both allogeneic and syngeneic contexts. The pattern of IL-2 production differed from IFNγ in that the $CD105^-$ allogeneic cells produced less IL-2 production than controls. This was the only setting that demonstrated this decrease. $CD105^{+/-}$ patterns in the syngeneic context of IL-2 production opposed those documented in the IFNγ assay.

Changes in transcription and secreted factors indicate that MSCs in an allogeneic differentiation culture promote $CD4^+$ cells toward a Th2 phenotype, with dependence upon the lack of CD105 expression for maximal induction. However, these studies indicate that the dynamic culture system did not eradicate all traces of Th1/Th17 lineages as seen by both the expression and secretion of these associated factors.

INTRODUCTION

There still exist many mysteries in the basic physiology of Mesenchymal stem cells (MSCs). It is known that MSCs from different sources behave differently in proliferative, differentiation, and colony forming capacities. *Kern et al* observed in their 2006 study that MSCs derived from bone marrow, adipocyte tissue, and umbilical cord blood are distinctly and quantitatively different in each of the aforementioned capacities.[77] Presently, the only consistency in the identification of a MSC population is its ability for plastic adherence, capacity for self-renewal, the ability to differentiate into cardiac, adipocyte, and vascular lineages, and the maintenance of immune-privilege. In fact, one review article by *Kolf et al* illuminated the fact that, despite hundreds of publications on MSCs, there are vast inconsistencies within the surface-marker profile employed to definitively identify a MSC.[1]

Endoglin (CD105) is a marker most known for its presence on endothelial cells.[78] While this protein is known as a member of the TGF-β receptor family, it has been studied thoroughly in the context of angiogenesis in solid tumor models. Endoglin expression is also induced on MSCs by culture in hypoxic conditions.[79] Interestingly, there has been some study of endoglin and MSC-related differentiation studies, showing down-regulation when MSC are differentiated into connective tissue cell types.[80] There have also been studies which indicate that the absence of CD105 on MSCs, presumably due to its capacity to modulate TGFβ signaling, results in a significant effect upon the proliferative capacities of several immune-cell populations.[3]

MSCs have the ability to modulate the immune system, and this modulation has been documented to create "immune privilege." This immune privilege is accomplished through several methods, including the production of anti-inflammatory cytokines such as Interleukin-10 (IL-10), Interleukin-5 (IL-5), Interleukin-6 (IL-6), and Transforming Growth Factor β (TGFβ).[81] These cytokines

alone have been shown to inhibit the proliferation of activated-T-cells, including MSC-induced inhibition in an allogeneic context.[82] . In addition to these suppressive cytokines, MSCs also have decreased MHC expression, allowing them to persist in allogeneic settings.[61] This makes these cells attractive candidates for cell therapies, and indeed, MSCs have been used for their capacity of immunomodulation to induce tolerance in clinical trials of graft vs. host disease.[83] However, despite this, few groups have sought to explore the corresponding link between the immunomodulatory capacities of $CD105^-$ MSCs in culture with T-cells, which would play the major role in their rejection.

By studying the characteristics of $CD105^-$ and $CD105^+$ MSC populations, in comparison with an unfractionated set of MSCs, we will identify which MSC phenotype is most apt to suppress specific immune-populations. If indeed there proves to be a difference in the immune modulating properties between the CD105-expressing phenotypes, it would be concerning for the *in vivo* maintenance of MSCs for cell therapies, including any subsequent downstream differentiated cells derived from an allogeneic source. In the following chapter, $CD4^+$ and $CD8^+$ T-cell suppression by MSCs with differential CD105 expression will be explored in the context of syngeneic and allogeneic *in vitro* models. This study includes optimizations of this *in vitro* model based on previous literature and our own laboratory findings. This chapter will demonstrate the characterization of $CD4^+$ T-cell differentiation as a product of their exposure to $CD105^{+/-}$ MSCs, in both the syngeneic and allogeneic settings.

METHODS

MSC Isolation

MSCs were procured from young-adult C57BL/6J mice (Jackson Laboratories). Previous data have shown that the MSC population available for isolation from bone marrow decreases as the mice age.[84] While this study was done in the context of MSC conversion to osteogenic progenitor cells, it has been noted in methodology that younger mice yield higher numbers of mononuclear cells from bone marrow extraction than their older counterparts, as younger marrow is more cellular than the adipose-laden aged marrow.[85] Therefore, all MSC extraction was performed on mice 9-11 weeks of age. The C57BL/6J mice were sacrificed by means of carbon dioxide asphyxiation, followed by opening of the chest cavity, in accordance with the approved animal usage protocol established. From here, the murine corpse was submerged in a 70% solution of 2-propanol (Fisher Chemicals) to limit contamination from the exterior of the mouse during bone isolation, and placed in a biosafety cabinet for manipulation in the following steps.

By removing skin and soft tissue over the femur, tibia, hip, and disarticulating the joints surrounding those bones, the bones were isolated and placed in an extraction medium. This medium is a filtered mixture of Dulbecco's Modified Eagle Medium (DMEM)-F12 (Invitrogen), 2% fetal bovine serum (FBS) (GIBCO), and 1% penicillin/streptomycin (5,000 μg/mL) (Cellgro). The bones were subsequently snipped at opposite ends, and flushed with this same medium into a new, separate culture dish. After a filtration step through a 70 μm cell strainer to remove any bone fragments or soft tissue that may have escaped the bones during flushing, the cells were washed, counted for efficiency of extraction, and then separated by means of a high density, low viscosity separation medium, known as Ficoll-Paque (GE HealthCare). After layering the cell-suspension over the Ficoll, the Ficoll-cell suspension was centrifuged at 300g, 4^{o}C, for 30 minutes with the brake off. Following this centrifugation step, distinct layers of cells are visible, and a mononuclear layer was identified by its position between the medium and Ficoll. This

mononuclear layer was carefully removed and washed twice with extraction medium to remove all traces of the separation procedure, and cells were counted for efficiency and plated on tissue-culture treated, plastic culture dishes.

As previously stated, mononuclear cells with plastic adherence are the minimum criteria for being classified as an MSC. Additionally, once plated, they are cultured in the same DMEM-F12 based medium, with a higher (10%) concentration of FBS. This medium is created as a low-glucose medium, which will not meet the energetic requirements of the non-adherent, non-mesenchymal mononuclear cells derived from bone marrow. These cells were cultured at 37^{o}C at normoxic conditions, with 5% CO_2. 3-4 days following extraction, after the MSCs have had time to adhere, the non-adherent mononuclear cells, unable to grow in the low glucose environment of the DMEM-F12, were siphoned off. The cells were passaged when they had achieved 80% confluence.

Flow Cytometry Based Sorting for CD105^{+}/CD105^{-} populations

Removal of the adherent MSCs was accomplished with a thin layer of 0.25% Trypsin EDTA (Cellgro) and placed at 37^{o}C for approximately 5 minutes, or until the MSCs began to release from the plastic. From there, those cells were washed and stained with a combination of antibodies for an initial sorting. The first sort is for CD90^{+},Sca-1^{+}, CD45^{-} c-kit^{-} cells using titrated concentrations of the following fluorescently conjugated antibodies: CD90.2-APC, Sca-1-PacBlue, CD45-FITC, and CD117 (c-kit)-PE (BioLegend). The final separation was for the establishment of experimental groups as described below. A titrated concentration of anti-mouse CD105-APC antibody was applied to the CD45^{-}/c-kit^{-} /CD90^{+}/Sca-1^{+} selected MSCs, thus establishing a set of CD105^{+} and CD105^{-} MSCs.

Splenocyte Isolation and Sorting

Splenocytes were harvested from 9-30 week-old male C56BL6/J or C3H/HeJ mice (Jackson Laboratories). The age range was increased for the splenocyte harvest to reflect the flexibility during

which these mice maintain a normal, healthy adult immune-phenotype.[86] The mouse strain C3H/HeJ was selected due to the extreme differences in histocompatibility, based on the protein configuration of the alloantigen markers between itself and the C56BL/6J mice. A table of alloantigen protein types in different mouse strains was procured from BioLegend.

Mice were sacrificed here in an identical fashion to the method described above. To harvest the spleen, an incision was made on the left dorsolateral side of the mouse, just inferior to the rib cage. The spleen is clearly visible through the peritoneal sac when opened from this angle. A second small incision was made directly lateral of the spleen tip, and the spleen was removed through this incision. Ensuring there was no extraneous tissue from the peritoneum, the spleen was transferred to a small culture dish containing enough supplemented RPMI to completely cover the organ. Supplemented RMPI consisted of a base of RPMI-1640 without L-Glutamine (Fisher Scientific), with 10% FBS (GIBCO), 5% Penicillin/Streptomycin (5,000 μg/mL) (Cellgro), 5% MEM-Non-essential Amino Acids (100x) (Corning), 5% Sodium Pyruvate (100mM) (Corning), 5% L-Glutamine (200mM) (Corning), and 0.025 μmol 2-mercaptoethanol (Sigma-Aldrich).

Using a 100μm cell strainer and the plunger of a syringe, the spleen was ground into a single cell suspension, before being strained through a second 100μm cell-strainer into a centrifuge tube. Cells were pelleted at 300g for 5 minutes at 4^{o}C, and the supernatant was subsequently aspirated. Cells were then suspended with 5mL of RBC Lysis Buffer (eBioscience) per spleen, and incubated at room temperature for 10 minutes with occasional gentle agitation. Cells were again pelleted using the same centrifugation parameters as listed above. After aspiration of the RBC-lysis buffer, the cells were then counted for proceeding directly with antibody incubation for sorting, or for proliferation-staining.

Cells were sorted using titrated concentrations of murine anti-CD4-PE (BioLegend) and anti-CD8-APC (BioLegend) for the experiments that required these T-cell populations. Experiments that required a $CD3^{+}$ enriched splenocyte group, a CD3-Magnisort Kit (eBioscience) was employed according to

manufacturer's instructions. When the experiments required whole-splenocytes, the cells were re-suspended in cold 1x Phosphate Buffered Saline without calcium or magnesium (PBS) (Corning) to commence proliferation staining.

Proliferation Staining

Cells that required carboxyfluorescein succinimidyl ester (CFSE) (eBioscience) staining for proliferation analyses were rinsed twice in cold 1xPBS. After the second wash, cells were re-suspended at a concentration of $2x10^7$cells/mL, again in cold 1xPBS. An equal volume of 20μM CFSE was created from 5mM CFSE stock in cold PBS. These CFSE-containing and cell-containing volumes were combined and incubated for 10 minutes at room temperature. The reaction was quenched by adding 10mL of cold, supplemented RPMI. The cells were washed twice in cold, supplemented RPMI, and the CFSE-signal was quantified by flow for a baseline in these proliferation analyses.

Proliferation Assays and MSC Co-culture

To induce proliferation, mouse anti-CD3 (eBioscience) and anti-CD28 (eBioscience) were employed in varying concentrations according to the experimental parameters (listed below). As a result of these experiments, the most effective method to induce T-cell stimulation was binding of 10μg/mL of anti-CD3 and 5μg/mL of anti-CD28 to non-tissue culture treated plates. This was accomplished by creating a plating mixture of these antibodies at the aforementioned concentrations, and coating the bottom of the plates. The plates were then incubated at 37^oC for 1-2 hours, and allowed to cool to room temperature. The wells were then washed twice with room-temperature 1xPBS, and supplemented RMPI was added to the wells to receive the splenocyte populations under examination.

For the direct-contact co-cultures described in the experiments below, $5x10^4$ MSCs of different experimental populations were added to the antibody-treated plates at this step. For the transwell co-culture systems described in the experiments below, varying experimental doses of MSCs were added to

the 0.4μm polycarbonate-membrane transwell inserts (VWR). When the optimal dose of MSCs was determined at a ratio of 1 MSC for every 5 splenocytes from the results of these experiments, all MSCs were plated at a concentration of $5x10^4$ MSCs per transwell insert. MSCs were irradiated prior to their placement in co-culture at a dose of 30Gy by x-ray irradiation, as determined by previous studies[87] to be a functional mitotically-arresting but non-lethal dose.

For each of the co-culture assays, $2.5x10^5$ CFSE-labeled splenocytes of different experimental populations were added to each of the antibody-coated wells and cultured with or without the MSC populations in supplemented RPMI. CFSE signals and analyses were conducted using BD FACS Diva software or with FlowJo. The CFSE results were tabulated and analyzed, employing a Student's t-test assuming equal variances for the calculations of statistical significance.

Differentiation Assays

In the differentiation assays, $2.5x10^5$ $CD4^+$ splenocytes of different experimental populations were added in a 5:1 ratio to each of the antibody-coated wells and cultured with or without the MSC populations in supplemented RPMI. 72 Hours after initiation of co-culture, the MSC-containing transwell inserts were removed. The $CD4^+$ populations were harvested and washed in a 1x PBS solution, then re-plated onto fresh, stimulation antibody-coated plates in supplemented RPMI. These cultures were allowed to expand for 24 hours, where the cells and supernatants were collected for analyses.

RT-PCR of Differentiated Splenocytes

Cells from the differentiation cultures were harvested as described above, washed in PBS, and resuspended in 1mL TRIazol reagent (Fisher Scientific). After a 5 minute incubation at room temperature, 200μL chloroform (Sigma Aldrich) was added to the samples, and briefly agitated. The samples were then centrifuged for 15 minutes with a speed of 12,000 RCF at 4^oC. The aqueous layer was isolated after this centrifugation, and placed in a new tube. 500mL of 100% isopropanol (Fisher

Scientific) was added to the aqueous layer. The samples were then incubated at -20°C for 20 minutes. Following the incubation, the samples were centrifuged for 10 minutes with a speed of 12,000g at 4°C. The supernatant was removed, and the pellet was washed with 1mL of 75% ethanol (Fisher Scientific), and returned for a final centrifugation step for 5 minutes at 7500g. The supernatant was removed and the pellet allowed to dry for 15-20 minutes prior to resuspension in water. Concentrations of RNA were measured using a BioTEK Take 3 instrument and Gen5.1.11 software.

To create the cDNA library, 1μg of RNA was taken from the extraction described above and used in a reverse-transcription kit (BioRad), adjusting the volume with water to 16μL dependent on the concentration of RNA in the sample. 4μL of the reverse-transcription mastermix was added to the RNA-suspension, and the reaction was placed in an Eppendorf Mastercycler Gradient Thermocycler. The reaction was incubated in the thermocycler for a priming step lasting 5 minutes at 25°C. This was followed by the reverse-transcription step for 30 minutes at 42°C, and finally 5 minutes at 85°C to inactivate the reaction.

The resultant cDNA from the reverse-transcription step was quantified prior to initiation of qPCR. 50pg of the cDNA product was required for each quantifying reaction. Keeping the reaction on ice, the cDNA was diluted to a concentration of 16.67pg/μL, and 3μL were transferred into 5μL of EvaGreen qPCR Mastermix-low ROX (MidSci). 2uL of 10uM factor-specific primer pairs were added to the reaction. Primer sequences can be found in supplemental table S2.1. Each qPCR reaction was performed in triplicate, and was cycled and analyzed in a sealed 384-well plate, using an Applied Biosystems ViiA7 instrument. Cycling conditions during the quantification consisted of an initial hold for 10 minutes at 95°C. This was followed by 40 cycles of 95°C for 5 seconds with a subsequent 30 seconds at 60°C. The temperature cycled at 1.6°C per second.

The resultant CT values from each of the reactions were normalized using the CT values of hypoxanthine phosphoribosyltransferase (HPRT) as an internal control, creating a ΔCT value for each

sample. The ΔΔCT was calculated by subtracting the factor-specific ΔCT from a non-co-cultured (NCC) controls. The fold change was calculated by the following equation:

$$Fold\ Change = 2^{-(\Delta\Delta CT)}$$

The fold changes for each group were tabulated and analyzed. Statistical comparisons were made using the Student's t-test assuming equal variances.

Quantification of Secreted Factors

Confirmation analyses for the Th1/Th2 differentiation were conducted on the supernatants harvested 24 hours after the restimulation of the MSC-co-culture groups (as described above). ELISA assays were performed for Interferonγ (IFNγ), Interleukin-4 (IL-4), Interleukin-2 (IL-2), and IL-10 using a Mouse Th1/Th2 ELISA Ready-SET-Go Kit (eBioscience) according to manufacturer's instructions. The necessary dilution of the supernatants was titrated in order to produce quantifiable signal for each of these factors. The completed reactions were subjected to absorbance spectroscopy using a BioTek plate reader using Gen5.1.11 software 450nm and 570nm.

For the analysis of these ELISA plates, the absorbance values from 570nm were subtracted from the absorbance at 450nm. Using the concentrations of standard curve for each factor as provided by the kit, linear regression models for correlating the concentration to absorbance were created. The equation generated by the factor-appropriate regression model was subsequently employed to quantify the concentration of each factor in the supernatant. These results were tabulated and analyzed.

RESULTS

Stimulation Cultures

In order to document a change in proliferation, a splenocyte stimulation assay was necessary to construct. Previously documented studies have shown that using a plate-bound anti-CD3 and soluble anti-CD28 have successfully induced T-cell specific stimulation and subsequent proliferation.[88] This was preferred over using phytohemagglutinin for activation, as it more closely mimics the mechanism induced for T-cell proliferation by antigen-presenting cells. One such protocol was attempted. Splenocytes from C56BL/6J mice were isolated and stained using CFSE as a measure of proliferation. These splenocytes were placed in culture in the appropriate supplemented RMPI medium (see methods) with plate-bound murine anti-CD3. For these assays, the anti-CD3 concentration was 10μg anti-CD3/mL PBS. 5μg/mL of anti-CD28 was added to these cultures in the soluble phase. CFSE signal was tracked in these cells over a period of 4 days. The percentage of cells that had divided in these cultures was determined by the construction of a gate on the histogram plot of CFSE signal, within the subpopulation of splenocytes falling within the expected size-range. Using the unstimulated control as a guide, the demarcating CFSE signal was determined for each experimental replicate to distinguish dividing cells from the other quiescent splenocytes. As documented in Figure 2.1A by representative images, these cultures produced no stimulation compared to their unstimulated controls.

Thus, the combination of stimulating antibodies that would result in proliferation of T-cells was reassessed. By incubating the anti-CD28 to bind to the non-tissue culture-treated plate concurrently with the anti-CD3, a proliferative effect was produced. This was titrated at varying doses of anti-CD3 at 100 μg/mL, 10 μg/mL, and 1μg/mL in PBS during antibody plating. In Figures 2.1B and 2.1C, the CFSE signal of the splenocyte cultures is displayed for 24 and 48 hours after the initiation of culture, respectively. Even at the lowest concentration of anti-CD3, the addition of the plate-bound anti-CD28 to the proliferation assay created a stimulatory effect on the T-cells in culture. Within the first 24 hours,

cells began to divide in a dose-dependent manner (Figure 2.1B). By 48 hours after induction of stimulation culture, 59.3% of splenocytes had demonstrated at least one division even at the lowest concentration of anti-CD3. The stimulation also had increased in a dose-dependent manner at 48 hours, but with very little differences between the 10μg/mL and 100μg/mL anti-CD3 doses. Therefore, in each of the subsequent assays, a plated antibody concentration of 10μg/mL anti-CD3 and 5μg/mL anti-CD28 was employed to induce stimulation.

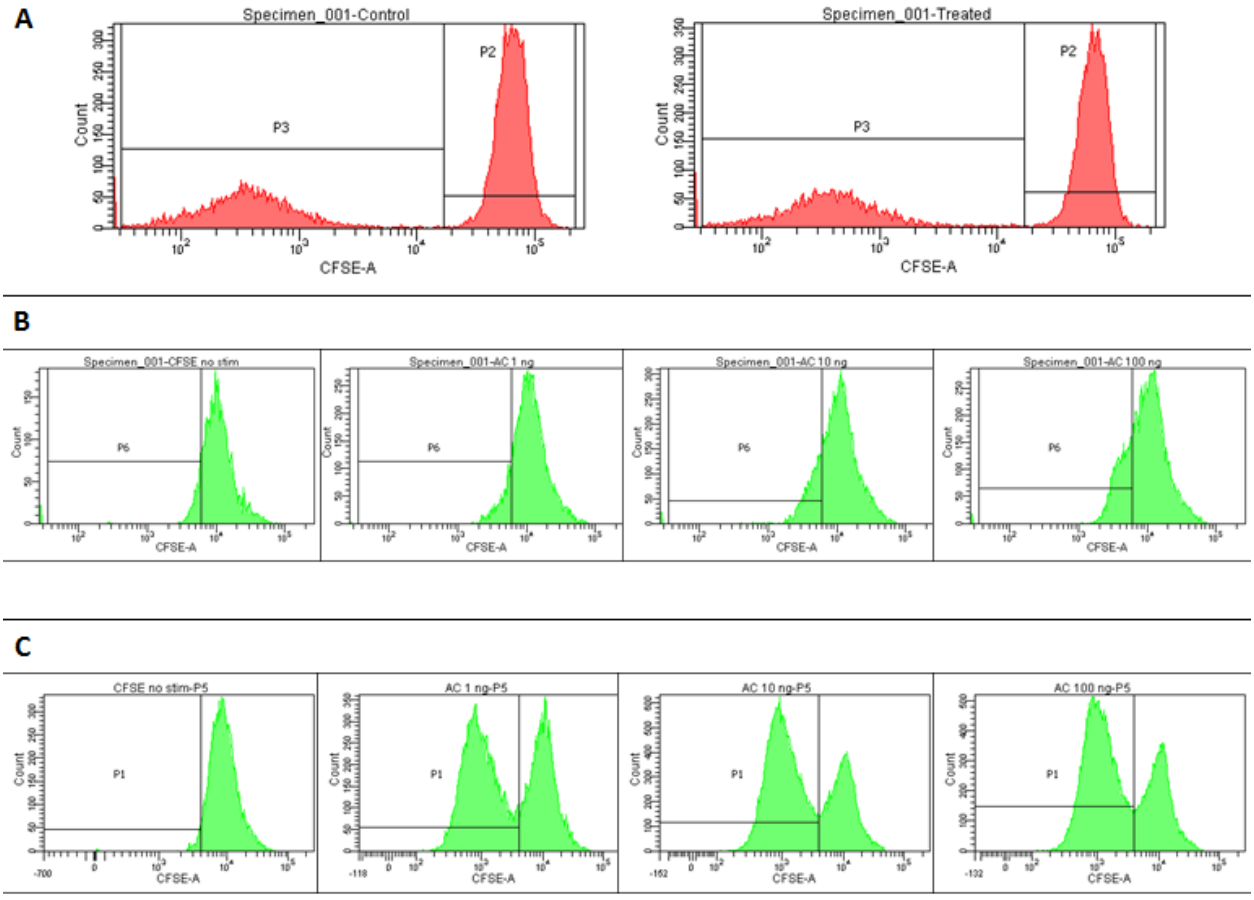

Figure 2.1: Dosage comparison of stimulation antibodies for splenocyte proliferation.
(A) Histogram of cell count by CFSE signal, 4 days after initiation of stimulation culture with only plate bound anti-CD3. Anti-CD28 was in soluble phase for these assays. The area designated by P3 in both panels indicates a weaker CFSE signal, typically indicating that the cells in these populations have divided. P3 on the left, control panel (without stimulation) contained 34.1% of the parent population gated from FSC and SSC for size. P3 on the right had 34.2% of the parent population; therefore containing no differences, despite treatment with 10μg/mL of plate bound anti-CD3 and 5μg soluble anti-CD28. **(B)** Histogram

of CFSE stained splenocytes, 24 hours after incubation with plate bound anti-CD3 and anti-CD28 at varying concentrations of CD3. Panels left to right indicate 0 stimulating antibodies, 1μg/mL of anti-CD3 with 5μg/mL anti-CD28, 10μg/mL of anti-CD3 with 5μg/mL anti-CD28, and 100μg/mL of anti-CD3 with 5μg/mL anti-CD28, respectively. These panels display a population selected for size by FSC and SSC. In each panel, P6 was created using the non-stimulated population to gate for divided cells. The cells without stimulation showed 12% of the parent population of having a halved CFSE signal, indicating division. The percentages for the increasing populations were 14.1%, 22.1%, and 26.5% for 1, 10, and 100 μg/mL anti-CD3, respectively. This demonstrates a population beginning to divide as a result of the combination of plate bound antibodies. **(C)** CFSE stained splenocyte stimulation cultures, structured in the same manner as described in part B, 48 hours after initiation of culture. Population P1 was created using the non-stimulated culture as a control for divided cells, indicating 4.9 % having divided without stimulation. There was a clear set of divided cells as indicated by the CFSE peaks. The percent divided of each increasing plate-bound anti-CD3 concentration was: 59.3%, 66.5%, and 66.7% for 1, 10, and 100 μg/mL anti-CD3, respectively.

Optimization of MSC Co-Culture Conditions

In their review article, *Yagi et al* assert that MSCs can affect their surrounding cells by both paracrine signaling and via direct contact.[89] To determine the most effective method by which to assess T-cell proliferation in the presence of MSCs for the subsequent experiments, a comparative study was conducted between direct co-culture and transwell co-culture. This study was initially comprised with multiple experimental variables, including the investigation of how the expression of CD105 on the $CD90^+$, $Sca\text{-}1^+$, $CD45^-$ $c\text{-}kit^-$ MSCs affects proliferation. It also utilized splenocytes from both C56BL/6J and C3H/HeJ mice, in an attempt to explore differences in an allogeneic and syngeneic setting. $CD105^+$ and $CD105^-$ MSCs were irradiated at 30Gy, and then plated in either direct or transwell stimulation cultures with CFSE-stained splenocytes from C56BL/6J or C3H/HeJ mice, in a ratio of 1 MSC for every 5 splenocytes. Proliferation was analyzed every 24 hours for 3 days.

However, upon reviewing the data, a MSC-washout artifact was discovered in the cultures that had direct contact. Figure 2.2A displays images of example cultures, taken after the artifact was found in the non-stimulated controls for the study. While there are more residual splenocytes in the harvested, direct contact samples, there are also no visible MSCs. MSCs, being plastic adherent cells, should still be present in the culture dishes after the process of splenocyte collection. In Figure 2.2B, the artifact of non-CFSE stained MSCs is clearly visible in the percentages indicated by the divided-cell gate compared to both the transwell cultures, and the cultures allowed to proliferate in the absence MSCs. These

images and analyses were both from CD105^{+} cultures in an allogeneic context, and therefore these differences cannot be due to experimental variables. The MSC-washout artifact was found in both the visualization and the CFSE-analyses of direct-contact cultures, regardless of CD105 expression or splenocyte source (data not shown). It is suspected that the necessary stimulating-antibody coating on the plates prevented proper adherence for these cells. Therefore, for the subsequent analyses, all suppression assays by MSCs were performed in a transwell setting, such that the MSC-washout artifact could not impact the data.

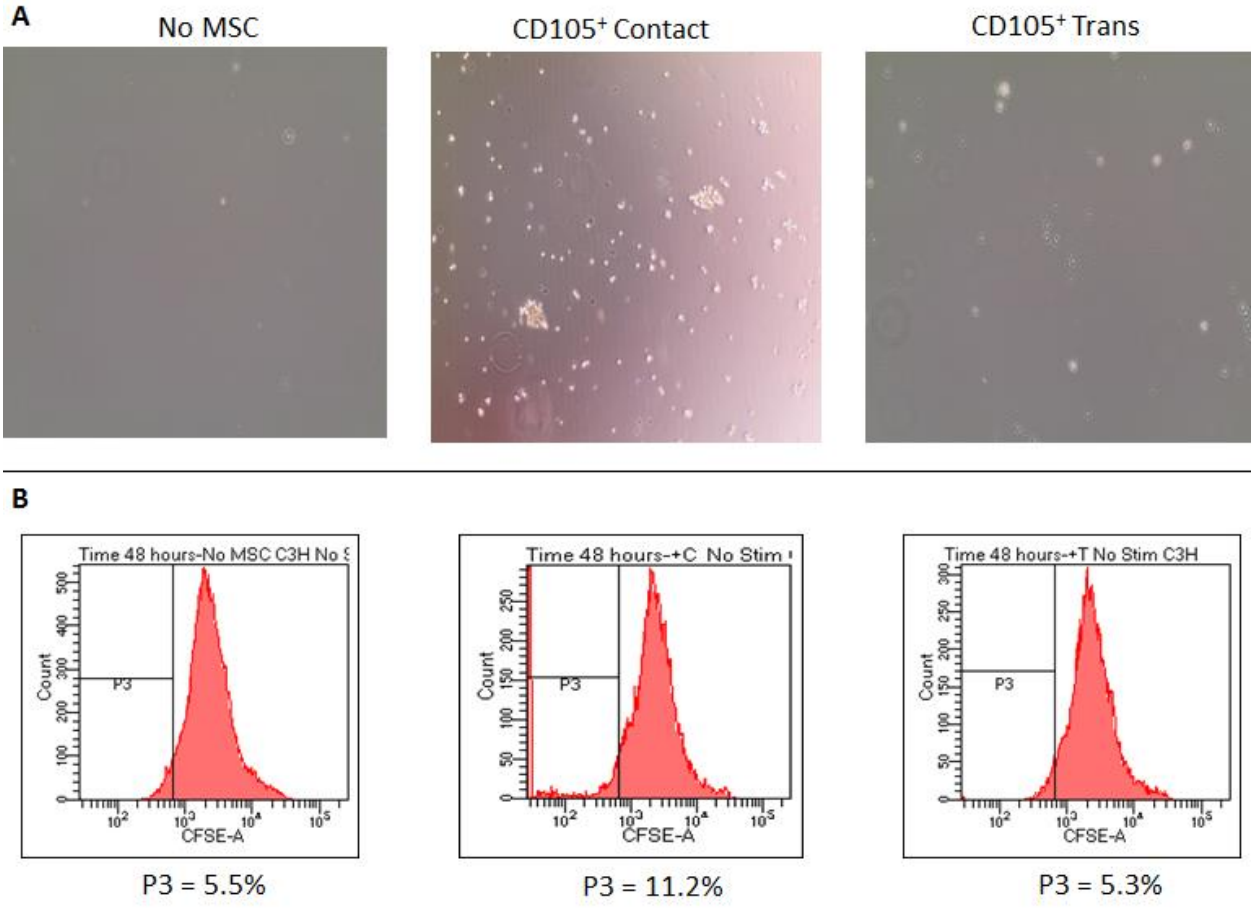

Figure 2.2: Optimization of co-culture assays for MSCs and splenocytes
(A) Representative images of co-culture dishes after cell collection for analysis. These images were procured from 48-hour stimulated co-cultures between CD105^{+} MSCs and CFSE-labeled splenocytes. As visible in the central panel, there were still

several blasting splenocytes remaining in the culture after rinsing the plates, but there are no visible MSCs, indicating that the adherent MSC population was isolated with the splenocytes. There were no expected MSCs in the left and right panels, where MSCs were either not present or were present in a removable transwell insert. **(B)** The MSC-washout effect is visible in the CFSE-based proliferation analyses for the splenocytes. P3 on all three panels was created based on the CFSE fluorescence pattern from the assays which contained neither stimulating antibodies nor MSCs. This gate applied to the subsequent analyses demonstrated a distinct population in the non-stimulated, direct contact co-culture without CFSE signal, indicating the MSCs were present in the gates needed to analyze the proliferation of the splenocytes, artificially skewing the analyses.

Optimization of Suppression Timeline and MSC Dosage

The analysis of T-cell proliferation has been extensively documented. There are multiple methods that have been devised to track and report the frequency at which various T-cell populations are dividing.[90, 91] However, with each different experimental manipulation of a T-cell expansion system, there are correspondingly different timeframes in which the T-cells are observed in order to conclude the efficacy of experimental effects upon proliferation.[92] To determine the timeframe in which the MSCs show the greatest effect upon $CD3^+$ T-cell expansion, CFSE-tracked proliferation was observed every 24 hours over the course of 3 days.

Additionally, there have been previous studies that demonstrated a dose-response in the suppressive effects of MSCs on T-cells, corresponding to the ratio of MSCs:T-cells in the suppression cultures. Increasing the dosage of MSCs creates a greater suppression of proliferation.[3] Therefore, in order to optimize the MSC:T-cell ratio at which these suppression assays should be performed, increasing doses of irradiated, $CD90^+$, $Sca\text{-}1^+$, $CD45^-$ $c\text{-}kit^-$ MSCs were added in a transwell system to $CD3^+$-splenocyte stimulation cultures. The MSCs were unsorted for CD105. The MSC:T-cell ratios in these studies were as follows: 2:1, 1:1, 1:5, and 1:50. The T-cells were placed in the bottom chamber, such that they could maintain contact with the plate-bound stimulating antibodies. The MSCs were placed in the upper chamber. A schematic of this experiment can be found in supplemental Figure 2.S1.

Figure 2.3A shows an example of the analyses used to assess the percent of the $CD3^+$ population that had divided in these cultures. The CFSE-stained, $CD3^+$ cells were gated for the expected sizes of the

proliferating and quiescent lymphocyte populations. A gate was constructed using the non-stimulated, CFSE control and the unstained samples. This was done to ensure that an accurate measure of the cells containing a CFSE-signal (at a lower level than the non-dividing population, but still containing CFSE) were the substance of the percent-divided population. These gates were then applied to the experimental samples of that particular time point, as the fluorescent signal of CFSE decreases with time. An example of these gates as applied to the 48-hour time-point on four of the experimental MSC:T-cell ratios may be found in Figure 2.3B.

At 24 hours, the $CD3^+$ splenocytes had not yet completed a division, as seen in Figure 2.3C. However, after 48 hours, cells had undergone several divisions. The unsorted MSCs in culture produced a distinct suppression in all groups. However, the dose-response that was previously reported was unable to be replicated in these assays. In fact, the 2:1 and the 1:5 ratios of MSCs:T-cells produced similar suppression at having 58.26%±6.74 and 61.08%±6.23 divided cells, respectively. This compares to the stimulation cultures without MSCs, which had a percent divided at 74.54%±3.07. After 72 hours in culture, the $CD3^+$ cells had proliferated to the extent that the percent divided was not reduced significantly at any MSC dosage, and there was again no correlation of a dose-response. Data for each time-point and cell-dosage can be found in Figure 2.3C. Therefore, for the subsequent assays where the experimental variable of CD105 expression could affect T-cell populations in their proliferation, all CFSE-data were gathered at 48 hours, employing a ratio of 1 MSC for every 5 T-cells.

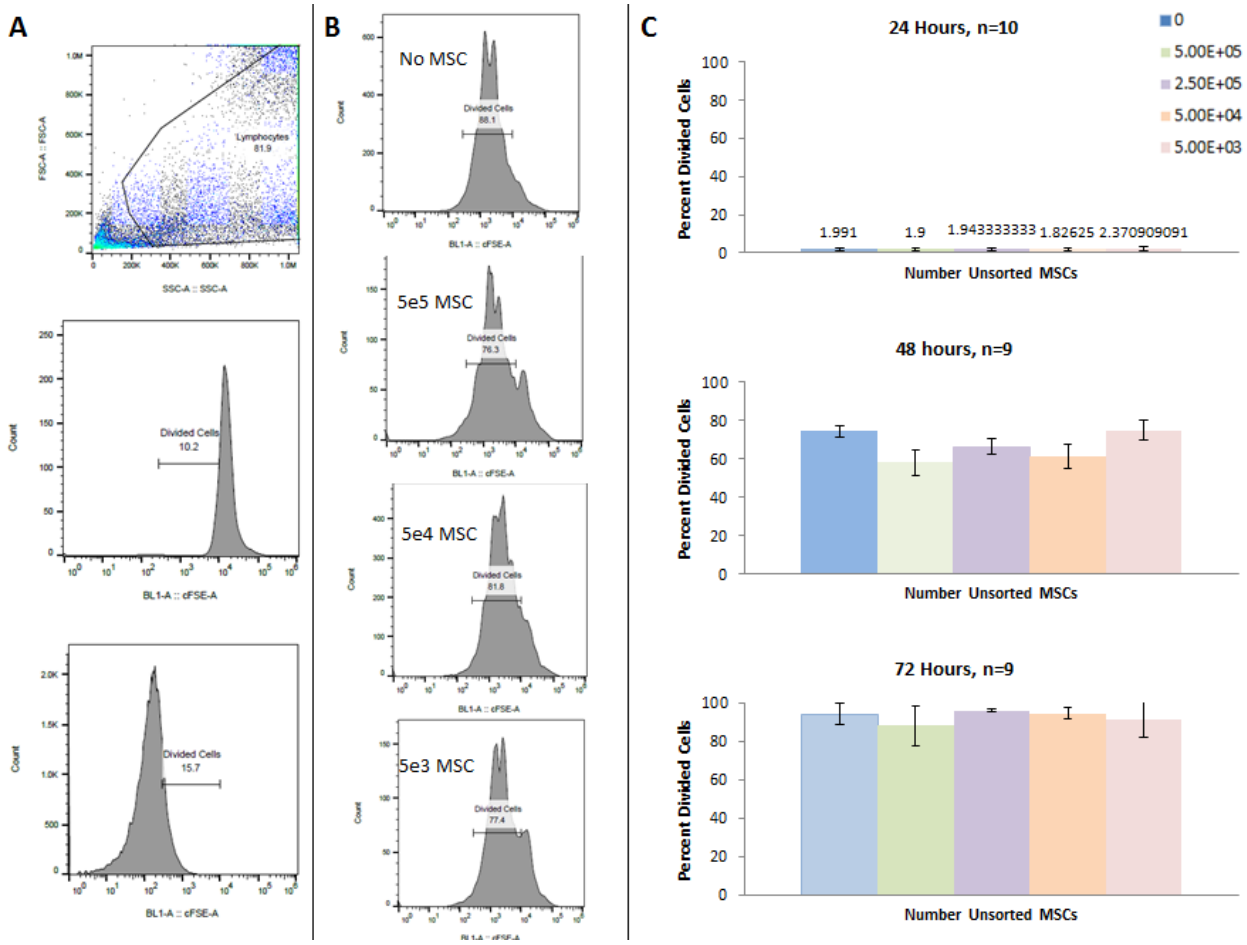

Figure 2.3: Optimization of suppression analyses for MSC and splenocyte co-culture
Increasing numbers of unsorted, irradiated MSCs were placed in transwell co-culture with $2.5x10^5$ $CD3^+$ splenocytes, and stained with CFSE at the initiation of co-culture. Unstimulated co-cultures were used as gating controls. **(A)** Gating for proliferation analysis. Stimulated splenocytes were gated based on size to include both blasting and quiescent cells, as seen in the top panel. This lymphocyte gate was isolated and the CFSE signal for both the unstimulated and the unstained cells (middle and bottom panels) were viewed. A "divided cells" gate was created based on these histograms to determine the percent divided. **(B)** Gates created in part A of this figure were subsequently applied to all samples in the experiments. The panels here are representative histograms of some samples in these analyses with the appropriate gates, and labeled for the amount of unsorted, irradiated MSCs that were placed in the co-culture. The percentages were tabulated for comparison. **(C)** Suppression of $CD3^+$ T-cells by unsorted MSCs, analyzed every 24 hours. Data are indicated as percent divided, +/- standard error.

Effect of CD105 Expression on T-cell Proliferation

There have been several studies that observed the effect of MSCs on the proliferation of $CD4^+$ and $CD8^+$ T-cells.[93] Some have even documented the anti-proliferative effect as a function of CD105 expression.[3] However, few have investigated whether the syngeneic or allogeneic source of T-cells can be a determining factor for the efficacy of suppression by MSCs with respect to the expression of CD105.

MSCs with the expression profile $CD90^+$, $Sca\text{-}1^+$, $CD45^-$ $c\text{-}kit^-$ were sorted based on CD105 positivity and placed in the previously described transwell co-culture system, after they were irradiated. A population that was unsorted for CD105 was also irradiated and placed in this system.

Splenocytes were isolated from either C57BL/6J or C3H/HeJ mice and sorted for CD4 or CD8 expression. Following CFSE staining, they were placed in stimulation cultures with the 3 MSC treatment groups in transwell inserts. The ratio of MSCs to $CD4^+$ or $CD8^+$ cells was 1 MSC for every 5 T-cells. Controls for this experiment included CFSE-stained T-cell stimulation cultures without MSCs, CFSE-stained T-cells without stimulation, and unstained, stimulated T-cells. CFSE-signals were obtained after 48 hours, and analyzed with the same method found in Figure 2.3A/B.

The results from these experiments can be found in Figure 2.4. The $CD4^+$ populations demonstrated very slight suppression compared to the non-MSC stimulated controls, as seen in Figure 2.4A. The $CD105^-$ suppression culture showed the most suppression at 73.79%±1.21 and 75.57%±1.23 for syngeneic and allogeneic, respectively. This compares to the 76.45%±1.41 for the syngeneic group and 78.05%±1.61 for the allogeneic group without MSCs. The $CD105^+$ populations produced less suppression than either the unsorted MSC or the $CD105^-$ groups in these $CD4^+$ co-cultures. No significant differences were found across all experimental groups.

A similar pattern held true for the $CD8^+$ cells in the syngeneic model, with $CD105^-$ cells producing the greatest suppression effect of 81.86%±3.35 divided cells compared to 85.69%±2.01 divided cells in the non-MSC containing, stimulated control. In contrast, an unexpected observation emerged for the $CD8^+$ allogeneic co-culture assays. Co-culture with all MSC groups produced a slight stimulation effect compared to controls. The least stimulatory effect was seen in the $CD105^-$ group, with the unsorted and $CD105^+$ populations creating more divided cells. With both patterns in the syngeneic and allogeneic CD8 suppression model, no groups reached statistical significance.

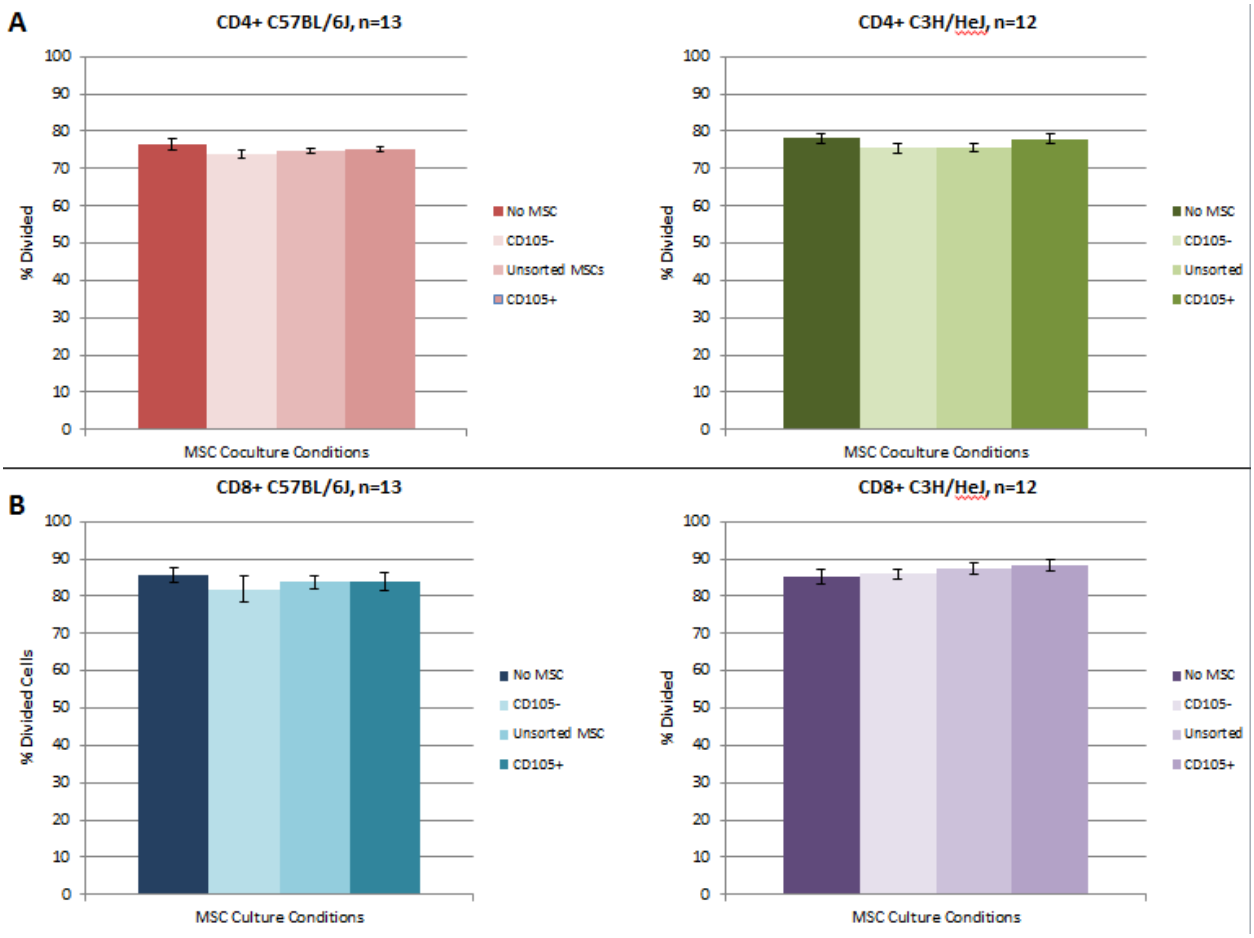

Figure 2.4: Suppression capacity of CD105$^{+/-}$ MSCs on CD4/8^{+} splenocytes
CFSE-based proliferation assays with anti-CD3 and anti-CD28 were initiated in co-culture with either CD105^{+}, CD105^{-}, or unsorted MSCs. Percent of divided cells was calculated 48 hours after incubation with MSC subgroups. Data are presented as percent-divided, +/- standard error. **(A)** CD4^{+} splenocytes were sorted from C57BL/6J mice for a syngeneic co-culture (left) and C3H/HeJ mice for an allogeneic co-culture (right). Both co-cultures produced a very slight suppression, with CD105^{-} MSCs suppressing at 73.79%±1.21 and 75.57%±1.23 for syngeneic and allogeneic, respectively. **(B)** CD8^{+} splenocytes were sorted from C57BL/6J mice for a syngeneic co-culture (left) and C3H/HeJ mice for an allogeneic co-culture (right). The syngeneic model also produced a slight suppression, with the most seen in the CD105^{-} group (81.86%±3.35). However, there was a stimulation effect seen in the CD8^{+} allogeneic model, with each MSC co-culture group producing a slight increase in percent divided cells.

Characterization of Differentiated Syngeneic CD4^{+} Cells

To address the question of how the presence of CD105 on MSCs influences the differentiation of CD4^{+} T-cells, CD4^{+} splenocytes were isolated from C57BL/6J mice for a syngeneic model. These sorted CD4^{+} populations were placed in stimulated co-cultures with or without CD105$^{+/-}$ MSCs and allowed to expand for 72 hours. The cultures were then refreshed and restimulated without their corresponding

experimental MSC-groups, and allowed to proliferate for 24 hours. The mRNA was harvested from these differentiated $CD4^+$ populations and subjected to quantification analyses for the identification of different T-cell phenotypes.

In Figure 2.5A, the constellation of GATA-binding protein 3 (GATA3), IL-4, and IL-5 test the relative amounts of these Th2-associated factors. GATA3 is a transcription factor which controls expression of both IL-4 and IL-5, and helps induce Th0 cells to a Th2 phenotype.[94] In these expression assays, the $CD105^+$ MSCs produced greater fold-changes than their $CD105^-$ counterparts. Interestingly, the IL-5 expression demonstrated a significant overall downregulation when compared to non-co-cultured (NCC) controls for the $CD105^-$ group. This differs from the upregulation seen in the $CD105^+$ cultures. The mRNA production between the NCC controls and the MSC-co-cultures reached a high level of significance ($p<0.005$) for the $CD105^-$ effect of downregulation in IL-5. The upregulation of GATA3 and IL-4 was significant when compared to NCC controls for the $CD105^+$ co-cultures only.

Factors associated with T-regulatory (Treg)-function are depicted in Figure 2.5B. There are minimal and non-significant differences for forkhead box P3 (FoxP3). The production of IL-10 is significantly increased for $CD105^+$ MSC-culture conditions compared to NCC controls. However, $CD105^-$ MSCs did demonstrate a higher numeric fold-change in comparison to the $CD105^+$ MSCs.

Figure 2.5C compares the pro-inflammatory, Th17-associated factors after differentiation cultures. Th17 cells have been associated with the suppression of the Treg phenotype,[95] and play an important role in maintaining an antimicrobial environment in mucosal barriers.[96] Aberrant Th17 induction has also been associated with autoimmune disease.[97] Additionally, Th17 cells require small amounts of TGFβ1 to differentiate,[98] which make their subset an interesting target for study in the context of $CD105^{+/-}$ co-culture. $CD105^-$ MSCs produced less Th17-associated transcription than the $CD105^+$ cells for each of the examined factors. However, Interleukin-17a (IL-17a), the hallmark cytokine of Th17 cells, shows significant downregulation in both MSC-co-culture groups compared to NCC

controls ($p<0.005$). In the examination of retinoid-related orphan receptor-γ (RORC), it is clear that both MSC culture groups upregulate its expression, but it is not significant for the $CD105^-$ MSC co-cultures. In Interleukin-22 (IL-22), a different pattern emerges, where the $CD105^-$ group comparatively produces a decrease in expression, but $CD105^+$ upregulates this cytokine. The reduction of IL-22 as influenced by $CD105^-$ MSCs reaches statistical significance ($p<0.005$) when compared to NCC controls.

Other pro-inflammatory cytokines and transcription factors associated with Th1 and γδ T-cells[99] were analyzed, the results of which can be found in Figure 2.5D. Interleukin-23 receptor (IL-23R) is also associated with the Th17 phenotype. Its presence has been conversely linked with T-box transcription factor 21 (Tbx21) and IFNγ for determining if naïve $CD4^+$ T-cells differentiate into a Th1 or Th17 functional T-cell.[99] All of the Th1/γδ T-cell associated factors examined had numerically greater fold-changes in the $CD105^+$ co-culture assays compared to the $CD105^-$, though these comparisons did not reach significance. IL-23R shows mild, non-statistically significant upregulation for both groups of MSCs in this syngeneic context. Tbx21 is a distinct Th1 transcription factor, which controls the expression of IFNγ.[100] MSC-co-cultures did upregulate Tbx21 to some degree, but predictably, the results were not statistically significant when compared to NCC controls. IFNγ, however, was consistently downregulated in all MSC-co-cultures. These results reached significance when compared to the NCC group ($p<0.05$).

A summary table of expression changes can be found in Table 2.1

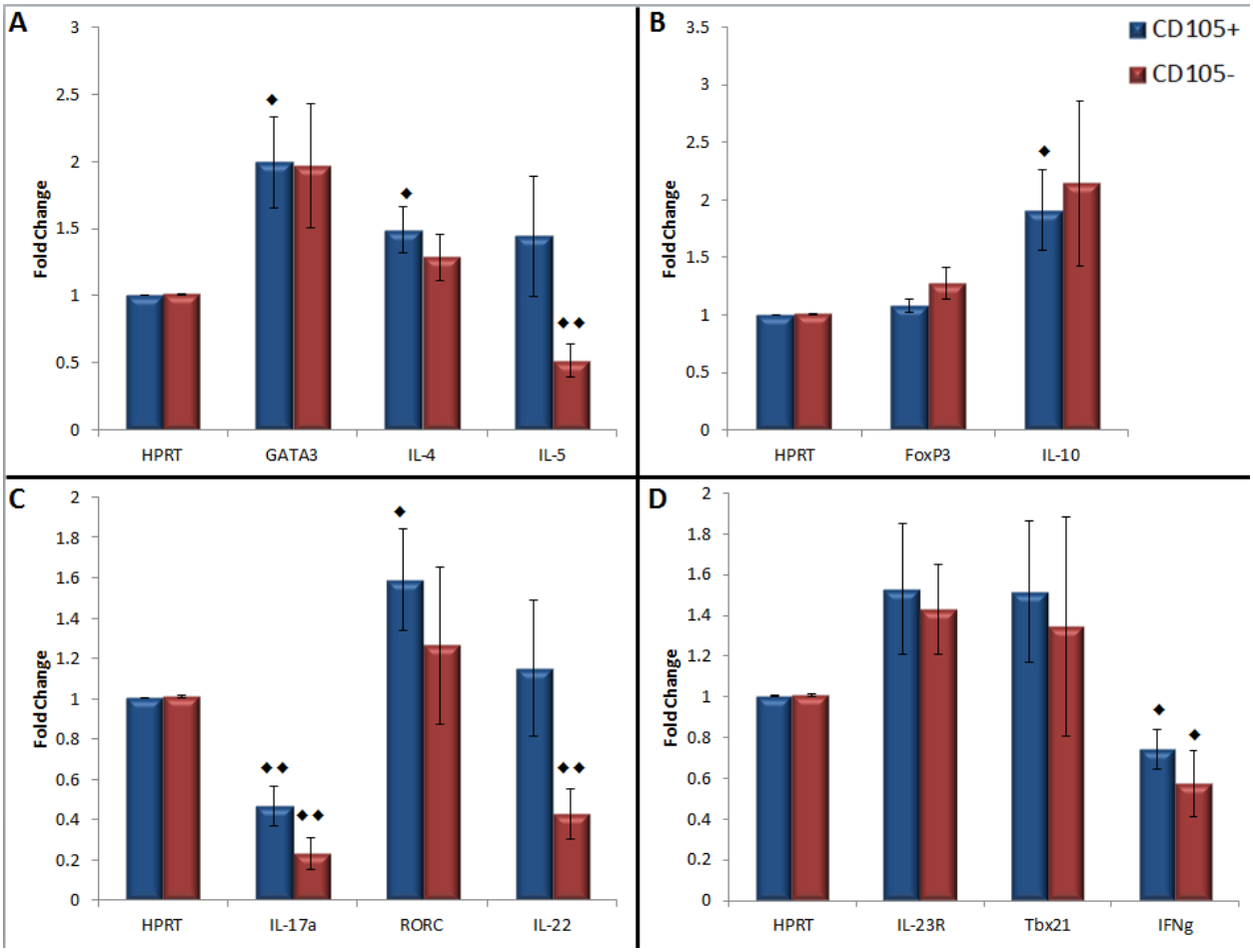

Figure 2.5: Differentiation of $CD4^+$-splenocytes after co-culture with syngeneic $CD105^{+/-}$ MSCs
Values are represented as means±SEM. **(A)** Comparison of transcription factors associated with the promotion of a Th2 phenotype after differentiation cultures. The $CD4^+$ T-cells co-cultured with $CD105^-$ MSCs demonstrated a slight decrease in these factors, but these did not reach significance. The syngeneic $CD105^-$ groups produced a fold-change of 1.28±0.17 and 0.517±0.12 for IL-4 and IL-5, respectively. **(B)** Comparison of Treg associated transcription factors after differentiation cultures. No significant changes were found in the regulation of FoxP3. However, each co-culture condition upregulated the expression of IL-10, with the $CD105^-$ co-culture having a higher 2.14±0.71-fold change compared to the 1.91+0.35-fold change for the $CD105^+$ group. **(C)** Comparison of pro-inflammatory, Th17-associated factors after differentiation cultures. IL-17a was downregulated by both co-culture conditions, with $CD105^-$ MSCs producing a more pronounced reduction in fold change by 0.26±.07 compared to the $CD105^+$, which reduced the expression by 0.46±0.09-fold. While both co-culture conditions did upregulate the expression of RORC, the $CD105^+$ group's expression was greater at 1.59±0.25-fold compared to $CD105^-$, producing only a 1.26±0.39-fold increase. The $CD105^-$ group had a more dramatic downregulation in expression for IL-22 at 0.43±0.13-fold compared to controls, while the $CD105^+$ co-culture group upregulated IL-22 slightly at 1.15±0.34. **(D)** Comparison of Th1-associated proinflammatory factors after differentiation culture. While IFNγ expression was suppressed by both co-cultures (0.74±0.09 for $CD105^+$ and 0.57±0.16 for $CD105^-$), IFNγ's controlling transcription factor: Tbx21, was upregulated. $CD105^-$ co-cultures did produce less expression of Tbx21 than their $CD105^+$ correlating co-cultures, however (1.35±0.54 and 1.52±0.35-fold, respectively). IL-23R also demonstrated upregulation, in a similar pattern with respect to co-culture conditions. None of these results reached statistical significance. ◆indicates that the fold-change is significant compared to the non-co-cultured controls, $p<0.05$. ◆◆indicated a significance factor of $p<0.005$**. n=12 for syngeneic cultures**

Table 2.1: Summary of syngeneic expression changes relative to NCC controls.
These are the data from $CD4^+$ C57BL/6-derived splenocytes co-cultured with $CD105^{+/-}$ MSCs that were assayed for differentiation. Red arrows indicate that changes were significant ($p<0.05$).

Factor	$CD105^+$	$CD105^-$
FoxP3	▲	▲
GATA3	▲	▲
IFNγ	▼	▼
IL-4	▲	▲
IL-5	▲	▼
IL-10	▲	▲
IL-17a	▼	▼
IL-22	▲	▼
IL-23R	▲	▲
RORC	▲	▲
Tbx21	▲	▲

Cytokine Production by Differentiated Syngeneic Co-Culture Products

From these same differentiation assays, the supernatants were simultaneously harvested. The fresh supernatant was then subjected to a Th1/Th2 ELISA characterization assay, wherein the factors

IFNγ, IL-2, IL-4 and IL-10 were quantified in each of the different experimental groups. For the Th2-cytokines IL-4 and IL-10, the expected pattern emerged in a most significant fashion. As visible in Figure 2.6A, experimental groups that were co-cultured with MSCs produced a greater amount of IL-4 than the NCC controls. The $CD105^-$ groups produced significantly more IL-4 than their $CD105^+$ counterparts in this syngeneic context. $CD105^-$ cultures also produced more IL-4 than the NCC controls in a significant fashion. This correlation was predicted by the mRNA expression data.

A nearly identical pattern also emerged for the production of IL-10 by these differentiated $CD4^+$ cells (Figure 2.6B). $CD105^-$ co-cultures produced more IL-10 than their $CD105^+$ correlates, the differences reaching statistical significance. In fact, this syngeneic $CD105^+$ group actually produced less IL-10 than the stimulated NCC controls, though these differences did not reach significance ($p=0.28$). Despite this minor discrepancy, the $CD105^-$ MSC co-cultures appear to shift the differentiation of these $CD4^+$ splenocytes to the more tolerant Th2 phenotype more efficiently than their $CD105^+$ correlates.

The expression of IL-2 was quantified from these same differentiated cultures using the ELISA assay described. In Figure 2.6C, the comparative concentrations for these co-cultures can be examined. The $CD105^+$ co-cultured cells followed a different pattern than would be predicted for a Th2-associated type. While both syngeneic cultures produced less IL-2 than the NCC controls, The $CD105^+$ syngeneic culture did not create as much IL-2 as the $CD105^-$ correlates. These did not reach statistical significance.

Interestingly, for the quantification of IFNγ in Figure 2.6D, there were divergent patterns from the anticipated production in these syngeneic populations: both syngeneic MSC-co-cultures produced more IFNγ than the NCC controls. This pattern was unanticipated as compared to the NCC controls, but the expression of CD105 as a factor for determining IFNγ production was predicted by the expression analyses documented in Figure 2.5D.

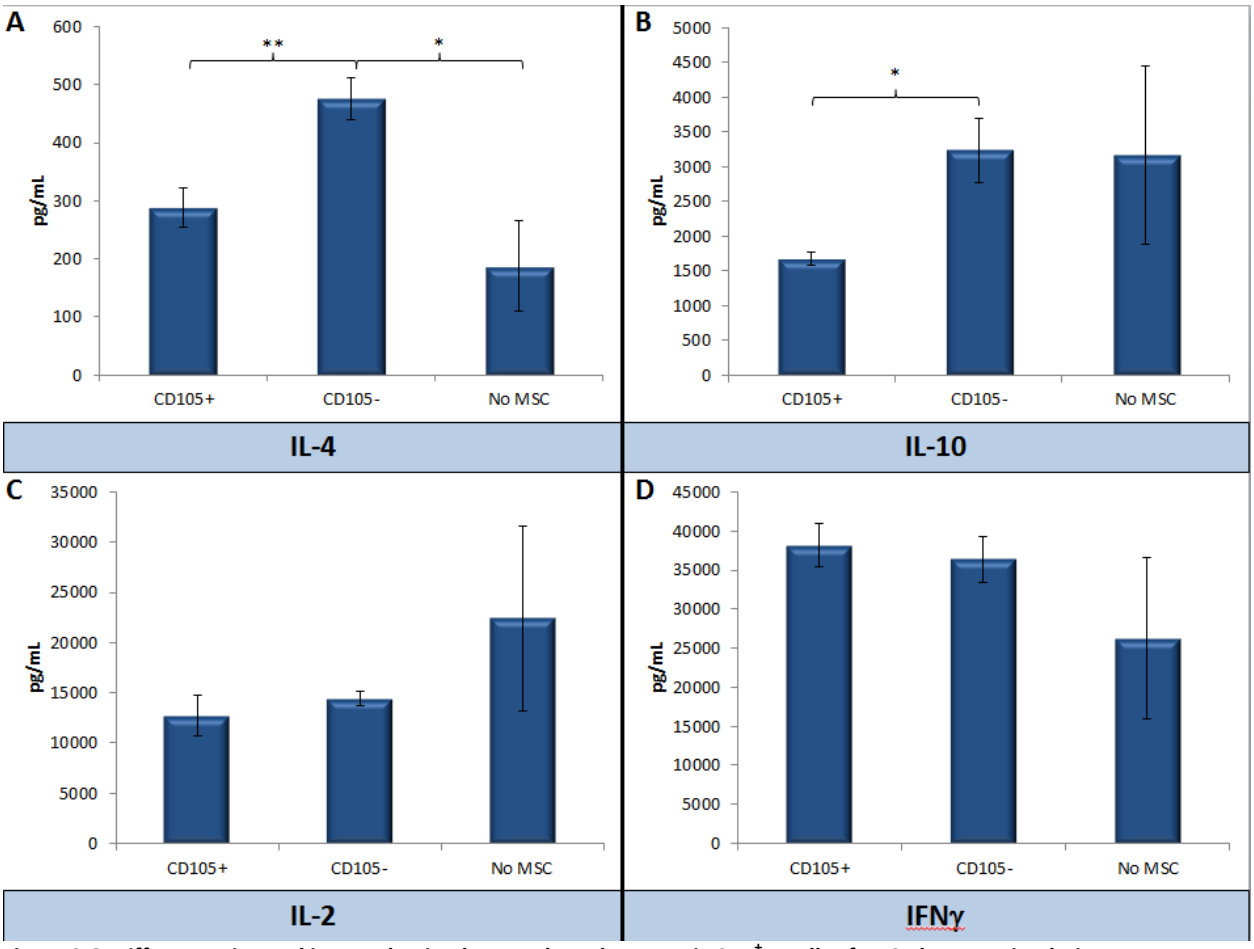

Figure 2.6: Differences in cytokine production by co-cultured syngeneic CD4$^+$ T-cells after 24 hour restimulation
Values represented as means±SEM. **(A) IL-4 Production**: In the syngeneic context, CD105$^+$ MSCs produced significantly less IL-4 (288.01±34.49pg/mL) compared to their CD105$^-$ counterparts (476.16+35.80pg/mL) ($p<0.01$). Differences between the MSC-cohort and the cohort without MSCs (187.60±78.23pg/mL) only reached significance in comparison to the CD105$^-$ co-culture group. However, there were numeric differences between the average concentration of the CD105$^+$ groups and the group without MSCs. The higher standard deviation within the non-co-cultured (NCC) syngeneic group could account for the lack of statistically significant differences between NCC controls and all MSC-containing co-cultures. **(B) IL-10 Secretion**: Within the syngeneic group, CD105$^+$ MSCs produced significantly less IL-10 (1675.21L±98.69pg/mL) compared to their CD105$^-$ counterparts (3237.29±458.95pg/mL) ($p<0.02$). Differences between the MSC-cohort and the NCC cohort (3166.88±1278.35pg/mL) did not have significant differences in IL-10 production. However, this may be due to the high standard deviation of the differentiated CD4$^+$ T-cells that were in the NCC group. **(C) IL-2 Production**: The syngeneic CD105$^+$ group demonstrated less IL-2 production (12740.9±2055.79pg/mL) than their CD105$^-$ counterparts (14385.15±729.06pg/mL), though this did not reach statistical significance. While both MSC-containing syngeneic groups did produce less IL-2 than the NCC controls, these results also did not reach statistical significance. This could, in part, be due to the high standard deviation of NCC group. (22425.9±9211.10pg/mL). **(D) Quantification of IFNγ:** Both CD105$^-$ co-cultures produced less than their CD105$^+$ correlates in both the syngeneic and allogeneic context, with 38194.49±2771.01pg/mL for the syngeneic CD105$^+$ and 36363.60±2953.92pg/mL for CD105$^-$ co-cultures. Surprisingly, all co-cultures resulted in increased IFNγ production when compared to their NCC controls, with only 26279.04±10260.43pg/mL produced from the C57BL6/J derived T-cells. **(n=4)**

Characterization of Differentiated Allogeneic CD4$^+$ Cells

The characterization of syngeneic CD4$^+$ differentiation in the presence of CD105$^{+/-}$ MSCs was distinctly novel. However, to address the role of allogeneic factors in this newly documented

immunomodulation, the same assays described above were repeated using splenocytes from C3H/HeJ mice. Surprisingly, they produced significant differences for several of the factors examined. In Figure 2.7, the results of the mRNA quantification and analysis can be found.

Figure 2.7A displays the data for Th2-associated factors created by the differentiated splenocytes. Here, the pattern observed in the syngeneic model is reversed, where $CD105^-$ MSC co-cultures creates a numerically higher upregulation of the Th2-associated factors. With the exception of IL-5, these allogeneic $CD105^-$ co-cultures produced more Th2-indicative cytokines than their $CD105^+$ counterparts, but these did not reach significance. Additionally, the CD105- co-cultures consistently and dramatically produced statistically significant variation from the NCC controls ($p<0.05$ and $p<0.005$). This suggests that the Th2 phenotype is more pronounced in the allogeneic co-cultures, particularly in the absence of CD105 expression on the MSCs. In these expression assays, the allogeneic co-culture group also produced consistently higher numeric upregulation in the fold changes of these Th2-promoting factors compared with their syngeneic counterparts.

Unlike the cells gathered from the syngeneic co-cultures, the $CD105^-$ allogeneic cells had statistically significant differentiation toward a Treg phenotype (Figure 2.7B), as indicated by the slight upregulation of FoxP3 ($p<0.05$). While the pattern of IL-10 production is consistent between syngeneic and allogeneic models, IL-10 expression is increased in the $CD105^-$ allogeneic context compared to the syngeneic. Additionally, the allogeneic upregulation of IL-10 reached statistical significance in both MSC co-culture groups compared to NCC controls ($p<0.005$). Since IL-10 is also a Th2-associated factor,[101] it is unsurprising that this pattern is similar to those for IL-4.

The data for Th17-associated factors can be found in Figure 2.7C. The allogeneic co-cultures downregulated expression of all Th17-associated factors. In the examination of RORC and IL-22, a different pattern emerges, where the $CD105^-$ allogeneic group comparatively produces the greatest decrease in expression. The allogeneic $CD105^{+/-}$ comparisons only reached significance for the

downregulation of IL-22. IL-22 is the only factor that had a compounding, statistically significant variation from the NCC controls in their downregulation for both MSC co-culture groups ($p<0.005$). Comparisons of IL-17a expression show a different pattern in this allogeneic analysis. While the allogeneic $CD105^{+}$ cells express the IL-17a mRNA to a lesser extent than the $CD105^{-}$ cells, neither of these values reached significance compared to NCC controls. These differences did become significant, however, between the $CD105^{-}$ syngeneic and allogeneic co-cultures.

As seen with the Th17 panel in Figure 2.7C, IL-23R shows downregulation in the allogeneic cultures compared to upregulation in the syngeneic context. Expression levels were similar in comparison of the $CD105^{+/-}$ co-cultures for IL-23R, with differing levels that did not reach significance. While all MSC-co-cultures did upregulate Tbx21 to some degree, it did not follow a pattern that was consistent with any other factor examined. IFNγ, however, was consistently downregulated in all MSC-co-cultures. The allogeneic groups produced the most downregulation, though there was no correlation with $CD105^{+/-}$ between syngeneic and allogeneic cultures. These results only reached significance in their comparison of IFNγ production from the NCC controls ($p<0.05$). A summary table of this information may be found in Table 2.2

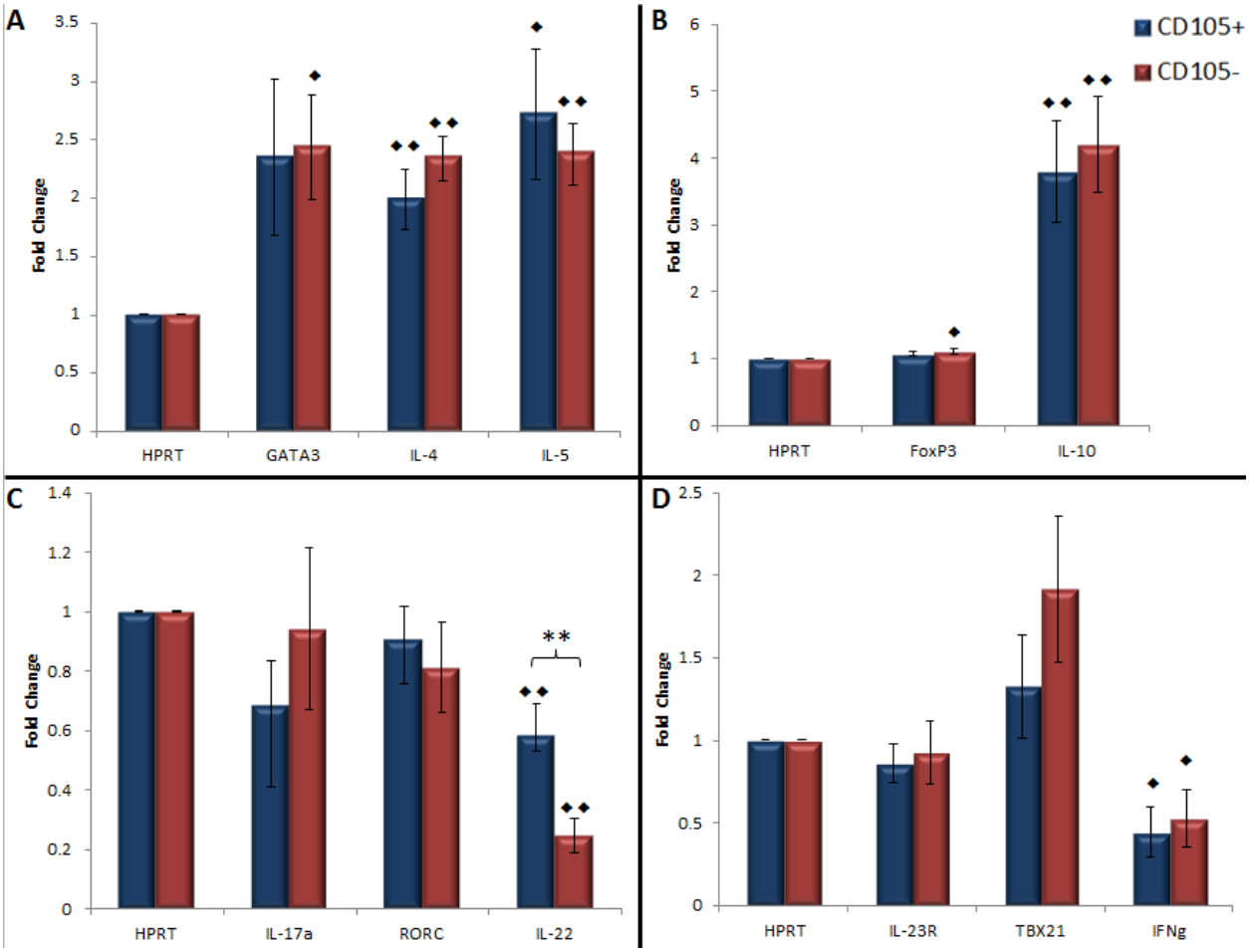

Figure 2.7: Differentiation of $CD4^{+}$-splenocytes after co-culture with allogeneic $CD105^{+/-}$ MSCs
Values are represented as means±SEM. **(A)** Comparison of transcription factors associated with the promotion of a Th2 phenotype after differentiation cultures**.** All of the MSC co-culture groups produced more Th2-associated factors when normalized to controls. With the exception of IL-5, the $CD105^{-}$ group demonstrated a slight increase in these factors compared to their $CD105^{+}$ counterparts, but these did not reach significance. The $CD105^{-}$ co-culture produced an upregulating effect for IL-4 and IL-5 by 2.34±0.19 and 2.37±0.26, respectively. This suggests that the Th2 phenotype is more pronounced in these allogeneic co-cultures, particularly in the absence of CD105 expression on the MSCs. **(B)** Comparison of Treg-associated transcription factors after differentiation cultures. Slight upregulation of FoxP3 was found to be significant in $CD105^{-}$ co-cultures ($p<0.05$). However, each co-culture condition upregulated the expression of IL-10. The greatest effect was seen in the allogeneic $CD105^{-}$ group (4.20±0.71-fold change) which had a statistically significant difference from the syngeneic $CD105^{-}$ co-culture (2.14±0.71-fold change) ($p<0.005$). **(C)** Comparison of pro-inflammatory, Th17-associated factors after differentiation cultures. All allogeneic co-cultures downregulated the expression of each Th17-associated factor. Statistically significant differences in IL-17a were seen between the $CD105^{-}$ syngeneic and allogeneic co-cultures, both downregulating by 0.26±.07 and 0.94±0.27-fold, respectively ($p<0.05$). For IL-22 and RORC, a different pattern emerges, where the $CD105^{-}$ allogeneic group comparatively produces the greatest decrease in expression (0.24±.05-fold and 0.81±0.15-fold, respectively). The allogeneic $CD105^{+/-}$ comparisons only reached significance for the downregulation of IL-22 ($p<0.005$). **(D)** Comparison of Th1-associated proinflammatory factors after differentiation culture. For both IL-23R and IFNγ, a pattern of downregulation for both co-cultures is apparent. While IFNγ was suppressed by all co-cultures, Tbx21 (which controls IFNγ expression) was upregulated. None of these results reached statistical significance. The $CD105^{-}$ culture group produced slight increases in expression for each of the Th1-associated factors, but none of these reach significance. ⬥indicates that the fold-change is significant compared to the non-co-cultured controls, $p<0.05$. ⬥⬥indicates a significance factor of $p<0.005$. ** indicates a $p<0.005$ between a $CD105^{+}$ and $CD105^{-}$ group**. n=8 for allogeneic cultures**

Table 2.2: Summary of allogeneic expression changes relative to NCC controls.
These are the data from co-cultured $CD4^+$ C3H/HeJ-derived splenocytes with $CD105^{+/-}$ MSCs and assayed for differentiation. Red arrows indicate that changes were significant ($p<0.05$).

Factor	$CD105^+$	$CD105^-$
FoxP3	▲	▲
GATA3	▲	▲
IFNγ	▼	▼
IL-4	▲	▲
IL-5	▲	▼
IL-10	▲	▲
IL-17a	▼	▼
IL-22	▼	▼
IL-23R	▼	▼
RORC	▼	▼
Tbx21	▲	▲

Cytokine Production by Differentiated Syngeneic Co-Culture Products

Performed in an identical fashion to the secreted cytokine assay above, the fresh supernatant from the allogeneic differentiation assays was subjected to a Th1/Th2 ELISA characterization experiment, wherein the factors IFNγ, IL-2, IL-4 and IL-10 were quantified in the control and experimental groups. For the Th2-cytokines IL-4 and IL-10, the same pattern emerged that was

ascertained from the data of the syngeneic group. However, these results were significantly more dramatic than their syngeneic $CD105^{+/-}$ correlates ($p<0.005$ between $CD105^{+}$ syngeneic and allogeneic, and $p<0.05$ for $CD105^{-}$). As visible in Figure 2.8A, all experimental groups that were co-cultured with MSCs produced a greater amount of IL-4 than the stimulated controls. Both $CD105^{+/-}$ allogeneic co-cultures produced significantly more IL-4 than the NCC controls. This correlation was predicted by the mRNA expression data.

A similar pattern became apparent for the production of IL-10 by these differentiated $CD4^{+}$ cells (Figure 2.8B). However, the production of IL-10 by the allogeneic group is more dramatic than their syngeneic counterparts ($p<0.005$). Allogeneic $CD105^{-}$ co-cultures produced more IL-10 than their $CD105^{+}$ correlates, but these did not reach significance. Both allogeneic groups produced significantly more IL-10 than the NCC controls ($p<0.05$ for $CD105^{+}$ and $p<0.005$ for $CD105^{-}$). $CD105^{-}$ MSC co-cultures appear to shift the differentiation of these $CD4^{+}$ splenocytes to the more tolerant Th2 phenotype more efficiently than their $CD105^{+}$ correlates: an effect that is most consistent in the allogeneic context.

In Figure 2.8C, the comparative concentrations of IL-2 produced from these co-cultures can be examined. The $CD105^{+}$ co-cultured cells in both syngeneic and allogeneic groups followed a different pattern than would be predicted for a Th2-associated type. In the allogeneic setting, the $CD105^{+}$ co-cultured cells exuded significantly more IL-2 than any other population, including the NCC controls. The allogeneic $CD105^{-}$ co-cultured cells, however, did follow the expected pattern of producing less IL-2 than all other co-culture groups, though this did not reach significance.

For the quantification of IFNγ in Figure 2.8D, there were patterns similar to the syngeneic group surrounding CD105 expression, namely: the absence of CD105 correlated with a decreased production of IFNγ in this allogeneic setting. The allogeneic $CD105^{+}$ co-cultures also produced significantly more IFNγ than their syngeneic correlates ($p<0.05$). Here, differences between secreted IFNγ from the $CD105^{+}$ co-cultures and the NCC controls from C3H/HeJ mice reached significance. This pattern was

unanticipated as compared to the NCC controls, but the expression of CD105 as a factor for determining IFNγ production was predicted by the expression analyses documented in Figure 2.7D.

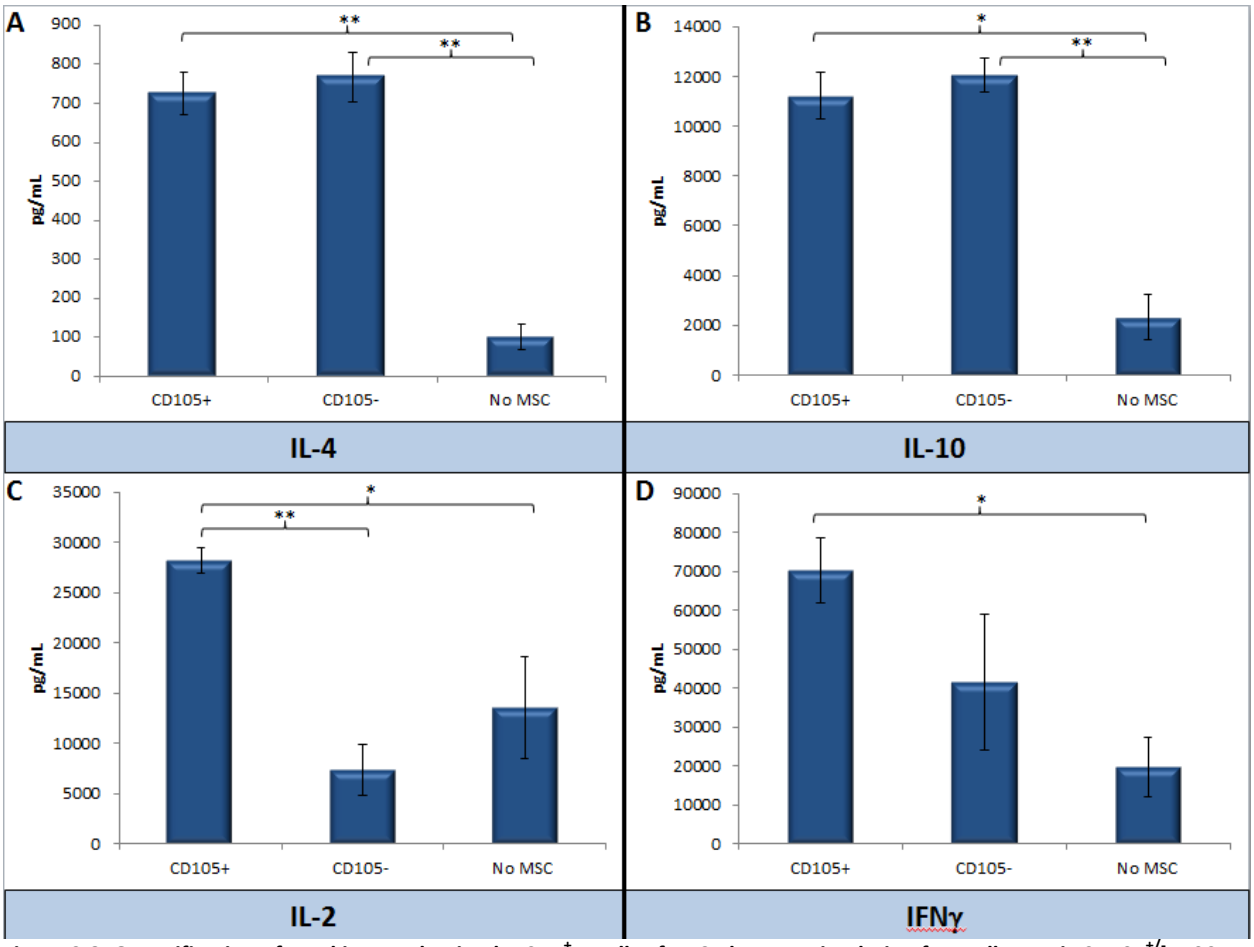

Figure 2.8: Quantification of cytokine production by $CD4^+$ T-cells after 24 hour restimulation from allogeneic $CD105^{+/-}$ MSC co-cultures

Values represented as means±SEM. **(A) IL-4 Production**: the allogeneic co-cultures did not display significant differences in IL-4 production between the $CD105^+$ and $CD105^-$ cohorts, though the amount from the $CD105^-$ co-culture contained a higher numeric average of produced IL-4 (767.94±63.83pg/mL) than the $CD105^+$ (725.44±53.58pg/mL) group. However, both MSC-co-cultured groups created significantly more IL-4 production than the corresponding syngeneic groups ($p<0.01$). Additionally, both allogeneic co-cultures produced significantly more IL-4 than their counterparts without MSCs (101.12±31.52pg/mL) ($p<0.0005$). **(B) IL-10 Secretion**: there were no significant differences between the $CD105^+$ and $CD105^-$ cohorts. However, both MSC-co-cultured groups created significantly more IL-10 than the corresponding syngeneic groups, with 11231.25±964.66pg/mL and 12057.29±659.68pg/mL for $CD105^+$ and $CD105^-$ co-culture groups, respectively ($p<0.0005$). Additionally, both allogeneic co-cultures produced significantly more IL-10 than their counterparts without MSCs (2328.54±906.21pg/mL) ($p<0.0005$). **(C) IL-2 Production**: statistically significant differences between the $CD105^+$ (28189.07±1262.47pg/mL) and $CD105^-$ (7357.3±2492.81pg/mL) co-cultures were found ($p<0.001$). The $CD105^+$ allogeneic cohort, surprisingly, produced significantly more IL-2 than the cultures that were not incubated with MSCs (1355.35±5020.49pg/mL) ($p<0.05$). Comparison of the syngeneic and allogeneic groups for $CD105^{+/-}$ expression did yield significant differences ($p<0.001$ and $p<0.05$, respectively). **(D) Quantification of IFNγ:** allogeneic co-cultures produced more IFNγ than both the syngeneic cultures and the NCC samples, at 70379.81±8404.86pg/mL and 41521.16±17354.67pg/mL for $CD105^+$ and $CD105^-$, respectively. These values reached statistical significance in the $CD105^+$ syngeneic vs. allogeneic comparison ($p<0.05$). All co-cultures resulted in increased IFNγ production when compared to their NCC controls, with only 19587.28±7671.95pg/mL produced from differentiated $CD4^+$ T-cells from C3H/HeJ mice. These values only reached significance between the allogeneic $CD105^+$ and NCC groups ($p<0.005$). **(n=4)**

DISCUSSION

The syngeneic T-cell suppression models that this study sought to replicate and apply in an allogeneic context for examining the effect of CD105 expression on MSCs were performed by *Anderson et al*. [3] The previous model, however, had some methodological differences that could potentially explain the inconsistencies in our results. In the previous studies, the greatest concentration of $CD105^{+/-}$ MSCs was plated at a ratio of 1 MSC for every 40 splenocytes. Despite this, they were able to produce a significant reduction in their proliferation index. However, these studies used only anti-CD3 at a low concentration of 1μg/mL for stimulation in the soluble phase. The methods described in our study were unable to produce stimulation without both anti-CD3 and anti-CD28 being plate-bound (Figure 2.1). Since the proliferative index is calculated based upon a control group which lacks the experimental variable to suppress proliferation (in these cases, MSCs), perhaps the reported values in the previous study are, in fact, comparable to the percent-divided that were reported in this study. However, the dose-response was still inconsistent. Alternatively, the induction of proliferation used in this study could potentially have overcome the suppressive effect of our MSC dosage. Some groups have even reported a necessary 100:1 ratio of MSCs:T-cells in order to suppress growth.[102]

One very interesting finding of this study is the seemingly stimulatory effect of all MSC-groups upon the allogeneic $CD8^+$ T-cell population. MSCs have been shown previously, even in an allogeneic system, to produce inhibition of $CD8^+$ cell proliferation.[103] However, this group performed their assays on APC-primed and antigen-specific $CD8^+$ T-cell lines, and concluded that MSCs inhibited proliferation by hampering interactions with antigen-presenting cells. Since this study did not make use of antigen-presenting cells, and used primary T-cells that had not previously been stimulated and maintained in culture, these results are difficult to directly compare.

An alternative idea that might explain the slight stimulation in our $CD8^+$ T-cells is this: the MSCs in these allogeneic cultures are promoting the growth of a specific, modulatory type of $CD8^+$ t-regulatory cell, with the $CD8^+CD28^-$ phenotype. *Liu et al* published findings that purified $CD3^+CD8^+$ T-cells had a greater proportion of $CD8^+CD28^-$ cells after co-culture with MSCs.[104] These $CD8^+CD28^-$ T-cells have shown the capacity to inhibit the proliferation-activated $CD4^+$ T-cell populations in co-culture.[105] Therefore, it is possible that this $CD8^+CD28^-$ population has been so enhanced in co-culture with the MSCs, that it actually is seen as having a proliferative effect on the overall $CD8^+$ co-culture.

The lack of statistically significant differences between $CD105^+$ and $CD105^-$ groups could therefore be explained by the fact that our assays were performed specifically on $CD4^+$ or $CD8^+$ T-cells. The differentiation effects of MSCs in a mixed-splenocyte reaction have been shown to increase the proportion of regulatory T-cell phenotypes,[106] and these cells could, in turn, decrease the overall proliferation of the mixed splenocytes via inhibitory cytokines.

These results have demonstrated that there are significant differences between syngeneic and allogeneic MSC-based differentiation cultures of $CD4^+$ T-cells. Additionally, some of these effects can be correlated to the expression of CD105 on the MSCs in co-culture. The expression data from these co-cultures suggest that the allogeneic setting induces the transcription of more Th2-associated factors, such as GATA3, IL-4, IL-5, and IL-10. Additionally, there were consistent differences seen in the allogeneic $CD105^-$ co-culture groups for GATA3, IL-4, and IL-10, which showed increased transcription of these factors compared to their $CD105^+$ counterparts. However, there were no significant differences or patterns detected in the FoxP3 expression, suggesting that the function of Treg cells and their suppression of Th1/Th17 subtypes[95] were not indirectly involved in the promotion of the Th2 population by means of depleting the other populations. It can therefore be concluded that MSCs themselves, in the allogeneic context, provide a mechanism for promotion of the Th2-phenotype, either by increasing the proportion of these cells directly or by suppressing the growth of Th1/Th17 populations. This is

perhaps a necessary mechanism for self-preservation, by inducing immune-tolerance in these allogeneic settings.

However, while there were differences between $CD105^{+/-}$ syngeneic and allogeneic co-cultures in the Th1 and Th17 expression panels, the pattern was inconsistent in its specific suppression of these subtypes. These factors were not expressed conversely from the Th2-associated factors, which would have indicated a promotion Th2-development by depletion of other Th-types. However, IL-17a, IL-22, IL23R and IFNγ were all downregulated in the allogeneic co-cultures, but there was no correlation in downregulation with the expression of CD105.

To elucidate the significance of the expression data in terms of actual T-cell functionality, the quantification of secreted proteins by the differentiated $CD4^+$ cells was characterized using a Th1/Th2 panel. The results seen in Figure 2.6A for IL-4 production was predicted by, and correlated with, the expression data. IL-10 production also correlated precisely with the expression data in both the syngeneic and allogeneic context. For both IL-4 and IL-10 production, however, the higher standard deviation within the NCC-syngeneic group could account for the lack of statistically significant differences between it and all MSC-containing co-cultures, like those seen in the allogeneic group.

The Th1-cytokine production patterns do not correlate with the expression data. In fact, all MSC-cultures appeared to induce the expression of IFNγ, the hallmark Th1 cytokine.[107] While the $CD105^-$ co-cultures for both syngeneic and allogeneic produced less IFNγ than their $CD105^+$ correlates, the results did not reach significance. The lack of CD105 also proved important for IL-2 reduction in the allogeneic context, but the opposite was true in the syngeneic setting. The production of IL-2 was less in these syngeneic MSC-groups compared to NCC controls, but here, $CD105^-$ demonstrated a greater concentration of IL-2 than the $CD105^+$ co-cultures. The higher standard deviation seen in the Th1-cytokine production by the NCC controls could account for some of the variability in these data.

Perhaps the existence of other Th-subtypes in the differentiation cultures could explain the Th1-associated cytokine-production. Namely, why it does not exhibit the converse patterns created by allotypes and CD105 expression in theTh2-cytokine panels. There has been documented compensatory reactions between Th17 and Th1 subtypes, which show the depletion of one group leads to increased production of the other.[108] Additionally, it is highly improbable that every $CD4^+$ cell was differentiated toward one, specific Th-lineage, and the Th1-cells that remain in these differentiation assays could be responsible for these unpredictable amounts of Th1-associated cytokines.

SUPPLEMENTAL FIGURES & TABLES

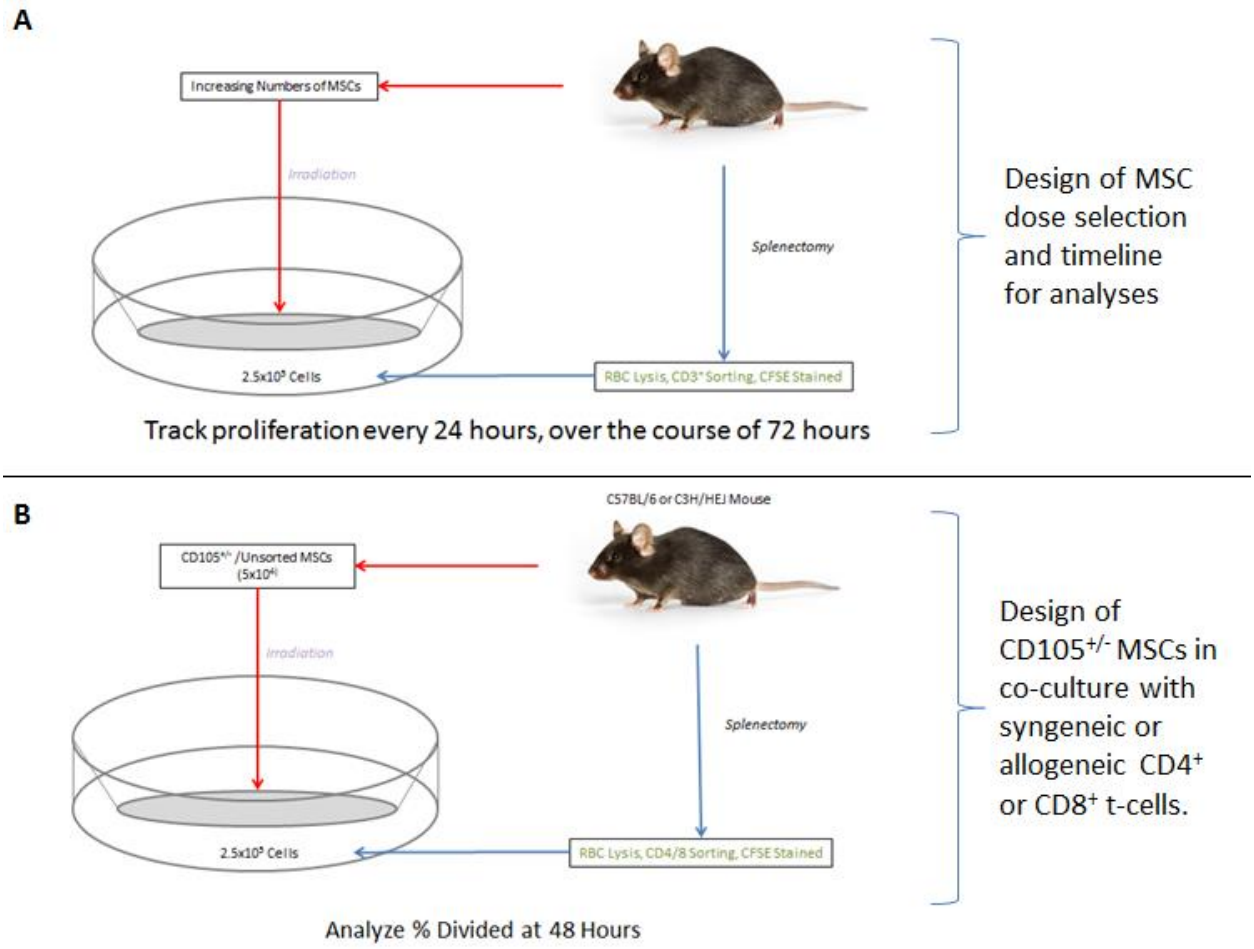

Figure 2.S2.9: Schematic of experimental co-culture designs with MSCs and various splenocyte populations.

Table 2.S2.3 qPCR Primer Sequences for Differentiation Assay. All primers are species-specific to murine cDNA libraries

Factor	Forward (5'->3')	Reverse (5' -> 3')
HPRT	GGC CAG ACT TTG TTG GAT TTG	CGC TCA TCT TAG GCT TTG TAT TTG
IFNγ	GGC CAT CAG CAA CAA CAT AAG	GTT GAC CTC AAA CTT GGC AAT AC

IL-17a	CGC AAT GAA GAC CCT GAT AGA T	CTC TTG CTG GAT GAG AAC AGA A
IL-22	CGA CCA GAA CAT CCA GAA GAA	GAG ACA TAA ACA GCA GGT CCA
IL-23R	GAG CCA GAC AGC AAG TAT GT	CAG TTT CTT GGG AAG TTT GGT G
IL-4	GAA GAA CAC CAC AGA GAG TGA G	TGC AGC TCC ATG AGA ACA C
IL-5	CCC AAC CTT AGC ATC CTT TCT	AGG GAG TTG AGG AGA GAT TGA
IL-10	TGC ACT ACC AAA GCC ACA A	GAT CCT CAT GCC AGT CAG TAA G
RORC	ATC TGG AGG AAG GAC AAC TTT C	CCT AGG GAT ACC ACC CTT CAT A
Tbx21	CCA GGG AAC CGC TTA TAT GT	CCT TGT TGT TGG TGA GCT TTA G
FoxP3	CCC AGT GCC CAT CCA ATA AA	TTC TCC TGC TGG GAT CTT AAA C
GATA3	CTG AGC GCC AAG GAA TCA	AGC AGA CAC GGA GGA ATA AAG

Chapter 3: Impact on Hyperbaric Oxygen on Post-UCB Transplant Transfusion Requirements and Time to Transfusion Independence

ABSTRACT

Limitations in umbilical cord blood (UCB) transplantations originate from decreased cell numbers available for infusion at time of transplant. Delayed engraftment and higher rates of engraftment failure subsequently increase the need for post-transplant transfusion support. Hyperbaric oxygen (HBO) has been shown to improve engraftment in an animal model of UCB transplantation, and these experiments proved sufficient to initiate a first-in-human trial of HBO for UCB transplantation.

This study seeks to evaluate time to packed red blood cell (PRBC) and platelet independence for the HBO study population, and compare to retroactively reviewed UCB transplant data from the same institution. Additionally, it seeks to compare the effects of conditioning regimens, and the number of cord units infused at time of transplant for transfusion independence.

Fifteen subjects underwent HBO therapy at the University of Kansas Cancer Center after reduced intensity conditioning (RIC) (n=9) or myeloablative conditioning (MAC) (n=6) regimens. 6 hours following therapy, they received single (n=8) or double (n=7) UCB units. The patient charts were reviewed for post-transplant PRBC and platelet transfusion requirements. These were compared to standard cord-blood recipient requirements from previous KUCC patients. These were further evaluated between preparative regimens and number of UCB units infused.

Patients who experienced relapse of disease or who expired during the first 100 days were excluded from the quantification of PRBC and platelet unit analyses. They were, however, evaluated to determine if transfusion independence had been reached prior to these events, and included if this was demonstrated in their records.

In the first 100 days, there were no significant differences found in the units of PRBC and platelets required for transfusion support between the HBO and standard groups. The consecutive days of neupogen support post-transplant were consistently fewer for the HBO patients, including analyses

segregated by regimen and number of cords infused. Most significantly, the HBO-group had drastically shorter times to both PRBC and platelet independence. In fact, by days 66 and 74 post-transplant, 100% of HBO-patients were PRBC and platelet independent, respectively. This compares to incomplete platelet (88.63%) and PRBC (86.36%) independence in their standard-transplant counterparts at day 100. While these did not reach statistical significance, it is most likely due to small sample size of the HBO-cohort and their subdivisions. For mechanistic purposes, the HBO-cohort had their erythropoietin levels assessed 8 hours after the HBO-therapy. At present, there has not been a definitive clinical correlation between EPO levels, transfusion requirements, or transfusion independence. The findings demonstrate a previously described increase in EPO levels with myeloablative therapy in contrast to a reduced conditioning regimen.

INTRODUCTION

The use of umbilical cord blood (UCB) for allogeneic hematopoietic stem/progenitor cell (HSPC) transplant has been beneficial for groups that had previously faced limitations based on HLA-requirements, such as racial and ethnic minorities.[109] Clinically, UCB is also associated with a lower incidence of GVHD despite HLA disparity for the recipient.[110] However, there has been documentation of higher rates of engraftment failure for UCB-recipients compared with the recipients of HLA-matched bone-marrow (BM). Patients also have been documented to experience delayed neutrophil and platelet engraftment, complicating the post-transplant course with higher rates of infection and emergent transfusions.[111] This has correlated, and therefore been associated with, decreased numbers of nucleated cells available for transplant in the case of UCB. [110, 112, 113] To resolve this, several groups have focused on the expansion of UCB-HSPCs ex-vivo and studying mechanisms of BM-homing.[114] It has been noted that a population of repopulating HSPCs loses its *in vivo* capacity when cultured briefly with stimulatory cytokines.[115] This has held true for HSPCs of different origins, including UCB-derived HSPCs in a NOD/SCID mouse model.[116]

Therefore, it would perhaps be more clinically useful to enhance the homing of the HSPCs, such that the lower starting numbers available in UCB would translate to a higher probability of engraftment *in* vivo. The mechanism of BM-homing for $CD34^+$ HSPCs has been extensively studied, but remains elusive in many aspects. It has been proposed that the expression of cell-surface molecules, including very late antigen (VLA)-4, VLA-5, C-X-C Motif Chemokine Receptor (CXCR)4, and B2-integrins expressed on $CD34^+$ cells, are important for interacting with marrow stromal cells to increase homing in the hematopoietic niche.[115] The maintenance of this specific $CD34^+$ phenotype is therefore important to ensure that transplanted cells reach their destination in the host marrow.

Erythropoietin (EPO) is an endogenous factor that has demonstrated the capacity to influence HSPC growth and differentiation toward an erythroid lineage.[117] In neonatal studies, circulating HSPCs decline in a manner that correlates with lower serum EPO concentration.[118] It was therefore hypothesized in our previous studies that EPO exposure causes changes in the homing capacity of HSPCs. We proved that there was a decrease in stromal-cell derived factor 1 (SDF-1)-driven migration of UCB-$CD34^+$ HSPCs when the EPO/EPO-receptor signaling pathway was induced. This was rescued by the inhibition of the EPO/EPOR signaling pathway.[119]

Since Hyperbaric Oxygen (HBO) has proven to decrease circulating levels of EPO in healthy subjects,[120] HBO was employed to induce an *in vivo* murine model for the reduction of EPO signaling in UCB-transplant. This demonstrated that myeloid, B-cell, and T-cell engraftment is enhanced compared to control mice. There were differences in early kinetics of UCB-$CD34^+$ cell distribution.[121]

These data were sufficient to conduct a first-in-human trial of HBO treatment for patients undergoing UCB-HSPC transplant. The primary aims were for evaluating the safety of HBO in the context of treatment for HSPC transplant, with secondary aims for efficacy to compare rates of engraftment and blood count recovery. This study is a comparison of the requisite transfusion support for these patients during the first 100 day-course in their transplant recovery.

METHODS

Patient Selection

The study was approved by the institutional review board at the University of Kansas Medical Center (KUMC) prior to initiation, and was registered at clinicaltrials.gov (NCT02099266). At the University of Kansas Cancer Center, fifteen patients with acute myeloid leukemia (AML) or acute lymphoblastic leukemia (ALL) who required HSPC transplant were consented according to Human-Subject Committee approved study number 13601 to undergo hyperbaric oxygen treatment. Given the increased risk for pulmonary complications in patients with severe pulmonary disease undergoing HBO, patients were excluded if they had a history of severe COPD or history of spontaneous pneumothorax.

Hyperbaric Oxygen Treatment

After a signed written consent, patients in the HBO-cohort were subjected to 2 hours of 100% oxygen at 2.5 ATM following their reduced intensity conditioning (RIC) (n=9) or myeloablative conditioning (MAC) (n=6) regimens. Patients rested during this time in a supine position in the transparent hyperbaric chamber while monitored by the hyperbaric medicine team. Six hours after the commencement of treatment with HBO, patients received either single (n=8) or double (n=7) units of UCB. They were monitored for adverse events and severe adverse events as a result of the HBO, in addition to standard-of-care post-transplant supportive treatment and monitoring. A schematic of the HBO treatment can be seen in supplemental figure S1. EPO levels were measured in these patients both before, and 8 hours after HBO treatment.

Chart Review

The fifteen patients of the HBO-cohort had their charts reviewed by research staff to collect the following data: demographic data including age, gender, and race/ethnicity of the subjects. In addition, transplant-related data include: date of transplant, preparative regimen (reduced intensity or

myeloablative), number of cord units (single or double), degree of HLA matching of each unit, donor chimerism on day +30, +60, +100, +180, and +365 post-transplant, date and cause of death, and date of relapse. Data was also collected on their post-transplant transfusion and growth factor requirements. The numbers of supportive platelet/packed red blood cell (PRBC) units required were tabulated, along with the time to transfusion independence (TTI) for both categories of blood products. The consecutive days of granulocyte-colony stimulating factor (G-CSF), also known as neupogen, support was also noted. These variables were obtained for the second group needed for comparison: UCB-recipients at the same institution, which underwent transplant between the years 2008 and 2014. (n=45)

Statistical Analysis

For these comparisons, Kaplan-Meier survival curves were used, Differences between HBO versus controls were determined using the log-rank test. Some of the observations were right-censored. For subjects with a value of 0, a small quantity (0.1) was imputed to facilitate including these subjects in the analyses. For determining significance, data were compared between the HBO and control groups using a two-tailed student's T-test.

RESULTS

HBO Tolerance and Exclusions

There were no adverse events or severe adverse events that were determined to be a result of the HBO during the follow-up period of 100 days for this study. Patients who experienced either relapse of disease or who expired during the first 100 days were excluded from the quantification of PRBC and platelet unit analyses and TTI calculations. They were, however, evaluated to determine if transfusion independence had been achieved prior to these events, and included if this was demonstrated in their records.

The means of the summative data for this study can be found in Table 3.1. Table 3.2 reports the median values for each of the transfusion and growth factor parameters measured.

Table 3.1: Comparison of means between HBO and standard historic patients according to preparative regimen and number of UCB units infused for transplant.

Group	Mean PRBC Units	Mean Platelet Units	Mean Days G-CSF Support	Mean TTI - PRBC	Mean TTI - Platelets
HBO-total (n=15)	9 (p=0.30)	16.35 (p=0.31)	29.4 (p=0.08)	32.87 (p=0.07)	33.53 (p=0.11)
Standard-Total (n=44)	9.29	17.14	35.02	56.09	54.8
HBO-Ablative (n=6)	5.43 (p=0.23)	7.86 (p=0.16)	26.63 (p=0.07)	24 (p=0.53)	25.5 (p=0.45)
Standard-Ablative (n=23)	11.93	22.29	35.65	66.13	67.78
HBO-RIC (n=9)	6.13 (p=0.66)	11.89 (p=0.78)	31.67 (p=0.44)	22.56 (p=0.02)	25.56 (p=0.11)
Standard-RIC (n=21)	7.52	13.71	34.33	45.09	40.57
HBO-Single UCB (n=8)	5.43 (p=0.19)	7.87 (p=0.26)	26.63 (p=0.06)	24 (p=0.06)	25.5 (p=0.06)
Standard-Single UCB (n=4)	10.25	24	36.2	74.4	70.2
HBO-Double UCB (n=7)	12.57 (p=0.87)	24.86 (p=0.95)	33.57 (p=0.70)	43 (p=0.74)	42.71 (p=0.95)
Standard-Double UCB (n=40)	9.19	16.19	34.87	53.74	52.82

Table 3.2 Median values for HBO and standard historic patients according to preparative regimen and number of UCB units infused for transplant.

Group	Median PRBC Units	Median Platelet Units	Median Days G-CSF Support	Median TTI - PRBC	Median TTI - Platelets
HBO-total (n=14)	9	9	29.5	34	30.5
Standard-Total (n=44)	7	16	32	40.5	35.5
HBO-Ablative (n=6)	12	19.5	29.5	51.5	46
Standard-Ablative (n=23)	11.5	19.5	34	41	41
HBO-RIC (n=8)	4	6	28	23.5	25.5
Standard-RIC (n=21)	6	11	31	38	33
HBO-Single UCB (n=7)	4.5	6	27.5	22	25
Standard-Single UCB (n=4)	11	22	37	37	49
HBO-Double UCB (n=7)	11	19	33	46	44
Standard-Double UCB (n=32)	7	13	31	40	35

Supportive Blood Product/Growth Factor Summations

As seen in Figure 3.1, the mean values of PRBC and platelet units were consistently lower from a numeric standpoint for all comparative categories for the HBO-cohort. The exception was found in the number of platelet units required for HBO patients in the setting of double cord-blood recipients. Differences in means most likely did not reach significance due to the small sample size of the HBO-cohort. Since HSPC-transplant recipients have specialized transfusion requirements after transplantation to deter alloimmunization to HLA-differences, minimizing the number of transfusions is advantageous from a clinical perspective.[122] Therefore, HBO-therapy would be an excellent choice for patients who are already at greater risk for developing immunohematologic consequences from their transplant.

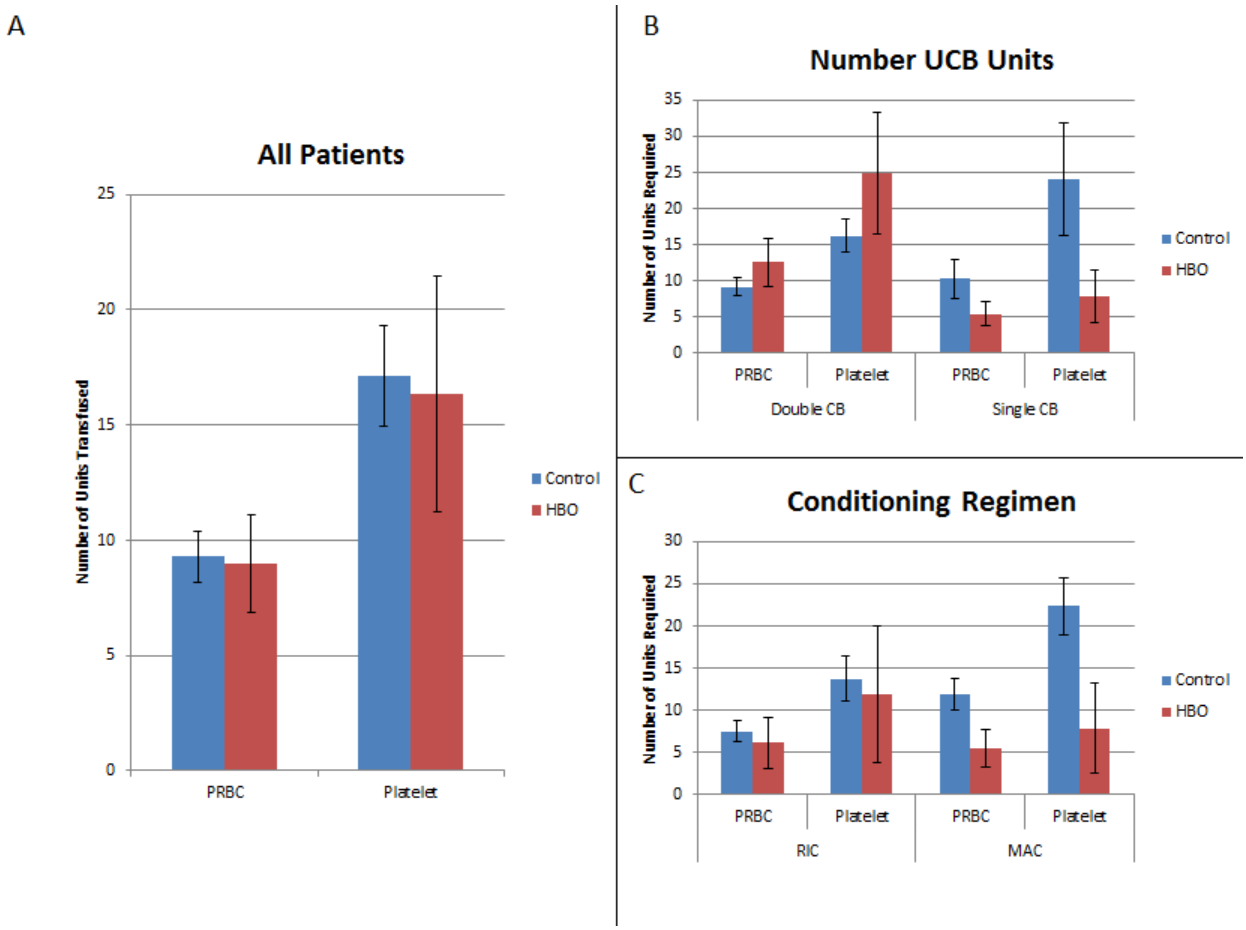

Figure 3.1: Comparison of means for supportive blood product usage in HBO-patients versus controls during the first 100 days post-transplant
Values represented as means +/- standard error. (A) HBO-therapy provides an overall decrease in blood product usage regardless of conditioning regimen or units transplanted. (B) Side-by-side comparison of blood products required as a function of the number of UCB-units infused for transplant for the HBO-cohort and control patients. (C) Side-by-side comparison of blood products required as a function of the pre-transplant conditioning regimen for the HBO-cohort and control patients.

Growth Factor Requirements

Standard of care for patients experiencing neutropenia secondary to their pre-transplant conditioning regimens is the administration of an exogenous growth factor, G-CSF, until neutrophil counts have stabilized above >1000 neutrophils/μL.[123] Decreasing the neutropenic time for these patients post-transplant reduces their risk for developing potentially fatal infections. Therefore, by tabulating the required days of G-CSF support, a comparison between the control UCB-patients and HBO-treated patients may be created. This measure gives information for the performance of the graft.

A graphic representation of the duration of G-CSF treatment for all patients may be found in Figure 3.2. In each stratification of the patient data, the mean values for days of G-CSF treatment are lower for patients in the HBO-cohort, though these results did not reach significance. With the exception of those patients receiving single-cord UCB-transplants (where n=4 of the control data, Figure 2D), the range of days for HBO-patients is less compared to their standard-treatment counterparts.

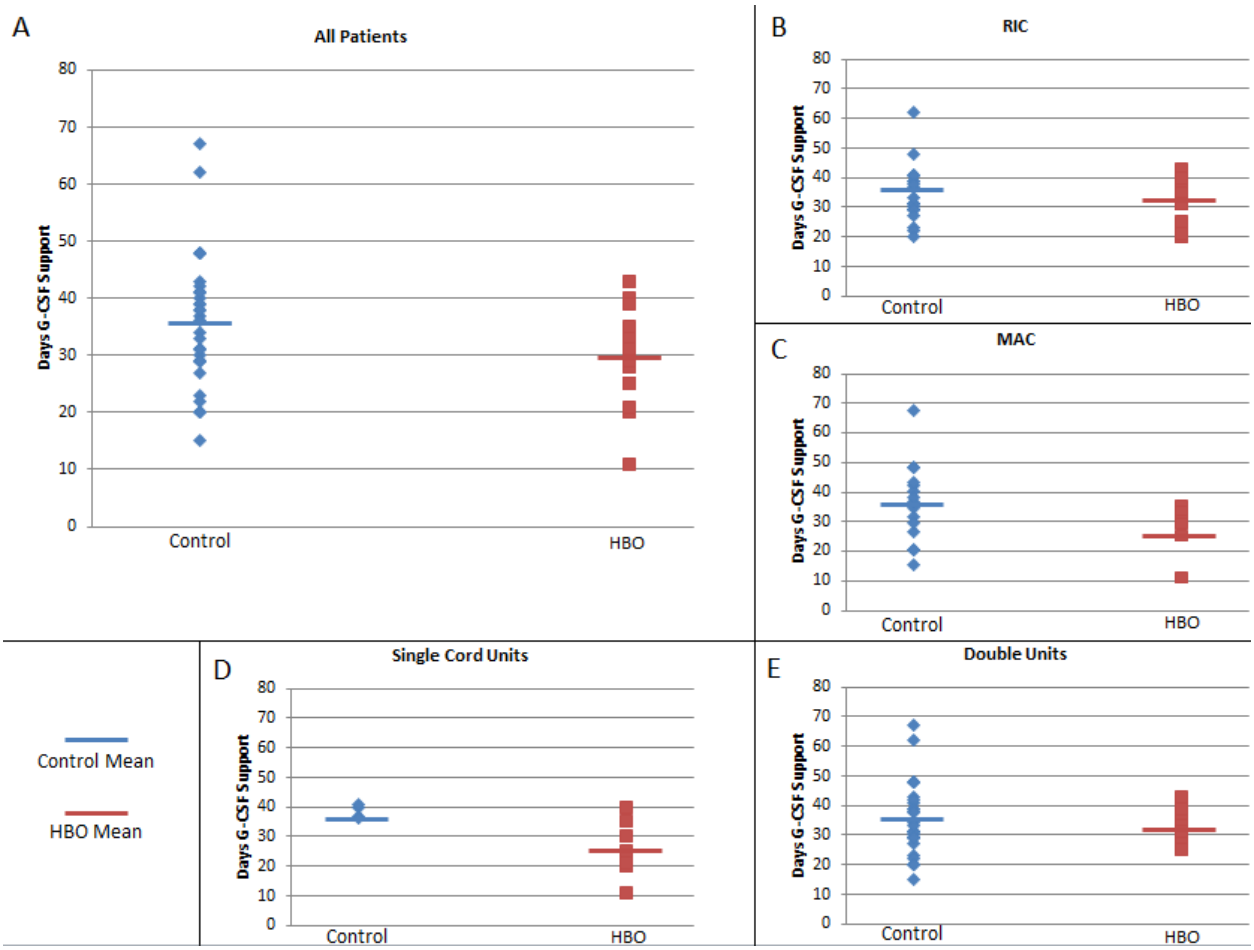

Figure 3.2: Comparative quantification of G-CSF support required post-UCB transplant
Each point represents an individual patient's requisite duration of treatment (days). Means are represented by bars – the values of which are tabulated for comparison in table 1. (A) Days of G-CSF support for all UCB-recipients, comparing HBO-treated patients with controls. (B) Comparison of control and HBO-patients who underwent reduced intensity conditioning. (C) Duration of G-CSF treatment for HBO-patients versus control, who underwent myeloablative conditioning. (D) Days of G-CSF support for patients who received single-cord infusions of UCB for transplant and (E) those who received double-cord infusions.

Time to Transfusion Independence

Most notably, patients in the HBO-cohort experienced significantly less time to transfusion independence (TTI) for both PRBC and platelet support than the standard UCB-recipients. TTI for platelets was defined as the day of the last, post-transplant platelet transfusion, with no platelet transfusions in the following seven days. Red blood cell TTI was defined as the day of the last PRBC transfusion with no transfusion in the following thirty days. For visualization purposes, the ratio of patients that were independent by day, compared to the total cohort, can be found in Figure 3.3. In fact, by days 66 and 74 post-transplant, 100% of HBO-patients were PRBC and platelet independent, respectively. This compares to incomplete platelet (88.63%) and PRBC (86.36%) independence in their standard-UCB-transplant counterparts at day 100. For reasons listed above, decreasing the TTI for patients in a post-transplant setting is crucial for minimizing allograft sensitivity.

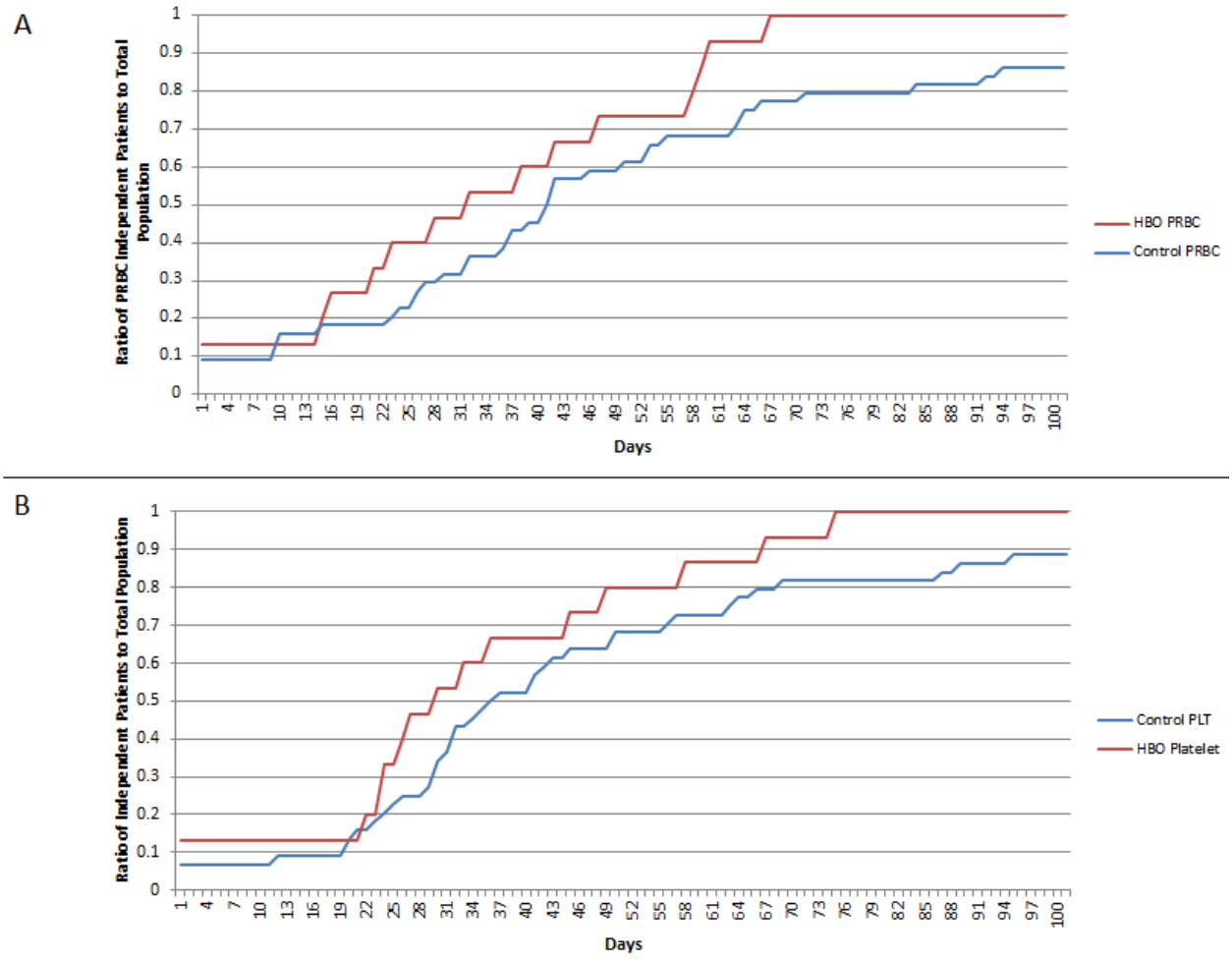

Figure 3.3: Time to transfusion independence for PRBC and platelets in the HBO-cohort, compared to standard UCB-transplant recipients
(A) Depicts the ratio of patients who have achieved PRBC-independence to the total cohort, by day. 100% of HBO patients were independent by day 66 post-transplant compared to incomplete (86.37%) independence by day 100 for standard-UCB recipients. (B) Graphic representation of the ratio of platelet independence for each patient cohort, by day. 100% of HBO patients were independent by day 74, where the standard-UCB recipient patients had incomplete cohort independence by day 100 (88.63%).

Erythropoietin and Mechanism

In our previous studies, the reduction in EPO *in vitro* demonstrated an increase in SDF-1 mediated chemotaxis of UCB-derived HSPCs. Therefore, EPO levels in patient serum were measured before HBO, and 8 hours after HBO, when the UCB-CD34^{+} cells would be actively homing to the bone marrow. Levels of EPO were reduced in all patients after HBO. The previously-described trend of MAC producing higher levels of endogenous EPO than RIC patients was observed, and can be found in Figure

3.4. However, there was no correlation between the serum levels of EPO, the units of PRBC/platelets required for supportive care, or TTI for PRBC/platelets (data not shown).

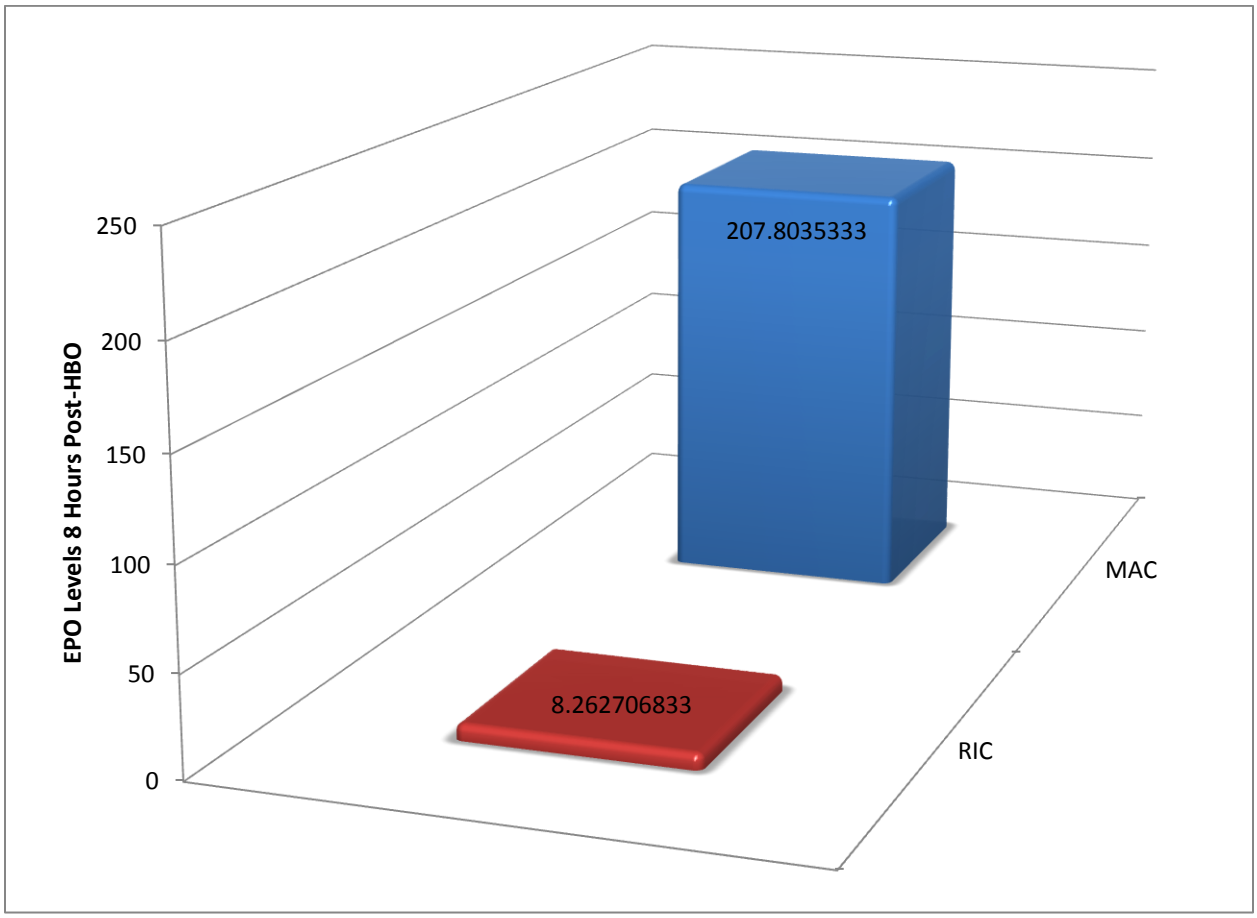

Figure 3.4: Comparative mean erythropoietin levels of patients in the HBO-cohort
Data is stratified by pre-transplant conditioning regimen. Levels of EPO were measured eight hours after HBO treatment.

DISCUSSION

The use of hyperbaric oxygen for aiding in HSPC transplant is a novel approach to improve bone-marrow (BM) homing of HSPC, and is of particular importance in the context of UCB transplants, where reduced $CD34^+$ numbers are available in the graft. HBO is a generally safe and well-tolerated therapy, with the most common risks being sinus and middle-ear barotrauma (2% of cases). [124] The only absolute contraindication to date for HBO is untreated pneumothorax. HBO-chambers are widely available in large academic medical centers globally, due to their use for emergent treatments in the instances of carbon monoxide toxicity and decompression sickness.[125]

In the case of HSPC transplant, it is noteworthy that these patients have a comparatively heavy pharmaceutical load at the time of transplant. However, concern that there might be a pharmacodynamic exacerbation of adverse drug events is mostly unfounded. In fact, no synergistic effect of pulmonary toxicity for bleomycin patients undergoing HBO therapy has been documented.[126] HBO has also mitigated the cardiotoxic effects of doxorubicin in a rat model of concurrent HBO and drug treatment. [127] While there may be some rare free-radical trauma associated with oxygen toxicity,[128] a single treatment of HBO that improves engraftment and minimizes the necessary supportive post-transplant care should be investigated.

The results for this study, at present – did not reach significance. This is most likely due to the small sample size of the HBO-cohort. The addition of more patients to this study will provide interesting insights for HBO therapy's effect on the post-transplant supportive transfusion requirements in these UCB-recipients. Most noteworthy in this study, however, was the fact that there was no correlation with the level of EPO in patient serum with any of the following metrics for improved clinical outcomes: the quantitative numeration of blood products received, the TTI, or the days of G-CSF support.

Previously, our group reported an inverse correlation between circulating levels of EPO and BM-homing of UCB-$CD34^+$ cells in mice. HBO increased the amount of UCB-$CD34^+$ cells present in the bone-

marrow after transplant – an effect that was mitigated by a post-HBO "rescue" dose of EPO.[119] It stands to reason, then, that the EPO levels in these human subjects should correlate to better engraftment. The serum levels of EPO were indeed transiently reduced immediately after HBO therapy; markers of engraftment such as neutrophil, platelet, and RBC recovery were improved compared to the historic controls (but did not reach significance). However, these did not correlate directly with EPO levels, or even a metered reduction in serum EPO. Therefore, while EPO has shown to play a mechanism in homing, it is possible that there are other physiological factors on a multi-organ-system-level that respond to HBO and aid in HSPC engraftment.

It has been demonstrated that there is a necessary polarized domain on $CD34^+$ cells to interact with the BM-microenvironment.[129] Specifically, CD82 is needed for osteoblastic adhesion, but CXCR4, VLA-4, and CD44 are also important on the $CD34^+$ HSPC for insertion into the BM-hematopoietic niche. Future studies for the mechanism of HBO-induced engraftment could target its specific effects on the regulation of these specific co-markers for this homing-capable population of $CD34^+$ HSPCs.

It is important to note that since HBO is a global therapy for *in vivo* models, there are other critical interactions, both in the vasculature and within the BM-microenvironment, which could shape the progress of HSPC engraftment. Within the marrow itself, HBO has shown to significantly treat transient BM-edema in the femoral head compared to controls.[130] In this same context of wound healing, HBO has attenuated inflammation and apoptosis in areas of ischemia, and has been shown to decrease neutrophil extravasation from blood vessels.[131] The attenuation of inflammation could feasibly increase the available $CD34^+$ HSPC available for engraftment: particularly in the case of UCB cells, where the required degree of HLA-matching is not as stringent.[109]

HBO can also affect another critical component of the BM-microenvironment: the mesenchymal stem cell (MSC). MSCs have been documented to provide an array of supportive factors within the hematopoietic niche.[61, 132] The effects of HBO on MSCs have been studied in the context of ischemic

injury repair, for which both HBO and MSC-therapy have been individually employed.[133] Via Wnt-signaling, HBO also increases the differentiation of MSCs into an osteogenic lineage.[134] Therefore, it is entirely possible that this crucial interaction between MSCs and HSPCs in the BM-microenvironment is improving homing and engraftment in the HBO model. Further *in vitro* studies of the immunomodulatory capacities of MSCs when subjected to HBO are currently underway to determine if this is a factor that contributes to the improved engraftment seen in our model.

SUPPLEMENTAL FIGURES

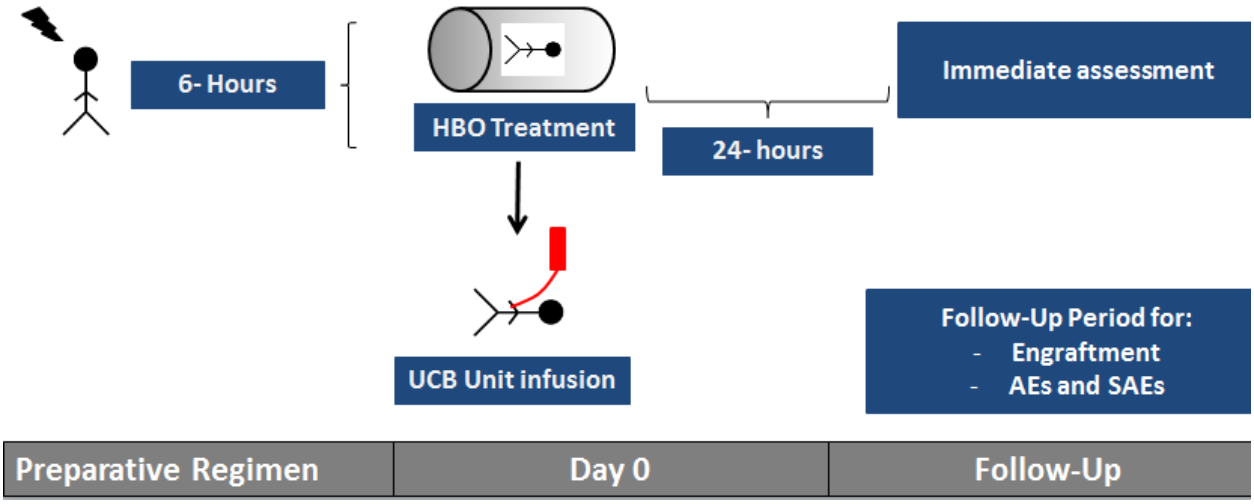

Figure 3.S3.5: Schematic of HBO Treatment

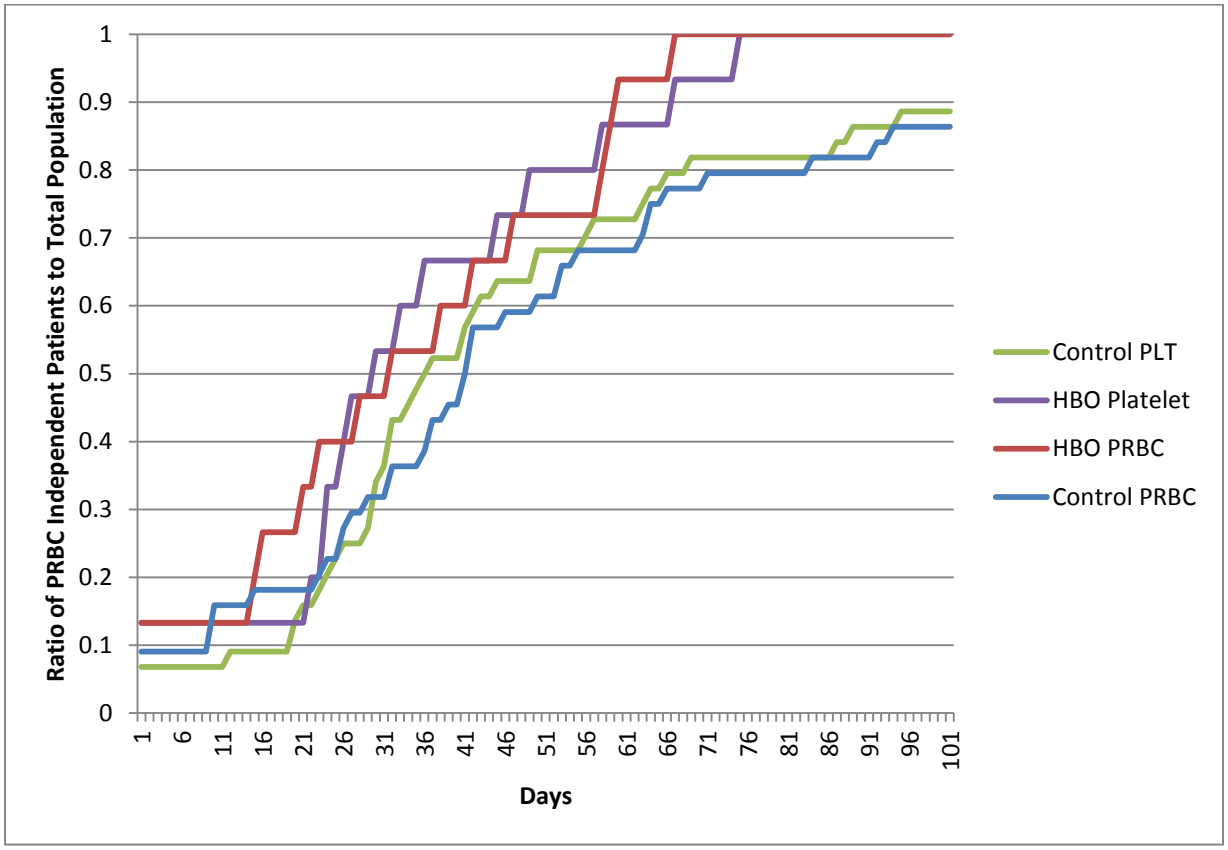

Figure 3.S3.6: All data for time to transfusion independence from HBO-clinical study

Chapter 4: A Brief Examination of Hyperbaric Oxygen on Mesenchymal Stem Cells and the Relation to CD105 Expression

ABSTRACT

The clinical use of hyperbaric oxygen (HBO) has been proven to improve clinical outcomes in HSPC-transplant. The correlation of these outcomes by post-transplant transfusion requirements to levels of erythropoietin did not replicate previous findings in animal data. Therefore, the manipulation of the immunomodulatory factors produced by mesenchymal stem cells (MSCs), a component in the hematopoietic niche, was examined. Differences between the functionality of $CD105^{+/-}$ MSCs have also been documented. Because of the relationship between CD105 expression and tissue oxygen tension, this study sought to examine how HBO affects the expression of CD105 in various MSC-populations and any correlative changes of selected immunomodulatory factors produced by these MSCs.

MSCs were procured from mouse bone marrow, sorted for their CD105 expression, and exposed to HBO. Expression analyses were performed before HBO-treatment, immediately following treatment, and 12 and 24 hours after treatment. Transcriptional changes in CCL2, CD105, IL-6, iNOS, PTGES, and TGFβ were assessed by qPCR after HBO treatment and normalized to controls. MSCs were subsequently procured from a human Wharton's Jelly source and subjected to identical treatments and qPCR analyses. These WJ-MSCs also had their CD105 surface expression tracked by flow cytometry at the aforementioned time-points.

IL-6 was consistently upregulated immediately following HBO treatment for $CD105^{+/-}$ BM-MSCs and WJ-MSCs. Potential subsequent effects of this upregulation showed increased expression of iNOS, PTGES, and TGFβ at the 24 hour time-point. These effects were exaggerated in the $CD105^{-}$ population compared to $CD105^{+}$ BM-MSCs. This increase in expression was not consistent in the WJ-MSCs, which demonstrated a statistically significant downregulation in PTGES and TGFβ at the 24 hour time-point. The expression of CD105 was consistently upregulated immediately following HBO treatment, followed

by a downregulation to its lowest expression level 12 hours after the termination of treatment. This held for all MSCs regardless of their source or prior CD105 expression, and was confirmed by flow cytometry.

Inconsistencies between the $CD105^{+/-}$ BM-MSCs and the WJ-MSCs may stem from the paracrine effects of the secreted immunomodulatory factors within the cell cultures, or from basic physiologic differences between the cell-source for these MSC populations. However, the consistent downregulation of CD105 may present a mechanism by which MSCs enhance homing of HPSCs to bone marrow, as the decrease corresponds to the window in which HPSC homing occurs.

INTRODUCTION

Hyperbaric Oxygen (HBO) presently has a therapeutic role for the treatment of a variety of conditions, including but not limited to: carbon monoxide poisoning, air embolism, traumatic ischemia, problematic wound healing and other conditions linked to poor perfusion.[128] Most notably, HBO has recently been used to improve the efficacy of bone marrow engraftment in the context of hematopoietic stem/progenitor cell (HSPC) transplant in both animal models and human trials.[119] In this study, both human and animal subjects were subjected to HBO-therapy prior to transplantation, and demonstrated significant improvement of graft performance over time. In the animal models, HBO-therapy was shown to reduce the production of erythropoietin (EPO), which subsequently and causatively led to improved homing of the graft.

However, the human studies indicated that neither the level of EPO nor HBO-induced EPO reduction correlated with need for supportive transfusion care post-transplant, which had been assessed as a marker of graft performance. Moreover, the patients did experience less need for transfusion support after transplant using HBO-conditioning. Therefore, perhaps there are other factors which led to the improved homing and engraftment seen in these patients. Since the entire host was treated with HBO prior to transplant, it is not unreasonable to believe that the HBO-therapy could have caused changes within the bone marrow niche itself that helped improve engraftment in these patients.

There is a cell type that exists within the bone marrow (BM) niche that plays a supportive role in maintaining the HSPC microenvironment: the mesenchymal stem cell (MSC). MSCs have been documented to provide supportive factors within the hematopoietic niche.[61, 132] Additionally, the effects of HBO on MSCs have been studied in the context of ischemic injury repair, for which both HBO and MSC-therapy have been individually employed.[133] Therefore, it is possible that this crucial interaction between MSCs and HSPCs in the BM-microenvironment is improving homing and engraftment in the HBO model.

However, MSCs are varied in source and have inconsistencies within their definitive marker profile.[1] The disparity in these marker profiles has led to the investigation of physiological differences between MSCs and their capacities for self-renewal, differentiation, and immunomodulation.[2, 3] One such marker that has been studied is endoglin (CD105). CD105 is a multifunctional protein with the capacity to modulate members of the transforming growth-factor β (TGFβ) superfamily,[18] and its presence/absence has led inquiries into its capacity to modify this signaling as it relates to the endogenous and therapeutic roles of MSCs.[2, 3] It is noteworthy that CD105 also increases as a response to hypoxia.[135] Therefore, changes in the expression of endoglin on MSCs is likely to change as a result of exposure to HBO - the capacity of that MSC to perform immunomodulatory functions may indeed be altered as a result.

Previously, we have demonstrated that differences in CD105 expression on MSCs play a role in the differentiation of T-cells *in vitro*. The mechanism by which this occurs is still currently under study. However, MSCs have been documented to produce C-C Motif Chemokine Ligand 2 (CCL2)[136], inducible Nitric Oxide Synthase (iNOS)[137] Interleukin-6 (IL-6)[138], Prostaglandin E2 (PGE2)[139], and members of the TGFβ superfamily. [139] There exists a possibility that HBO-therapy can modify the immunomodulatory capacity of MSCs by changing the levels of these secreted factors during the crucial homing-window of HSPC transplant. Therefore, by examining the effects of HBO on these factors, and any resultant correlations with the expression of CD105, insight into how HBO changes the BM-microenvironment will be ascertained in this study.

METHODS

Murine BM-MSC Isolation

The method for murine BM-MSC isolation can be found in Chapter 2: Methods, under MSC Isolation.

Flow Cytometry Based Sorting for $CD105^{+}/CD105^{-}$ BM-MSC populations

The method for sorting of these BM-MSC populations can be found in Chapter 2: Methods. The BM-MSCs in this study were subjected to experimental variables between passages 7-10.

Human Wharton's Jelly-MSC Isolation

Wharton's Jelly MSCs (WJ-MSCs) are isolated from human umbilical cord segments following an IRB approved-informed consent process. Potential donors were expectant mothers between 38-42 weeks in gestation and have negative viral serology for Human Immunodeficiency Virus Type 1 & 2, Hepatitis A, B and C, HTLV 1 & 2, Treponema pallidum, Chlamydia trachomatis and Neisseria gonorrhea. Donors who meet these criteria were consented to donate the umbilical cord from their parturition. Following birth, donated umbilical cords are placed in cool 1x-phosphate buffered saline (1xPBS) containing 100 IU/mL of penicillin and 100 µg/mL of streptomycin (Cellgro) and stored at 4°C until transfer to the laboratory.

To process the donated cord, the tissue is thoroughly washed with the same antibiotic/PBS mixture used for transport, in order to remove traces of blood and minimize potential bacterial contamination. The cord is cut into small segments and washed in sterile PBS, supplemented with a greater antibiotic concentration of 200 IU/mL of penicillin and 200 µg/mL of streptomycin (Cellgro). The cord sections are then opened such that three blood vessels can be removed. The clean cord is then minced with sterile scissors into 2- to 3-mm fragments and incubated in xeno-free, serum-free media

(Miltenyi), to permit cellular migration and extravasation from the tissue and adhere to the tissue culture dish.

WJ-MSC migration and adherence to the tissue culture plates occurs over a 2-3 week period. Following the migration of WJ-MSCs out of the umbilical cord, cord tissue is removed and the cells are allowed to expand to approximately 80-90% confluency, at which time they are harvested using TrypLE (ThermoFisher Scientific) and are ready for expansion. The cultures are expanded to Passage 5, increasing the number of available WJ-MSCs approximately 1300-fold. Cells recovered from Passage 5 are counted and stored in liquid nitrogen until use for the hyperbaric oxygen assays.

Hyperbaric Oxygen Treatment of MSC Groups

Both BM-MSCs and WJ-MSCs were cultured for 2-3 passages following recovery from the frozen state. The cells were then plated into T-75 tissue culture flasks. Once the confluence of these passaged cells reached 70-80%, one set of the MSCs were harvested for a pre-treatment comparative control. The remaining MSCs were treated with 100% O2 for 2 hours at 2.5 ATM. To control for the influence of temperature change and hypocarbia, control plates were incubated in room air adjacent to the HBO-chamber for the same duration of time. Cells were harvested for mRNA and protein immediately following treatment (Time 0) and at 12 and 24 hours following the termination of the HBO treatment.

Flow Cytometric Analysis of CD105 Expression

WJ-MSCs were harvested before HBO treatment and at the experimental time points listed above. 5μL of FITC-conjugated anti-CD105 was added to $1x10^6$ cells for each of the control and treatment groups for the identification of $CD105^+$ cells. Using BD FACS Diva software, MSCs were gated for the appropriate size and the doublet-fraction was excluded. An example of the creation of these gates can be found in Figure 4.2A. Using unstained controls for each sample, a histogram gate was

created for determining the percentage of $CD105^{+}$ cells in the sample. These results were tabulated and compared for significance using a student's t-test.

Isolation and Quantification of mRNA

The method for RNA isolation and cDNA conversion can be found in Chapter 2: Methods. Primer sequences for the studies in this chapter can be found in supplemental tables 4.S1 and 4.S2 for mouse and human specific primers, respectively.

The resultant CT values from each of the reactions were normalized using the CT values of hypoxanthine phosphoribosyltransferase (HPRT) as an internal control for the murine cells and Glyceraldehyde 3-phosphate dehydrogenase (GAPDH) for the human cells, creating a ΔCT value for each sample. The $\Delta\Delta$CT was calculated by subtracting the factor-specific ΔCT from time-correlated non-HBO treated controls. The fold change was calculated by the following equation:

$$Fold\ Change = 2^{-(\Delta\Delta CT)}$$

The fold changes for each group were tabulated and analyzed for significance using a student's t-test.

RESULTS

Transcriptional Changes for HBO Treated $CD105^{+/-}$ BM-MSCs

To determine the potential effects of HBO-treatment on BM-MSCs, the sorted $CD105^{+/-}$ experimental groups underwent transcriptional expression analysis via qPCR for the factors: CCL2, iNOS, IL-6, prostaglandin E2 synthase (PTGES; for the production of PGE2), TGFβ1, and CD105. The data were normalized to an internal control (HPRT) and fold change was calculated by use of control samples that were not treated with HBO. The changes in these immunomodulatory factors can be seen in Figure 4.1. Figure 4.1A depicts changes from the $CD105^{+}$ population of cells. There were some differences between the replicates. The first replicate shows increasing fold changes in the 12 and 24 hour time points for iNOS, PTGES, and TGFβ1. The second replicate shows these are upregulated to their highest degree immediately following HBO-treatment (Time 0). However, both consistently show that IL-6 is most prominently upregulated immediately following HBO-treatment. The expression of CD105 for both replicates, however, demonstrates a transient upregulation immediately following HBO-treatment, followed by a downregulation at 12 hours. There were minor and inconsistent changes for CCL2.

The changes in response to HBO-treatment demonstrated by the $CD105^{-}$ MSCs were dramatic compared to $CD105^{+}$ correlates, but there were consistencies in the pattern of CD105 expression over time. While these cells were $CD105^{-}$ by surface marker expression at the beginning of this experiment (data not shown) the transcriptional levels of CD105 transiently increased immediately post-HBO and then decreased to its lowest level at 12 hours, as seen in Figure 4.1B. There was also consistency regardless of CD105 expression for the immediate upregulation of IL-6 post-HBO. This was followed by a downregulation in one of the CD105- replicates. The other replicate did not follow this pattern, showing a marked 17.64-fold upregulation 12 hours after treatment.

However, there were differences in the patterns of expression for iNOS. Figure 4.1C shows the 24 hour transcriptional data for all factors in the $CD105^{-}$ HBO-treated BM-MSCs, such that the intensity

of the fold-changes did not diminish the other data by scale, seen in Figure 4.1B. While the $CD105^+$ BM-MSCs did show iNOS upregulation in one replicate at 24 hours, the $CD105^-$ cells showed a 38.15-fold and a 8.23-fold upregulation in their replicates, which dominates the $CD105^+$ cells' upregulation at 2.45-fold. Similarly, PTGES and TGF$\beta 1$ were dramatically upregulated at the 24 hour time point in both replicates for the $CD105^-$ populations. For all time points, CCL2 did not have drastic or consistent changes, much like the $CD105^+$ groups.

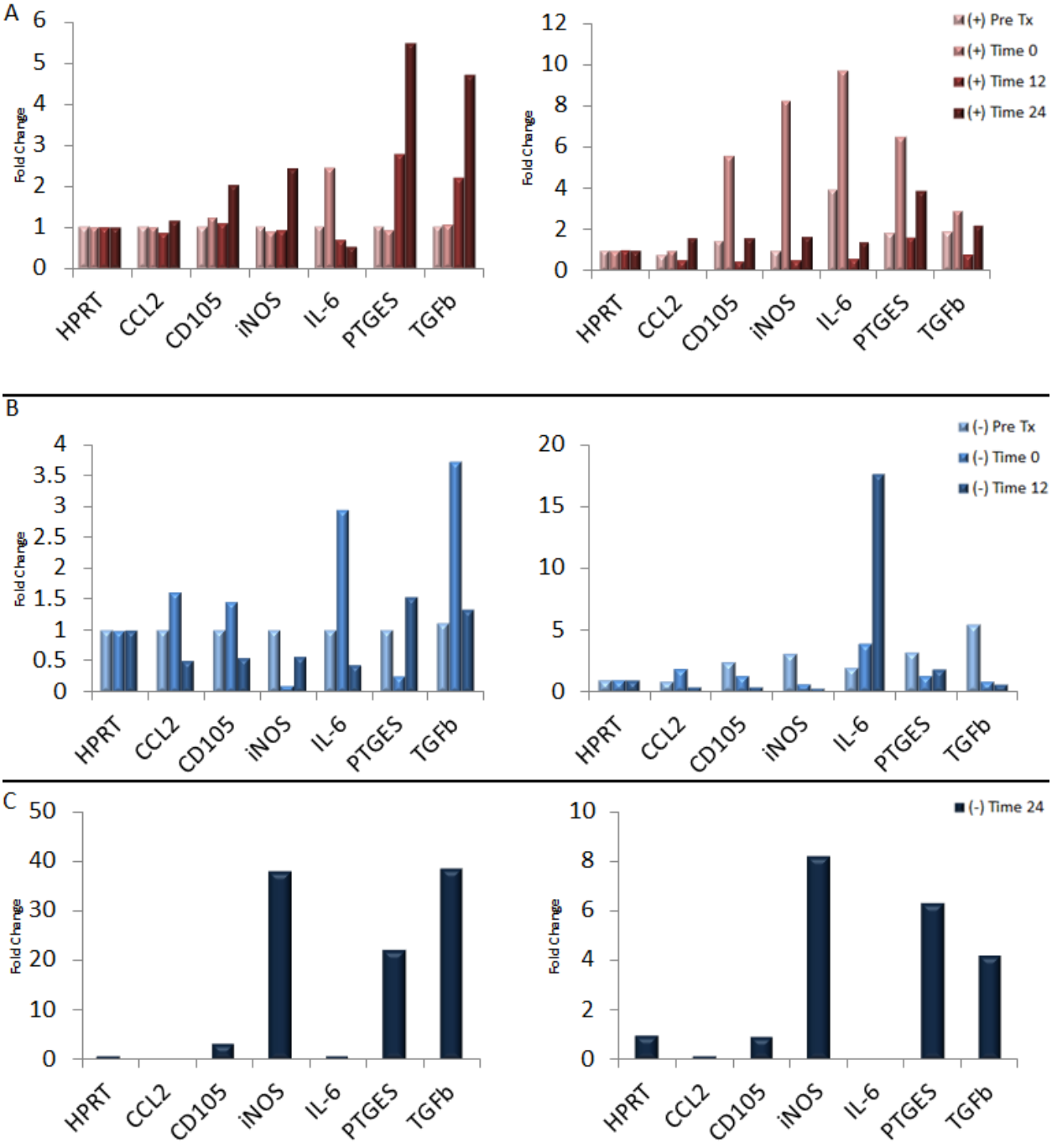

Figure 4.1: Expression data for CD105+/- BM-MSCs treated with HBO

Represented is the qPCR analysis for immunomodulatory factors from HBO-treated BM-MSCs for two separate replicates of the HBO-treatment. **(A)** $CD105^{+}$ BM-MSCs responded to treatment with HBO with factor changes that were consistently upregulated between replicates for PTGES and TGFβ1 at the 24 hour time-point. PTGES was upregulated 5.47 and 3.91-fold, where TGFβ1 changed with a 4.71 and 2.19-fold increase in expression. Both trials also demonstrate a transient increase in CD105 expression immediately post-treatment (1.24 and 5.60-fold at Time 0) followed by a decrease 12 hours later (1.12 and 0.48-fold). These data also demonstrate a consistent increase in IL-6 expression at Time 0 (2.44 and 9.71-fold), which tapers off at later time-points. **(B)** $CD105^{-}$ data are represented here without the 24 hour time-point such that they are not diminished by the necessary increases in scale. Compared with the $CD105^{+}$ cells, there were similar patterns for IL-6 production with a transient increase in expression immediately post-treatment, (2.95 and 3.91-fold) but this pattern does not persist for the replicate depicted on the right, where IL-6 is upregulated by 17.64-fold 12 hours after HBO treatment. The pattern of a transient increase in CD105 expression immediately post-HBO, followed by a downregulation at the 12 hour time point, is

consistent with the $CD105^+$ counterparts in the replicate seen on the left (1.46-fold for Time 0 and 0.55-fold for Time 12). The figure on the right also demonstrates this decrease at 12 hours (0.48-fold), but not the transient increase at Time 0 compared to the pre-treatment sample (1.32 and 2.42-fold, respectively). **(C)** The 24 hour $CD105^-$ HBO treatment expression values are depicted separately such that the scale does not interfere with visualization of the fold-changes of other time points. Similar to the $CD105^+$ cells, the expression of IL-6 normalized for both replicates by 24 hours despite the upregulation seen in earlier time-points (1.02 and 0.08-fold at 24 hours). CD105-expression also increased (3.4-fold) and normalized (0.96-fold) for the replicates depicted on the left and right. This is consistent with the pattern seen between time-points for the $CD105^+$ BM-MSCs. TGFβ1, PTGES, and iNOS all had the most dramatic upregulation in expression at the 24 hour time-point. iNOS increased 38.15-fold for the replicate on the left and 8.23-fold for the right. This compares with mild upregulation for the $CD105^+$ counterparts at 2.44 and 1.66-fold. PTGES was upregulated 22.33-fold and 6.35-fold in these two $CD105^-$ replicates. TGFβ1 expression increased by 38.56 and 4.21-fold for the two trials. Both PTGES and TGFβ show upregulation in $CD105^+$ at the 24 hour time-points, but not to the degree that was seen in the $CD105^-$ cells.

CD105 Expression of WJ-MSCs with HBO Treatment

Since the hyperbaric oxygen clinical study was performed on human subjects, human WJ-MSCs were employed in a similar expression analysis. Using flow cytometry at the following time points: established pretreatment, immediate post-treatment, 12 hours, and 24 hours post treatment, the functional surface expression of CD105 was ascertained from these cell populations. These were compared to non-HBO-treated controls in Figure 4.2. Using gating parameters to isolate the size-appropriate WJ-MSC population (Figure 4.2A), the percent of cells expressing CD105 was assessed. Consistent with the BM-MSC transcription data, WJ-MSCs experience a statistically significant, transient increase in surface CD105 expression immediately following HBO-treatment compared to controls. As seen in Figure 4.2B, the expression of CD105 then diminishes significantly between Time 0 and Time 12, before it normalizes with controls at 24 hours. Differences between the Time 0 treatment group and the pre-treatment cells reach significance in comparison to the 24 hour HBO-treated groups, but not with controls.

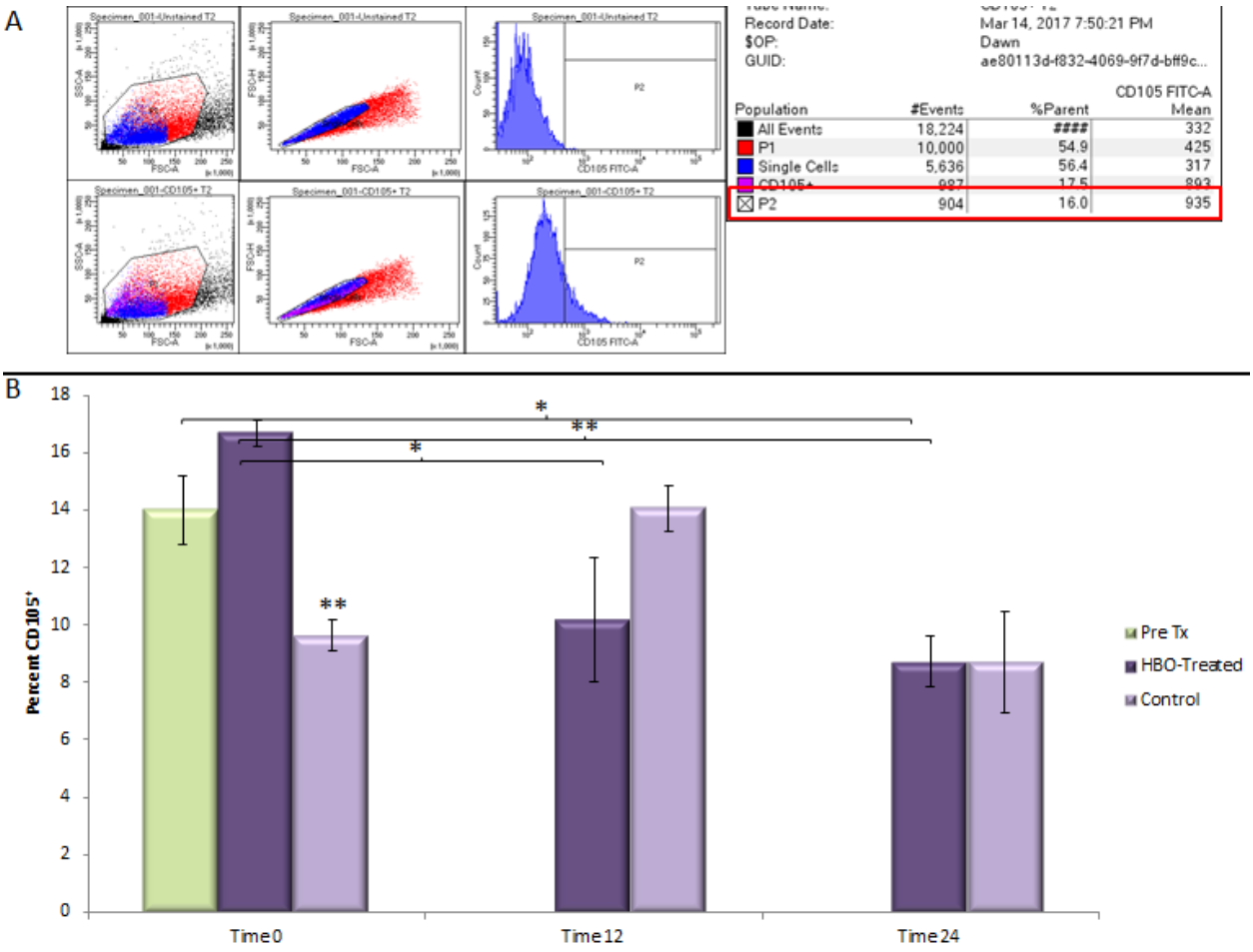

Figure 4.2: Expression of CD105 on WJ-MSCs during the course of HBO treatment assessed by flow cytometry
Values represented as means±SEM. **(A)** Construction of gates for size by SSC-A vs. FSC-A (left), and exclusion of doublets by FSC-H and FSC-A (second from left) isolated the WJ-MSCs for examination of CD105 expression. The top histogram panel demonstrates the creation of a gate (P2) for the demarcation of CD105 expression from an identical sample that was unstained with FITC-conjugated anti-CD105. The bottom histogram panel depicts the same sample stained with antibody. Highlighted in red on the statistics view (right) is the percentage value of the parent population for $CD105^+$ cells. This was tabulated for each sample. **(B)** Graphic representation of CD105 expression at each time point, compared with controls. The pre-treatment group (far left) is indicated by the green color. Statistically significant changes in percent CD105 expression occurred at Time 0 between HBO-treated and control samples at 16.675%±0.46 and 9.65%±0.53, respectively ($p<0.0005$). The decrease of the CD105 also reached statistical significance between Time 0 and both 12 and 24-hours post-treatment with expression of 10.17%±2.18 at Time 12 ($p<0.05$) and 8.73%±0.87 for Time 24 ($p<0.0005$). The pre-treatment group expressed CD105 at 14%±1.22 which was significantly greater than the HBO-treated group (8.725%±0.87) at the final time-point ($p<0.05$), though the treatment group had normalized to controls by this time post-treatment (8.70%±1.77 for controls). **(n=4)**

Transcriptional Changes for HBO-Treated WJ-MSCs

Compared with the BM-MSC groups, the fold-changes seen in the WJ-MSCs were both smaller in scale and demonstrated different patterns of expression by time-point for several of the observed factors. However, among the factors where patterns were consistent between BM-MSCs and WJ-MSCs

was IL-6, where there was an initial upregulation at the termination of HBO-treatment that subsequently tapers off over time. CCL2 also did not demonstrate consistent or drastic changes in upregulation, as with the $CD105^{+/-}$ BM-MSCs. Interestingly, PTGES and TGFβ1 – which demonstrated prominent expression in both BM-MSC groups at 24 hours, showed a statistically significant downregulation over time in the WJ-MSCs.

The expression of CD105, however, correlated with the BM-MSC transcriptional changes and with the data acquired by use of flow for functional CD105 expression. The transient increase seen in the aforementioned groups was not seen at the Time 0 collection, however, the lowest level of expression was consistently found 12 hours after HBO-treatment. While these did not reach statistical significance, they may have clinical relevance, as discussed in later sections. These data may be found in Figure 4.3.

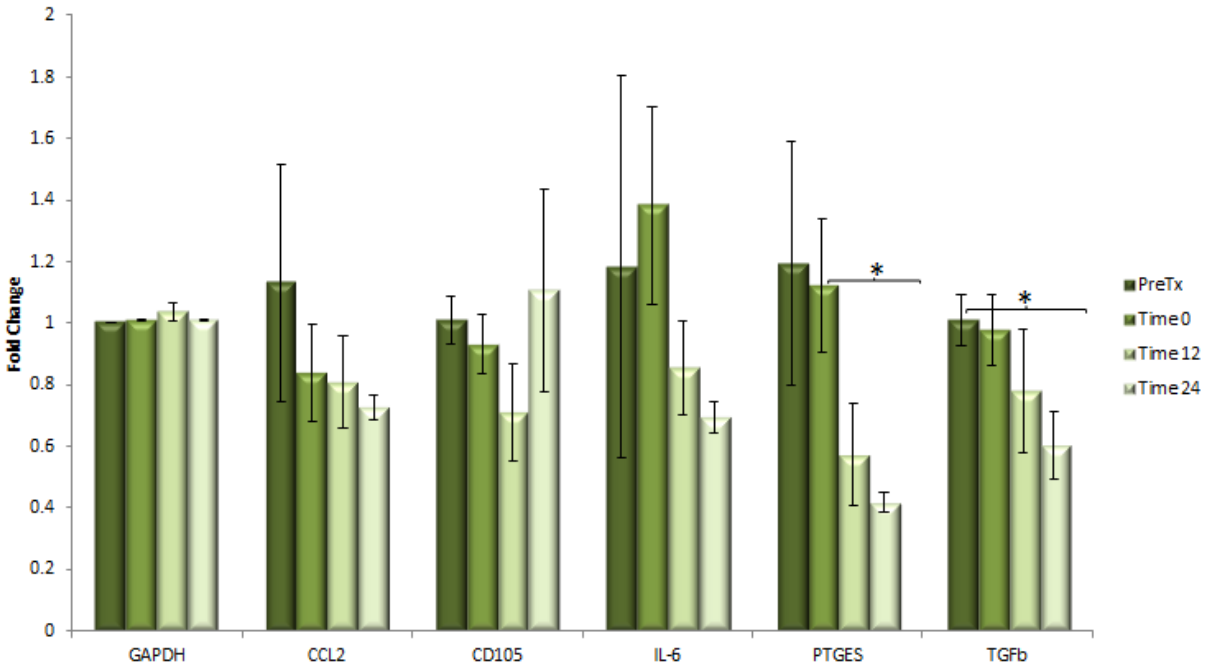

Figure 4.3: Transcriptional changes for HBO-treated WJ-MSCs over 24 hours
Values represented as means±SEM. Treatment of the WJ-MSCs revealed differences in patterns than those from the BM-MSCs with HBO treatment. For the factor PTGES, samples between which differences reached statistical significance were Time 0 (1.12-fold±0.21) and Time 24 (0.41-fold±0.03) ($p<0.05$). The only factor which demonstrated similar significance was for TGFβ1 between the pretreatment group that had very little change in expression (1.01-fold±0.08) and the 24 hour post-treatment group with 0.60-fold ±0.11 change. ($p<0.05$) Similar patterns were seen for CD105 expression in both the active expression by flow (Figure 4.2B) and the HBO-treated BM-MSC experimental groups. The 12-hour time point for CD105 demonstrates the lowest level of expression (0.71-fold±0.15) consistently across all groups with HBO-treatment. **(n=4)**

DISCUSSION

This study provides interesting data comparing the functionality of MSCs from different sources and with varying expression of CD105. Some of the limitations for this study were created by insufficient $CD105^{+}$ BM-MSC numbers, halting the transcriptional analysis for BM-MSCs at only two replicates. However, the patterns demonstrated by $CD105^{+/-}$ BM-MSCs in those two replicates may have some basis in the physiology of these immunomodulatory factors. Since these experiments are concerned with the expression of secreted factors, it is not unreasonable to suspect that these factors have paracrine effects on their neighboring cells, causing changes in their transcription profile. Therefore, the initial transcription changes could have a cascading effect for the subsequent immunomodulatory factors. IL-6 has been documented to induce iNOS, [140] which is consistent across $CD105^{+/-}$ BM-MSC groups. IL-6 is consistently upregulated in response to HBO, either immediately following or 12 hours after treatment, and iNOS follows suit 24 hours later – most dramatically in the $CD105^{-}$ groups.

Interestingly, TGFβ1 has been shown to attenuate iNOS expression in the context of *in vitro* hypoxia-reperfusion models of cardiomyocyte injury. [141] The upregulation of iNOS that may be caused by IL-6 could, in fact, be evoking this drastic TGFβ-response in the BM-MSCs 24 hours after HBO exposure. PGE2, the product of PTGES, also is an enhancing element of TGFβ1 which could be a response to iNOS upregulation. [142] PGE2 could also be causative for the iNOS upregulation, as it has been demonstrated to mediate its presence in the context of breast cancer studies.[143] Therefore, the interplay between these factors could be causing the drastic differences seen in the BM-MSC context. These effects could potentially be exaggerated in the $CD105^{-}$ group, as the lack of endoglin could prohibit the attenuating of TGFβ responses via Smad signaling.[14]

These transcriptional changes were not present in the WJ-MSC treated with HBO. In fact, both TGFβ1 and PTGES demonstrated opposite trends of downregulation at 24 hours. It is noteworthy, however, that there have been studies dedicated to documenting the functional differences between

WJ-MSCs and BM-MSCs in the context of enhancing HSPC transplantation.[144] In this study, they demonstrate that WJ-MSCs have a more suppressive effect than the BM-MSC counterparts on T-cell proliferation. Additionally, co-culture of $CD34^{+}$ HSPCs with BM-MSCs yield more erythroid colonies than WJ-MSCs, which yield more myeloid/granuloid colonies. Therefore, there is a physiologic and functional difference between these cell groups. This is visible even in the baseline, pre-treatment expression data for the WJ-MSCs compared to the BM-MSC populations. In light of these differences, making direct comparisons of the WJ-MSCs and BM-MSCs may not be informative for determining the differences in immunomodulatory factor change with HBO treatment. Additionally, limitations in primer design for human iNOS prohibited the examination of this integral piece that could connect the immunomodulatory factors examined.

This study was novel in its examination of the responsive expression of endoglin to hyperoxia. As stated previously, CD105 is a well-documented hypoxia response element.[135] Here, this study demonstrates that there is a consistent change in the expression of CD105 on MSCs as a result of HBO. Both $CD105^{+/-}$ BM-MSC and WJ-MSCs demonstrate a consistent, transient increase in CD105 expression immediately following treatment, followed by the most significant decrease at 12 hours. This was validated both by flow cytometry and by qPCR. The timeline of CD105 downregulation might be important in the context of using HBO for improving engraftment in HSPC-transplant studies. Our previous clinical study made use of cord-blood derived HSPCs infused 6 hours after the initiation of HBO. Since BM-homing occurs within the first 18 hours after infusion into these irradiated hosts,[129] the timing of CD105 downregulation by MSCs in the hematopoietic bone marrow niche may play a role in the ability of HSPC to home and engraft in these spaces.

To confirm the hypothesized roles of HBO-changes in both MSC-immunomodulation and modification of MSCs in the bone marrow niche, further studies are currently being conducted to

strengthen existing data and explore how these transcriptional changes relate to the expression of their corresponding proteins.

SUPPLEMENTAL TABLES

Table 4.S4.1: qPCR primer sequences for mouse-specific immunosuppressive factors secreted by MSCs

Primer Name	Primer Sequence (5'-3')
Mouse HPRT Forward	GGCCAGACTTTGTTGGATTTG
Mouse HPRT Reverse	CGCTCATCTTAGGCTTTGTATTTG
Mouse iNOS Forward	CAGGGAGAACAGTACATGAACAC
Mouse iNOS Reverse	TTGGATACACTGCTACAGGGA
Mouse CCL2 Forward	TAAAAACCTGGATCGGAACCAAA
Mouse CCL2 Reverse	GCATTAGCTTCAGATTTACGGGT
Mouse IL-6 Forward	CTGCAAGAGACTTCCATCCAG
Mouse IL-6 Reverse	AGTGGTATAGACAGGTCTGTTGG
Mouse TGFβ1 Forward	CTTCAATACGTCAGACATTCGGG
Mouse TGFβ1 Reverse	GTAACGCCAGGAATTGTTGCTA
Mouse PTGES Forward	CACACTGCTGGTCATCAAGAT
Mouse PTGES Reverse	TCACTCCTGTAATACTGGAGGC
Mouse CD105 Forward	AGGGGTGAGGTGACGTTTAC
Mouse CD105 Reverse	GTGCCATTTTGCTTGGATGC

Table 4.S4.2: Human-specific primer sequences for immunosuppressive factors secreted by MSCs

Primer Name	Primer Sequence (5'-3')
Human HPRT Forward	CCTGGCGTCGTGATTAGTGAT
Human HPRT Reverse	AGACGTTCAGTCCTGTCCATAA
Human GAPDH Forward	TCGACAGTCAGCCGCATCTT
Human GAPDH Reverse	GTCTGAGCGATGTGGCTCGG
Human CCL2 Forward	CAGCCAGATGCAATCAATGCC
Human CCL2 Reverse	TGGAATCCTGAACCCACTTCT
Human IL-6 Forward	ACTCACCTCTTCAGAACGAATTG
Human IL-6 Reverse	CCATCTTTGGAAGGTTCAGGTTG
Human TGFβ1 Forward	CTAATGGTGGAAACCCACAACG
Human TGFβ1 Reverse	TATCGCCAGGAATTGTTGCTG
Human PTGES Forward	TCCTAACCCTTTTGTCGCCTG
Human PTGES Reverse	CGCTTCCCAGAGGATCTGC
Human CD105 Forward	CGCCAACCACAACATGCAG
Human CD105 Reverse	GCTCCACGAAGGATGCCAC

Chapter 5: Conclusions and Future Directions

Rationale for Study

The expression of endoglin (CD105) on mesenchymal stem cells (MSCs) has been a subject of study for several groups attempting to identify a more therapeutically beneficial MSC. Because endoglin modulates TGFβ signaling,[18] it has presented itself as a target for several groups that seek to understand and improve the inherent MSC capacities for differentiation[2], self-renewal,[145] and immunomodulation.[3] As members of the TGFβ superfamily are involved in all these processes,[145-147] the modulation of its effect by an endogenous factor like CD105 has provided an attractive candidate for study.

The work for this doctoral dissertation began with evidence from our previous studies that showed $CD105^-$ BM-MSCs provided more effective therapy than unfractionated controls for the maintenance of cardiac function when injected intramyocardially in an ischemia/reperfusion model of infarction. *In vitro* modeling also demonstrated that $CD105^-$ BM-MSCs had a greater propensity to differentiate into cardiomyocytes and form capillaries than unfractionated BM-MSCs. However, the work of *Freyman et al* in the *European Heart Journal* showed in a porcine model that the delivery of MSCs by multiple methods to an infarct only resulted in a maximum of 6% of retained cells.[148] Because of this low retention, the mechanism by which the MSCs were reducing infarct-area fraction could not be solely the regeneration of new tissues. Because MSCs are known for their immunomodulatory capacity, it was hypothesized that the lack of CD105 expression on MSCs contributed to an immunologic milieu that reduced scarring following cardiac injury.

Suppression and Differentiation by $CD105^{+/-}$ MSCs

By this rationale, the work presented in this dissertation attempted to clarify differences in immunomodulation between $CD105^{+/-}$ BM-MSCs. Initially, the short-term goal was to replicate findings

that were reported in the 2013 publication from *Anderson et al*. The work in their paper showed that $CD105^-$ MSCs derived from adipose tissue had a greater suppressive effect on the proliferation of T-cells.[3] In Chapter 2 of this dissertation work, the establishment of a method that resulted in the proliferation of T-cells was accomplished. Factors under consideration to translate these into suppressive assays were: dosage of stimulating antibodies, dosage of MSCs to induce suppression, the benefits of a transwell culture system, and timeframe at which T-cell proliferation was to be assessed. Once these factors were determined, the examination of the suppressive effects of $CD105^{+/-}$ MSCs on $CD4^+$ and $CD8^+$ T-cells was undertaken.

However, as indicated by Figure 2.4, suppressive effects were mild and did not reach statistical significance between the $CD105^{+/-}$ MSC treatment groups for $CD4^+$ syngeneic and allogeneic models. $CD8^+$ cells, in fact, appeared to be stimulated in the allogeneic context. The lack of statistically significant differences between $CD105^+$ and $CD105^-$ groups could be explained by the fact that these assays were performed specifically on $CD4^+$ or $CD8^+$ T-cells. The differentiation effects of MSCs in a mixed-splenocyte reaction have been shown to increase the proportion of regulatory T-cell phenotypes,[106] and these cells could, in turn, decrease the overall proliferation of the mixed splenocytes via inhibitory cytokines.

The next logical step, therefore, was to compare the effects on differentiation for $CD4^+$ T-cells by $CD105^{+/-}$ MSCs in both syngeneic and allogeneic models. The results in Figures 2.5 and 2.6 have demonstrated significant differences between syngeneic and allogeneic MSC-based differentiation cultures of $CD4^+$ T-cells. Additionally, some of these effects can be correlated to the expression of CD105 on the MSCs in co-culture. The expression data from these co-cultures suggest that the allogeneic setting induces the transcription of more Th2-associated factors. There were also consistently documented differences seen in the allogeneic $CD105^-$ co-culture groups for upregulation of these Th-2 factors compared to their $CD105^+$ counterparts. This prominent Th2 phenotype was confirmed by quantification of the secreted factors IL-4 and IL-10, which was significantly greater in the allogeneic

setting and for $CD105^-$ co-cultures. The quantification of IFNγ and IL-2 showing inconsistent results might be due to the timeline of the method for assaying these factors.

Hyperbaric Oxygen and Hematopoietic Stem Cell Transplant

Throughout the course of these explorations into the immunomodulatory effects of $CD105^{+/-}$ MSCs, there was a concurrent novel clinical study for using hyperbaric oxygen (HBO) to improve the transplant outcomes of umbilical cord blood (UCB) recipients. The use of HBO was clinically significant in the reduction of supportive blood-product requirements by these transplant patients as seen in Figure 3.1, which decreased their risk for transfusion-related adverse events. It also decreased the time to transfusion independence (TTI) for both packed red blood cells and platelets in these patients (Figure 3.3). These data correlated to and confirmed the animal models that had been documented by this same group. [119]

In the previous study, HBO-therapy was shown to reduce the production of erythropoietin (EPO) which subsequently and causatively led to improved homing of the graft in these animal models. However, the human studies indicated that neither the level of EPO nor HBO-induced EPO reduction correlated with a need for supportive transfusions in the post-transplant course (Figure 3.4)… Perhaps, then, there were other factors which led to the improved homing and engraftment seen in these patients. Thus, the hypothesis was developed that HBO-therapy could have caused changes within the bone marrow (BM) niche itself that helped improve the engraftment in these patients. MSCs have been shown to provide supportive factors within the hematopoietic niche.[61, 132] The effects of HBO on MSCs have also been studied in the context of ischemic injury repair, for which both HBO and MSC-therapy have been individually employed.[133] Therefore the hypothesis became that the interactions between MSCs and HSPCs in the BM-microenvironment is improving homing and engraftment in the HBO model.

Correlations between CD105 Expression of MSCs and Hyperbaric Oxygen Treatment

By examining the effects of HBO on secreted immunomodulatory factors, and potential resultant correlations with the expression of CD105, some insight was gained on this hypothesis. There were some consistent patterns in secreted-factor expression in the BM-MSC portion of the study between $CD105^{+/-}$ populations (Figure 4.1). However, limitations in these experiments only allowed the production of two replicates. Repetitions of this assay to strengthen these data are included in the future directions for the study. The studies on the human WJ-MSCs did not provide as dramatic or consistent data as the BM-MSC counterparts.

However, studies on the human WJ-MSCs were consistent in the most novel portion of these experiments, which was the examination of the HBO-responsive expression of endoglin. CD105 is a well-documented hypoxia response element.[135] This study demonstrated a consistent, reproducible change in the expression of CD105 on MSCs as a result of HBO. Both $CD105^{+/-}$ BM-MSC and WJ-MSCs demonstrate a transient increase in expression immediately following treatment, followed by the most significant decrease at 12 hours. This was validated in multiple assays, and can be seen in Figures 4.1, 4.2, and 4.3. Since BM-homing occurs within the first 18 hours after infusion into these conditioned hosts,[129] the timing of CD105 downregulation by MSCs in the hematopoietic BM- niche may play a role in the ability of HSPC to home and engraft in these spaces.

Conclusions and Future Work

The picture of CD105 in the mesenchymal stem cell is incomplete, but there are several pieces that would give clarity to its physiologic and potentially therapeutic role. Primarily, a marker profile for which to define the mesenchymal stem cell is necessary. As previously stated, there are contradictory reports regarding the capacity of CD105 as a marker for a sub-set of MSCs with distinct capabilities, because there is such heterogeneity in the population. Additionally, the mechanism by which endoglin

functions to provide these differing MSC capacities should be explored as it has been in other cell types. As the field stands, the characterization of $CD105^+$ versus $CD105^-$ cells is primarily characteristic instead of mechanistic. Discussed here were several papers and our own evidence, commenting on differentiation and functional capacities of these two different cell types, but there was very little decisive, conclusive evidence of how endoglin functions in these contexts. A greater understanding of endoglin's function in TGFβ, BMP signaling, and TGFβ-independent mediated effects should be undertaken in order to explain the variety of phenotypic differences in these two distinct MSC populations.

The studies outlined in Chapter 2, where MSCs affected the differentiation of stimulated $CD4^+$ T-cells, are novel and thorough in their description of this phenomenon. However, there are further avenues through which the mechanism could be explored. All of these studies have generated data from observing changes in the T-cell portion of the co-culture. By the quantification of MSC-secreted factors that drive Th2-differentiation, such as IL-5 and IL-4, it could perhaps illuminate the mechanism by which MSCs influence differentiation. To elucidate the role of CD105 in the secretion of these factors, a direct comparison of $CD105^{+/-}$ cells should be undertaken; wherein an effective siRNA-based CD105-knockdown could be applied.[149] Applying these methods to a $CD105^+$ population would be interesting to determine if the MSCs maintained their distinct differentiation-influencing capacities. These studies would identify CD105-negativity as a primary factor for Th2 differentiation as regulated by MSCs, if this hypothesis is proven by future data.

Additionally, exploring the *in vivo* consequences of increased Th2 differentiation in an allogeneic setting would be a logical subsequent step for investigating this phenomenon. Previously, our group has demonstrated that $CD105^-$ MSCs are more adept at preserving cardiac function than an unfractionated set of MSCs, when injected in areas of reperfused-ischemia. To determine if these cells are accomplishing functional preservation by increasing the number of Th2 cells in the immunologic milieu

after infarct, tissue-sections could be fluorescently stained with antibodies that detect Th2-specific markers. The cells with Th2-indicators could be quantified and compared in syngeneic and allogeneic settings, and with varying endoglin expression. This would correlate *in vivo* functional data with a potential mechanism that does not include direct transdifferentiation of the MSCs themselves. Instead, it would prove that the MSCs are serving as a therapeutic intermediate to help quell reperfusion-based tissue damage.

These experiments and the works of others have barely scratched the surface for the mechanism by which endoglin expression is regulated via HBO. While HBO was shown in clinical trials to be therapeutically beneficial for HSPC transplant patients, the role of CD105 has not been defined. In previous work, HSPCs have had visualized interactions with osteoclasts to explore the osteoclastic role in the BM-niche microenvironment.[150] The application of this technique for exploratory assays using $CD105^{+/-}$ MSCs and HSPCs might give clarity as to their purposes in this setting. Using HBO to determine the part that MSC-regulation plays in the niche, and for the identification of other potential endoglin-modified cell types as a result of HBO-therapy, would also be important future studies.

References

1. Kolf CM, Cho E, Tuan RS. Mesenchymal stromal cells. Biology of adult mesenchymal stem cells: regulation of niche, self-renewal and differentiation. Arthritis research & therapy. 2007;9(1):204.
2. Gaebel R, Furlani D, Sorg H, et al. Cell Origin of Human Mesenchymal Stem Cells Determines a Different Healing Performance in Cardiac Regeneration. PLoS ONE. 2011;6(2):e15652.
3. Anderson P, Carrillo-Gálvez AB, García-Pérez A, et al. CD105 (Endoglin)-Negative Murine Mesenchymal Stromal Cells Define a New Multipotent Subpopulation with Distinct Differentiation and Immunomodulatory Capacities. PLoS ONE. 2013;8(10):e76979.
4. Oconnell PJ, McKenzie A, Fisicaro N, et al. Endoglin: a 180-kD endothelial cell and macrophage restricted differentiation molecule. Clinical & Experimental Immunology. 1992;90(1):154-159.
5. Augustin HG, Kozian DH, Johnson RC. Differentiation of endothelial cells: analysis of the constitutive and activated endothelial cell phenotypes. BioEssays : news and reviews in molecular, cellular and developmental biology. 1994;16(12):901-906.
6. El-Gohary YM, Silverman JF, Olson PR, et al. Endoglin (CD105) and Vascular Endothelial Growth Factor as Prognostic Markers in Prostatic Adenocarcinoma. American Journal of Clinical Pathology. 2007;127(4):572-579.
7. Li C, Guo B, Wilson PB, et al. Plasma levels of soluble CD105 correlate with metastasis in patients with breast cancer. International Journal of Cancer. 2000;89(2):122-126.
8. Yang L-y, Lu W-q, Huang G-w, et al. Correlation between CD105 expression and postoperative recurrence and metastasis of hepatocellular carcinoma. BMC Cancer. 2006;6(1):110.
9. Velasco S, Alvarez-Muñoz P, Pericacho M, et al. L- and S-endoglin differentially modulate TGFβ1 signaling mediated by ALK1 and ALK5 in L6E9 myoblasts. Journal of Cell Science. 2008;121(6):913-919.
10. Venkatesha S, Toporsian M, Lam C, et al. Soluble endoglin contributes to the pathogenesis of preeclampsia. Nat Med. 2006;12(6):642-649.
11. López-Novoa JM, Bernabeu C. The physiological role of endoglin in the cardiovascular system. American Journal of Physiology - Heart and Circulatory Physiology. 2010;299(4):H959-H974.
12. Koleva RI, Conley BA, Romero D, et al. Endoglin Structure and Function: DETERMINANTS OF ENDOGLIN PHOSPHORYLATION BY TRANSFORMING GROWTH FACTOR-β RECEPTORS. Journal of Biological Chemistry. 2006;281(35):25110-25123.
13. Guerrero-Esteo M, Sanchez-Elsner T, Letamendia A, et al. Extracellular and cytoplasmic domains of endoglin interact with the transforming growth factor-beta receptors I and II. The Journal of biological chemistry. 2002;277(32):29197-29209.
14. Barbara NP, Wrana JL, Letarte M. Endoglin is an accessory protein that interacts with the signaling receptor complex of multiple members of the transforming growth factor-beta superfamily. The Journal of biological chemistry. 1999;274(2):584-594.
15. Conley BA, Koleva R, Smith JD, et al. Endoglin controls cell migration and composition of focal adhesions: function of the cytosolic domain. The Journal of biological chemistry. 2004;279(26):27440-27449.
16. Sanz-Rodriguez F, Guerrero-Esteo M, Botella LM, et al. Endoglin regulates cytoskeletal organization through binding to ZRP-1, a member of the Lim family of proteins. The Journal of biological chemistry. 2004;279(31):32858-32868.
17. Muenzner P, Rohde M, Kneitz S, et al. CEACAM engagement by human pathogens enhances cell adhesion and counteracts bacteria-induced detachment of epithelial cells. The Journal of cell biology. 2005;170(5):825-836.

18. Valluru M, Staton CA, Reed MWR, et al. Transforming Growth Factor-β and Endoglin Signaling Orchestrate Wound Healing. Frontiers in Physiology. 2011;2:89.
19. Cuppen E, van Ham M, Wansink DG, et al. The zyxin-related protein TRIP6 interacts with PDZ motifs in the adaptor protein RIL and the protein tyrosine phosphatase PTP-BL. European journal of cell biology. 2000;79(4):283-293.
20. McAllister KA, Grogg KM, Johnson DW, et al. Endoglin, a TGF-[beta] binding protein of endothelial cells, is the gene for hereditary haemorrhagic telangiectasia type 1. Nat Genet. 1994;8(4):345-351.
21. Jonker L, Arthur HM. Endoglin expression in early development is associated with vasculogenesis and angiogenesis. Mechanisms of Development. 2002;110(1–2):193-196.
22. Mancini ML, Verdi JM, Conley BA, et al. Endoglin is required for myogenic differentiation potential of neural crest stem cells. Developmental Biology. 2007;308(2):520-533.
23. Akhurst RJ, Lehnert SA, Faissner A, et al. TGF beta in murine morphogenetic processes: the early embryo and cardiogenesis. Development (Cambridge, England). 1990;108(4):645-656.
24. Qu R, Silver MM, Letarte M. Distribution of endoglin in early human development reveals high levels on endocardial cushion tissue mesenchyme during valve formation. Cell and tissue research. 1998;292(2):333-343.
25. Toporsian M, Gros R, Kabir MG, et al. A Role for Endoglin in Coupling eNOS Activity and Regulating Vascular Tone Revealed in Hereditary Hemorrhagic Telangiectasia. Circulation Research. 2005;96(6):684-692.
26. Garcia-Cardena G, Fan R, Shah V, et al. Dynamic activation of endothelial nitric oxide synthase by Hsp90. Nature. 1998;392(6678):821-824.
27. Ma X, Labinaz M, Goldstein J, et al. Endoglin is overexpressed after arterial injury and is required for transforming growth factor-beta-induced inhibition of smooth muscle cell migration. Arteriosclerosis, thrombosis, and vascular biology. 2000;20(12):2546-2552.
28. Wysocki SJ, Zheng MH, Fan Y, et al. Expression of transforming growth factor-beta1 (TGF-beta1) and urokinase-type plasminogen activator (u-PA) genes during arterial repair in the pig. Cardiovascular research. 1996;31(1):28-36.
29. Thyberg J, Palmberg L, Nilsson J, et al. Phenotype modulation in primary cultures of arterial smooth muscle cells. Differentiation. 1984;25(1-3):156-167.
30. Bourdeau A, Cymerman U, Paquet ME, et al. Endoglin expression is reduced in normal vessels but still detectable in arteriovenous malformations of patients with hereditary hemorrhagic telangiectasia type 1. The American journal of pathology. 2000;156(3):911-923.
31. Matsubara S, Bourdeau A, terBrugge KG, et al. Analysis of endoglin expression in normal brain tissue and in cerebral arteriovenous malformations. Stroke; a journal of cerebral circulation. 2000;31(11):2653-2660.
32. Seghers L, de Vries MR, Pardali E, et al. Shear induced collateral artery growth modulated by endoglin but not by ALK1. Journal of Cellular and Molecular Medicine. 2012;16(10):2440-2450.
33. Sánchez-Elsner T, Botella LM, Velasco B, et al. Endoglin Expression Is Regulated by Transcriptional Cooperation between the Hypoxia and Transforming Growth Factor-β Pathways. Journal of Biological Chemistry. 2002;277(46):43799-43808.
34. Forsythe JA, Jiang BH, Iyer NV, et al. Activation of vascular endothelial growth factor gene transcription by hypoxia-inducible factor 1. Molecular and cellular biology. 1996;16(9):4604-4613.
35. Maxwell PH, Dachs GU, Gleadle JM, et al. Hypoxia-inducible factor-1 modulates gene expression in solid tumors and influences both angiogenesis and tumor growth. Proceedings of the National Academy of Sciences of the United States of America. 1997;94(15):8104-8109.

36. Semenza GL, Wang GL. A nuclear factor induced by hypoxia via de novo protein synthesis binds to the human erythropoietin gene enhancer at a site required for transcriptional activation. Molecular and cellular biology. 1992;12(12):5447-5454.
37. Melillo G, Musso T, Sica A, et al. A hypoxia-responsive element mediates a novel pathway of activation of the inducible nitric oxide synthase promoter. The Journal of experimental medicine. 1995;182(6):1683-1693.
38. LI C, HAMPSON IN, HAMPSON L, et al. CD105 antagonizes the inhibitory signaling of transforming growth factor β1 on human vascular endothelial cells. The FASEB Journal. 2000;14(1):55-64.
39. Fujinaga H, Baker CD, Ryan SL, et al. Hyperoxia disrupts vascular endothelial growth factor-nitric oxide signaling and decreases growth of endothelial colony-forming cells from preterm infants. American Journal of Physiology - Lung Cellular and Molecular Physiology. 2009;297(6):L1160-L1169.
40. Santibanez JF, Letamendia A, Perez-Barriocanal F, et al. Endoglin increases eNOS expression by modulating Smad2 protein levels and Smad2-dependent TGF-beta signaling. Journal of cellular physiology. 2007;210(2):456-468.
41. Paepe MED, Patel C, Tsai A, et al. Endoglin (CD105) Up-regulation in Pulmonary Microvasculature of Ventilated Preterm Infants. American Journal of Respiratory and Critical Care Medicine. 2008;178(2):180-187.
42. Burrows FJ, Derbyshire EJ, Tazzari PL, et al. Up-regulation of endoglin on vascular endothelial cells in human solid tumors: implications for diagnosis and therapy. Clinical cancer research : an official journal of the American Association for Cancer Research. 1995;1(12):1623-1634.
43. Chen F, Hong H, Zhang Y, et al. In vivo tumor targeting and image-guided drug delivery with antibody-conjugated, radiolabeled mesoporous silica nanoparticles. ACS nano. 2013;7(10):9027-9039.
44. Seon BK, Matsuno F, Haruta Y, et al. Long-lasting complete inhibition of human solid tumors in SCID mice by targeting endothelial cells of tumor vasculature with antihuman endoglin immunotoxin. Clinical cancer research : an official journal of the American Association for Cancer Research. 1997;3(7):1031-1044.
45. Takahashi N, Haba A, Matsuno F, et al. Antiangiogenic therapy of established tumors in human skin/severe combined immunodeficiency mouse chimeras by anti-endoglin (CD105) monoclonal antibodies, and synergy between anti-endoglin antibody and cyclophosphamide. Cancer research. 2001;61(21):7846-7854.
46. Chen CZ, Li M, de Graaf D, et al. Identification of endoglin as a functional marker that defines long-term repopulating hematopoietic stem cells. Proceedings of the National Academy of Sciences of the United States of America. 2002;99(24):15468-15473.
47. Begley CG, Green AR. The SCL Gene: From Case Report to Critical Hematopoietic Regulator 1999.
48. Perlingeiro RCR. Endoglin is required for hemangioblast and early hematopoietic development. Development (Cambridge, England). 2007;134(16):3041-3048.
49. Mirabelli P, Di Noto R, Lo Pardo C, et al. Extended flow cytometry characterization of normal bone marrow progenitor cells by simultaneous detection of aldehyde dehydrogenase and early hematopoietic antigens: implication for erythroid differentiation studies. BMC physiology. 2008;8:13.
50. van Dongen JJ, Lhermitte L, Bottcher S, et al. EuroFlow antibody panels for standardized n-dimensional flow cytometric immunophenotyping of normal, reactive and malignant leukocytes. Leukemia. 2012;26(9):1908-1975.
51. Sanchez-Elsner T, Ramirez JR, Sanz-Rodriguez F, et al. A cross-talk between hypoxia and TGF-beta orchestrates erythropoietin gene regulation through SP1 and Smads. Journal of molecular biology. 2004;336(1):9-24.

52. Machherndl-Spandl S, Suessner S, Danzer M, et al. Molecular pathways of early CD105-positive erythroid cells as compared with CD34-positive common precursor cells by flow cytometric cell-sorting and gene expression profiling. Blood Cancer Journal. 2013;3:e100.
53. Chimenti I, Smith RR, Li TS, et al. Relative roles of direct regeneration versus paracrine effects of human cardiosphere-derived cells transplanted into infarcted mice. Circ Res. 2010;106(5):971-980.
54. Tseliou E, Reich H, de Couto G, et al. Cardiospheres reverse adverse remodeling in chronic rat myocardial infarction: roles of soluble endoglin and Tgf-beta signaling. Basic research in cardiology. 2014;109(6):443.
55. Toma C, Pittenger MF, Cahill KS, et al. Human Mesenchymal Stem Cells Differentiate to a Cardiomyocyte Phenotype in the Adult Murine Heart. Circulation. 2002;105(1):93-98.
56. Silva GV, Litovsky S, Assad JAR, et al. Mesenchymal Stem Cells Differentiate into an Endothelial Phenotype, Enhance Vascular Density, and Improve Heart Function in a Canine Chronic Ischemia Model. Circulation. 2005;111(2):150-156.
57. Fink T, Zachar V. Adipogenic differentiation of human mesenchymal stem cells. Methods in molecular biology (Clifton, NJ). 2011;698:243-251.
58. Owen M, Friedenstein AJ. Stromal stem cells: marrow-derived osteogenic precursors. Ciba Foundation symposium. 1988;136:42-60.
59. Solchaga LA, Penick KJ, Welter JF. Chondrogenic differentiation of bone marrow-derived mesenchymal stem cells: tips and tricks. Methods in molecular biology (Clifton, NJ). 2011;698:253-278.
60. Sarugaser R, Hanoun L, Keating A, et al. Human mesenchymal stem cells self-renew and differentiate according to a deterministic hierarchy. PLoS One. 2009;4(8):e6498.
61. Gebler A, Zabel O, Seliger B. The immunomodulatory capacity of mesenchymal stem cells. Trends in molecular medicine. 2012;18(2):128-134.
62. Lee OK, Kuo TK, Chen W-M, et al. Isolation of multipotent mesenchymal stem cells from umbilical cord blood 2004.
63. Wang HS, Hung SC, Peng ST, et al. Mesenchymal stem cells in the Wharton's jelly of the human umbilical cord. Stem cells (Dayton, Ohio). 2004;22(7):1330-1337.
64. Zuk PA, Zhu M, Ashjian P, et al. Human adipose tissue is a source of multipotent stem cells. Molecular biology of the cell. 2002;13(12):4279-4295.
65. Tang Y, Wu X, Lei W, et al. TGF-beta1-induced migration of bone mesenchymal stem cells couples bone resorption with formation. Nat Med. 2009;15(7):757-765.
66. Zhen G, Wen C, Jia X, et al. Inhibition of TGF-[beta] signaling in mesenchymal stem cells of subchondral bone attenuates osteoarthritis. Nat Med. 2013;19(6):704-712.
67. Ng F, Boucher S, Koh S, et al. PDGF, TGF-β, and FGF signaling is important for differentiation and growth of mesenchymal stem cells (MSCs): transcriptional profiling can identify markers and signaling pathways important in differentiation of MSCs into adipogenic, chondrogenic, and ost… 2008.
68. Kim YJ, Hwang SJ, Bae YC, et al. MiR-21 regulates adipogenic differentiation through the modulation of TGF-beta signaling in mesenchymal stem cells derived from human adipose tissue. Stem cells (Dayton, Ohio). 2009;27(12):3093-3102.
69. Gaafar T, Osman O, Osman A, et al. Gene expression profiling of endometrium versus bone marrow-derived mesenchymal stem cells: upregulation of cytokine genes. Molecular and cellular biochemistry. 2014;395(1-2):29-43.
70. Chung MT, Liu C, Hyun JS, et al. CD90 (Thy-1)-positive selection enhances osteogenic capacity of human adipose-derived stromal cells. Tissue engineering Part A. 2013;19(7-8):989-997.
71. Mark P, Kleinsorge M, Gaebel R, et al. Human Mesenchymal Stem Cells Display Reduced Expression of CD105 after Culture in Serum-Free Medium. Stem cells international. 2013;2013:698076.

72. Rada T, Reis RL, Gomes ME. Distinct Stem Cells Subpopulations Isolated from Human Adipose Tissue Exhibit Different Chondrogenic and Osteogenic Differentiation Potential. Stem Cell Reviews and Reports. 2011;7(1):64-76.
73. Ninagawa N, Murakami R, Isobe E, et al. Mesenchymal stem cells originating from ES cells show high telomerase activity and therapeutic benefits. Differentiation. 2011;82(3):153-164.
74. Pablo Rodríguez J, González M, Ríos S, et al. Cytoskeletal organization of human mesenchymal stem cells (MSC) changes during their osteogenic differentiation. Journal of Cellular Biochemistry. 2004;93(4):721-731.
75. McAndrews KM, McGrail DJ, Quach ND, et al. Spatially coordinated changes in intracellular rheology and extracellular force exertion during mesenchymal stem cell differentiation. Physical biology. 2014;11(5):056004.
76. Huang IH, Hsiao CT, Wu JC, et al. GEF-H1 controls focal adhesion signaling that regulates mesenchymal stem cell lineage commitment. J Cell Sci. 2014.
77. Kern S, Eichler H, Stoeve J, et al. Comparative analysis of mesenchymal stem cells from bone marrow, umbilical cord blood, or adipose tissue. Stem cells (Dayton, Ohio). 2006;24(5):1294-1301.
78. Fonsatti E, Del Vecchio L, Altomonte M, et al. Endoglin: An accessory component of the TGF-beta-binding receptor-complex with diagnostic, prognostic, and bioimmunotherapeutic potential in human malignancies. Journal of cellular physiology. 2001;188(1):1-7.
79. Duff SE, Li C, Garland JM, et al. CD105 is important for angiogenesis: evidence and potential applications. FASEB journal : official publication of the Federation of American Societies for Experimental Biology. 2003;17(9):984-992.
80. Jin HJ, Park SK, Oh W, et al. Down-regulation of CD105 is associated with multi-lineage differentiation in human umbilical cord blood-derived mesenchymal stem cells. Biochemical and biophysical research communications. 2009;381(4):676-681.
81. Kyurkchiev D, Bochev I, Ivanova-Todorova E, et al. Secretion of immunoregulatory cytokines by mesenchymal stem cells. World Journal of Stem Cells. 2014;6(5):552-570.
82. Krampera M, Glennie S, Dyson J, et al. Bone marrow mesenchymal stem cells inhibit the response of naive and memory antigen-specific T cells to their cognate peptide. Blood. 2003;101(9):3722-3729.
83. Ringden O, Uzunel M, Rasmusson I, et al. Mesenchymal stem cells for treatment of therapy-resistant graft-versus-host disease. Transplantation. 2006;81(10):1390-1397.
84. Beane OS, Fonseca VC, Cooper LL, et al. Impact of Aging on the Regenerative Properties of Bone Marrow-, Muscle-, and Adipose-Derived Mesenchymal Stem/Stromal Cells. PLOS ONE. 2014;9(12):e115963.
85. Bergman RJ, Gazit D, Kahn AJ, et al. Age-related changes in osteogenic stem cells in mice. Journal of bone and mineral research : the official journal of the American Society for Bone and Mineral Research. 1996;11(5):568-577.
86. Connoy AC, Trader M, High KP. Age-related changes in cell surface and senescence markers in the spleen of DBA/2 mice: A flow cytometric analysis. Experimental Gerontology. 2006;41(2):225-229.
87. Li J, Kwong DL, Chan GC. The effects of various irradiation doses on the growth and differentiation of marrow-derived human mesenchymal stromal cells. Pediatric transplantation. 2007;11(4):379-387.
88. Trickett A, Kwan YL. T cell stimulation and expansion using anti-CD3/CD28 beads. J Immunol Methods. 2003;275(1-2):251-255.
89. Yagi H, Soto-Gutierrez A, Parekkadan B, et al. Mesenchymal Stem Cells: Mechanisms of Immunomodulation and Homing. Cell transplantation. 2010;19(6):667-679.

90. Quah BJC, Warren HS, Parish CR. Monitoring lymphocyte proliferation in vitro and in vivo with the intracellular fluorescent dye carboxyfluorescein diacetate succinimidyl ester. Nat Protocols. 2007;2(9):2049-2056.
91. Lyons AB. Divided we stand: Tracking cell proliferation with carboxyfluorescein diacetate succinimidyl ester. Immunol Cell Biol. 1999;77(6):509-515.
92. Lyons AB, Parish CR. Determination of lymphocyte division by flow cytometry. Journal of Immunological Methods. 1994;171(1):131-137.
93. Ramasamy R, Tong CK, Seow HF, et al. The immunosuppressive effects of human bone marrow-derived mesenchymal stem cells target T cell proliferation but not its effector function. Cellular immunology. 2008;251(2):131-136.
94. Yagi R, Zhu J, Paul WE. An updated view on transcription factor GATA3-mediated regulation of Th1 and Th2 cell differentiation. International immunology. 2011;23(7):415-420.
95. Eisenstein EM, Williams CB. The Treg/Th17 Cell Balance: A New Paradigm for Autoimmunity. Pediatr Res. 2009;65(5 Part 2):26R-31R.
96. Aujla SJ, Dubin PJ, Kolls JK. Th17 cells and mucosal host defense. Seminars in immunology. 2007;19(6):377-382.
97. Ghilardi N, Ouyang W. Targeting the development and effector functions of TH17 cells. Seminars in immunology. 2007;19(6):383-393.
98. Volpe E, Servant N, Zollinger R, et al. A critical function for transforming growth factor-beta, interleukin 23 and proinflammatory cytokines in driving and modulating human T(H)-17 responses. Nature immunology. 2008;9(6):650-657.
99. Chognard G, Bellemare L, Pelletier A-N, et al. The Dichotomous Pattern of IL-12R and IL-23R Expression Elucidates the Role of IL-12 and IL-23 in Inflammation. PLoS ONE. 2014;9(2):e89092.
100. Fyall KM, Fong AM, Rao SB, et al. The TBX21 transcription factor T-1993C polymorphism is associated with decreased IFN-gamma and IL-4 production by primary human lymphocytes. Human immunology. 2012;73(6):673-676.
101. O'Garra A, Vieira P. Regulatory T cells and mechanisms of immune system control. Nat Med. 2004;10(8):801-805.
102. Usha Shalini P, Vidyasagar JV, Kona LK, et al. In vitro allogeneic immune cell response to mesenchymal stromal cells derived from human adipose in patients with rheumatoid arthritis. Cellular immunology. 2017.
103. Li Pira G, Ivaldi F, Bottone L, et al. Human bone marrow stromal cells hamper specific interactions of CD4 and CD8 T lymphocytes with antigen-presenting cells. Human immunology. 2006;67(12):976-985.
104. Liu Q, Zheng H, Chen X, et al. Human mesenchymal stromal cells enhance the immunomodulatory function of CD8+CD28- regulatory T cells. Cell Mol Immunol. 2015;12(6):708-718.
105. Mikulkova Z, Praksova P, Stourac P, et al. Numerical defects in CD8+CD28- T-suppressor lymphocyte population in patients with type 1 diabetes mellitus and multiple sclerosis. Cellular immunology. 2010;262(2):75-79.
106. Del Papa B, Sportoletti P, Cecchini D, et al. Notch1 modulates mesenchymal stem cells mediated regulatory T-cell induction. European journal of immunology. 2013;43(1):182-187.
107. Szabo SJ, Sullivan BM, Stemmann C, et al. Distinct effects of T-bet in TH1 lineage commitment and IFN-gamma production in CD4 and CD8 T cells. Science (New York, NY). 2002;295(5553):338-342.
108. Damsker JM, Hansen AM, Caspi RR. Th1 and Th17 cells: Adversaries and collaborators. Annals of the New York Academy of Sciences. 2010;1183:211-221.
109. Barker JN, Byam CE, Kernan NA, et al. Availability of cord blood extends allogeneic hematopoietic stem cell transplant access to racial and ethnic minorities. Biology of blood and marrow

transplantation : journal of the American Society for Blood and Marrow Transplantation. 2010;16(11):1541-1548.
110. Gluckman E, Rocha V, Boyer-Chammard A, et al. Outcome of cord-blood transplantation from related and unrelated donors. Eurocord Transplant Group and the European Blood and Marrow Transplantation Group. The New England journal of medicine. 1997;337(6):373-381.
111. Ballen KK, Gluckman E, Broxmeyer HE. Umbilical cord blood transplantation: the first 25 years and beyond. Blood. 2013;122(4):491-498.
112. Laughlin MJ, Eapen M, Rubinstein P, et al. Outcomes after transplantation of cord blood or bone marrow from unrelated donors in adults with leukemia. The New England journal of medicine. 2004;351(22):2265-2275.
113. Rubinstein P, Carrier C, Scaradavou A, et al. Outcomes among 562 recipients of placental-blood transplants from unrelated donors. The New England journal of medicine. 1998;339(22):1565-1577.
114. Bari S, Seah KK, Poon Z, et al. Expansion and homing of umbilical cord blood hematopoietic stem and progenitor cells for clinical transplantation. Biology of blood and marrow transplantation : journal of the American Society for Blood and Marrow Transplantation. 2015;21(6):1008-1019.
115. Becker PS, Nilsson SK, Li Z, et al. Adhesion receptor expression by hematopoietic cell lines and murine progenitors: modulation by cytokines and cell cycle status. Experimental hematology. 1999;27(3):533-541.
116. Gan OI, Murdoch B, Larochelle A, et al. Differential Maintenance of Primitive Human SCID-Repopulating Cells, Clonogenic Progenitors, and Long-Term Culture-Initiating Cells After Incubation on Human Bone Marrow Stromal Cells. Blood. 1997;90(2):641-650.
117. Grover A, Mancini E, Moore S, et al. Erythropoietin guides multipotent hematopoietic progenitor cells toward an erythroid fate. The Journal of experimental medicine. 2014;211(2):181-188.
118. Gonzalez S, Amat L, Azqueta C, et al. Factors modulating circulation of hematopoietic progenitor cells in cord blood and neonates. Cytotherapy. 2009;11(1):35-42.
119. Aljitawi OS, Paul S. Erythropoietin modulation is associated with improved homing and engraftment after umbilical cord blood transplantation. 2016;128(25):3000-3010.
120. Balestra C, Germonpre P, Poortmans JR, et al. Serum erythropoietin levels in healthy humans after a short period of normobaric and hyperbaric oxygen breathing: the "normobaric oxygen paradox". Journal of applied physiology (Bethesda, Md : 1985). 2006;100(2):512-518.
121. Aljitawi OS, Xiao Y, Eskew JD, et al. Hyperbaric oxygen improves engraftment of ex-vivo expanded and gene transduced human CD34(+) cells in a murine model of umbilical cord blood transplantation. Blood cells, molecules & diseases. 2014;52(1):59-67.
122. Gajewski JL, Johnson VV, Sandler SG, et al. A review of transfusion practice before, during, and after hematopoietic progenitor cell transplantation. Blood. 2008;112(8):3036-3047.
123. Mehta HM, Malandra M, Corey SJ. G-CSF and GM-CSF in Neutropenia. Journal of immunology (Baltimore, Md : 1950). 2015;195(4):1341-1349.
124. Camporesi EM, Bosco G. Mechanisms of action of hyperbaric oxygen therapy. Undersea & hyperbaric medicine : journal of the Undersea and Hyperbaric Medical Society, Inc. 2014;41(3):247-252.
125. Moon RE. Hyperbaric oxygen treatment for air or gas embolism. Undersea & hyperbaric medicine : journal of the Undersea and Hyperbaric Medical Society, Inc. 2014;41(2):159-166.
126. Torp KD, Carraway MS, Ott MC, et al. Safe administration of hyperbaric oxygen after bleomycin: a case series of 15 patients. Undersea & hyperbaric medicine : journal of the Undersea and Hyperbaric Medical Society, Inc. 2012;39(5):873-879.
127. Karagoz B, Suleymanoglu S, Uzun G, et al. Hyperbaric oxygen therapy does not potentiate doxorubicin-induced cardiotoxicity in rats. Basic & clinical pharmacology & toxicology. 2008;102(3):287-292.

128. Leach RM, Rees PJ, Wilmshurst P. Hyperbaric oxygen therapy. BMJ (Clinical research ed). 1998;317(7166):1140-1143.
129. Larochelle A, Gillette JM, Desmond R, et al. Bone marrow homing and engraftment of human hematopoietic stem and progenitor cells is mediated by a polarized membrane domain. Blood. 2012;119(8):1848-1855.
130. Capone A, Podda D, Ennas F, et al. Hyperbaric oxygen therapy for transient bone marrow oedema syndrome of the hip. Hip international : the journal of clinical and experimental research on hip pathology and therapy. 2011;21(2):211-216.
131. Zhang Q, Chang Q, Cox RA, et al. Hyperbaric oxygen attenuates apoptosis and decreases inflammation in an ischemic wound model. The Journal of investigative dermatology. 2008;128(8):2102-2112.
132. Méndez-Ferrer S, Michurina TV, Ferraro F, et al. Mesenchymal and haematopoietic stem cells form a unique bone marrow niche. Nature. 2010;466(7308):829-834.
133. Khan M, Meduru S, Mohan IK, et al. Hyperbaric oxygenation enhances transplanted cell graft and functional recovery in the infarct heart. Journal of molecular and cellular cardiology. 2009;47(2):275-287.
134. Lin SS, Ueng SW, Niu CC, et al. Effects of hyperbaric oxygen on the osteogenic differentiation of mesenchymal stem cells. BMC musculoskeletal disorders. 2014;15:56.
135. Guo B, Kumar S, Li C, et al. CD105 (Endoglin), Apoptosis, and Stroke. Stroke; a journal of cerebral circulation. 2004;35(5):e94-e95.
136. Rafei M, Hsieh J, Fortier S, et al. Mesenchymal stromal cell-derived CCL2 suppresses plasma cell immunoglobulin production via STAT3 inactivation and PAX5 induction. Blood. 2008;112(13):4991-4998.
137. Sato K, Ozaki K, Oh I, et al. Nitric oxide plays a critical role in suppression of T-cell proliferation by mesenchymal stem cells. Blood. 2007;109(1):228-234.
138. Di G-h, Liu Y, Lu Y, et al. IL-6 Secreted from Senescent Mesenchymal Stem Cells Promotes Proliferation and Migration of Breast Cancer Cells. PLOS ONE. 2014;9(11):e113572.
139. Sotiropoulou PA, Perez SA, Gritzapis AD, et al. Interactions between human mesenchymal stem cells and natural killer cells. Stem cells (Dayton, Ohio). 2006;24(1):74-85.
140. Saini AS, Shenoy GN, Rath S, et al. Inducible nitric oxide synthase is a major intermediate in signaling pathways for the survival of plasma cells. Nature immunology. 2014;15(3):275-282.
141. Berg DT, Gupta A, Richardson MA, et al. Negative regulation of inducible nitric-oxide synthase expression mediated through transforming growth factor-beta-dependent modulation of transcription factor TCF11. The Journal of biological chemistry. 2007;282(51):36837-36844.
142. Ramirez-Yanez GO, Hamlet S, Jonarta A, et al. Prostaglandin E2 enhances transforming growth factor-beta 1 and TGF-beta receptors synthesis: an in vivo and in vitro study. Prostaglandins, leukotrienes, and essential fatty acids. 2006;74(3):183-192.
143. Timoshenko AV, Lala PK, Chakraborty C. PGE2-mediated upregulation of iNOS in murine breast cancer cells through the activation of EP4 receptors. Int J Cancer. 2004;108(3):384-389.
144. van der Garde M, van Pel M, Millán Rivero JE, et al. Direct Comparison of Wharton's Jelly and Bone Marrow-Derived Mesenchymal Stromal Cells to Enhance Engraftment of Cord Blood CD34(+) Transplants. Stem Cells and Development. 2015;24(22):2649-2659.
145. Jian H, Shen X, Liu I, et al. Smad3-dependent nuclear translocation of beta-catenin is required for TGF-beta1-induced proliferation of bone marrow-derived adult human mesenchymal stem cells. Genes & development. 2006;20(6):666-674.
146. Roelen BA, Dijke P. Controlling mesenchymal stem cell differentiation by TGFBeta family members. Journal of orthopaedic science : official journal of the Japanese Orthopaedic Association. 2003;8(5):740-748.

147. Wahl SM, McCartney-Francis N, Mergenhagen SE. Inflammatory and immunomodulatory roles of TGF-beta. Immunology today. 1989;10(8):258-261.
148. Freyman T, Polin G, Osman H, et al. A quantitative, randomized study evaluating three methods of mesenchymal stem cell delivery following myocardial infarction. European heart journal. 2006;27(9):1114-1122.
149. Ziebarth AJ, Nowsheen S, Steg AD, et al. Endoglin (CD105) contributes to platinum resistance and is a target for tumor-specific therapy in epithelial ovarian cancer. Clinical cancer research : an official journal of the American Association for Cancer Research. 2013;19(1):170-182.
150. Calvi LM, Adams GB, Weibrecht KW, et al. Osteoblastic cells regulate the haematopoietic stem cell niche. Nature. 2003;425(6960):841-846.